HUNGARIAN AGRICULTURAL ENGINEERING

28/2015

HUNGARIAN ACADEMY OF SCIENCES

Hungarian Agricultural Engineering

N° 28/2015

PERIODICAL OF THE COMMITTEE OF AGRICULTURAL ENGINEERING OF THE HUNGARIAN ACADEMY OF SCIENCES

Published by

Szent István University, Gödöllő
Faculty of Mechanical Engineering
H-2103 Gödöllő, Páter K. u. 1.

Gödöllő
2015

Published online: http://hae-journals.org
HU ISSN 0864-7410 (Print)
HU ISSN 2415-9751(Online)

PREFACE

In the name of the Comittee of Agricultural and Biosystem Engineering of the Hungarian Academy of Sciences we would like to welcome everyone who is interested in reading our journal. The Hungarian Agricultural Engineering (HAE) journal was published 28 years ago for the very first time with an aim to introduce the most valuable and internationally recognized (in these years already DOI numbered) Hungarian studies about mechanization in the field of agriculture and environmental protection. Initially the "Hungarian Institute of Agricultural Engineering" was responsible for the publication of the magazine which was mostly based on the articles and the presentations of the biannually organized International Mechanization Conference. Focusing on up-to-date technical and technological development, the conference discusses synergic trends between agriculture and industry, renewable energy production, newest environmental technology challenges, academic and applied research and technical education matters. According to the main objective, the conference brings together experts from different geographic regions with similar interdisciplinary scientific interest, research activities and shares ideas in the fields of bio-system engineering. During the sessions on the event that was organized between October 12-15, 2015 researchers, scientists, engineers gave summarizing presentations of their works. Overview of the best papers – after strict peer viewing process – is published in this issue of the Hungarian Agricultural Engineering. All papers have been selected by our editorial board and double blind reviewed by prominent experts. We do hope that this unique publication can give a good coverage of the scientific conference's work and can inspire many of the Readers to take part in the next Synergy conference in 2017.

Gödöllő, 30.12.2015.

Dr. István SZABÓ
editor in chief

Dr. László TÓTH
editor in chief

HUNGARIAN AGRICULTURAL ENGINEERING
N° 28/2015 5-10
Published online: http://hae-journals.org/
HU ISSN 0864-7410 (Print) / HU ISSN 2415-9751(Online)
DOI: 10.17676/HAE.2015.28.5

PERIODICAL OF THE COMITTEE OF AGRICULTURAL AND BIOSYSTEM ENGINEERING OF
THE HUNGARIAN ACADEMY OF SCIENCES
and
SZENT ISTVÁN UNIVERSITY
Faculty of Mechanical Engineering

CONDITIONS OF USING PROPELLER STIRRING IN BIOGAS REACTORS

Author(s):
Z. Bártfai – I. Oldal – L. Tóth – I. Szabó – J. Beke

Affiliation:
Szent István University, Faculty of Mechanical Engineering, 1.Páter K. street. Gödöllő, H2100

Email address:
bartfai.zoltan@gek.szie.hu, toth.laszo@gek.szie.hu, oldal.istvan@gek.szie.hu, szabo.istvan@gek.szie.hu, beke.janos@gek.szie.hu

Abstract

Preparing and further cutting of bovine dung which also contains straw, and of corn silage happens in special cutters, from which it is fed into the pre-fermentation tank. The primary mixing of liquid manure, and sewage water, including other fluids happens in a heated pre-container. The foodstuffs which are their expiration dates, and various other waste (household waste, greasy materials from washing, depleted frying oil, fats from grease-traps, etc.) are accepted in the pounder. This is where the cutting and separation of wrappings of boxed products happens as well, after which the thin parts are fed into an autoclave, and kept at 70oC for at least four hours to sterilise them.

The profit-oriented biogas plants consider the static, calculable production of electric and heat energy a fundamental goal, which requires the gas production to be continuous and free of hindrances [1]. In case of these factories, the gas yield for time unit may be lowered by various operation factors, but mainly malfunctions (errors, the foam within fermentation tanks from time to time, etc.). Incorrectly mixing or homogenising the materials arriving in the fermentation tanks also counts as a hindering operation factor. Our work details the basic questions of how the stirring inside fermentation tanks happens physically.

Keywords

biogas, stirring attributes, propeller fans, fermentation tanks

1. Introduction

Requirements for the stirring system are as follows:
- The density can be set for the entire mass even after mixing more dense, or more thin materials.
- Constant temperature and pH values can be achieved for the entire volume.
- The heat can be transferred from heating surfaces, and can be equalised.
- The micro-organisms are in a forced interaction with the nutrients.
- The entire volume is used, there are no so-called "dead areas".
- The hindering material parts are thinned.
- The subsidence of the substrate is prevented, and the nutrient content is homogenised.
- The bacteria release gas into the mass, which then reaches its surface in bubble form due to the so-called velocity shear of the material masses shifting compared to each other due to stirring.

Research analyses' conducted in biogas plants conclude that the homogenisation of materials fed into the fermentation tanks is not sufficient. Defining efficiency isn't simple due to the number of parameters which have an effect on fermentation. The physical constitution of materials, the level of cutting, the size of individual grains, the length of individual strands in materials which contain f.e. straw, etc. all have to be evaluated. The chemical constitution of materials, the contents of the materials - f.e. C/N ratios, pH values, dry material contents, etc., their inhibitor content, etc. all have to be calculated. Kamarad et al. [2] believes that most of the energy supplied is used for stirring, which is dependent on the viscosity of the material. The quality of stirring also determines the intensity of gas yield. During the stirring, they used a hydroxide-monohydrate solvent as a tracing indicator, and checked its quantity in various areas. The method proved to be feasible. In case of high concentrations, the fluid behaved as a non-Newton fluid. The indicator method helped to verify the usefulness of CFD (Computational Fluid Dynamics) modelling. Below are contour graphs of bladed stirring fans for their velocity (a) in [m/s], and viscosity (b) in [Pas] (Figure 1).

International literature discusses the stirring process inside biogas reactors in great length [3, 4]. Various small samples were constructed for the goal of modelling the process, using simpler, cheaper methods. The main problem of these small samples is that the physical form of the material is hard to match with the system, and a model mass close to the original is hard to create. In order to raise reliability, the processes are simulated both in small scale, and close to real values, using various simulation software. These modelling processes are plagued by the problem of following the viscosity, and the susceptibility to fraction of materials. Therefore, they are riddled with errors. CFD modelling is considered to be one of the most effective method for determining main attributes [5, 6].

The small sample and the CFD method together are sufficient for solving basic problems in their entirety, f.e. identifying the dead areas which form during the stirring process, determining the velocity shear values, and the overall visual simulation of the stirring [7]. We can also make a guess on the energetic implementation, since calculating the hydraulic resistance of

various stirring machines is possible as well [8]. Hydraulic resistance has a significant impact on energy consumption, which becomes substantial in case of big tanks. Another problem is the factory safety situation in case of some stirring methods. This factor is defined by two perspectives: the possible errors in the system, and the technological problems, meaning the fact that various materials stick to the stirring machine's surface; and to defend against and minimise the materials chipping the machinery away. During the stirring of various materials, various behaviours can be seen, as materials which contain strands are different to materials which contain heavy grains, the second of which includes both sand and small pebbles.

Nowadays' most widely used stirring methods can be seen on Figure 2.

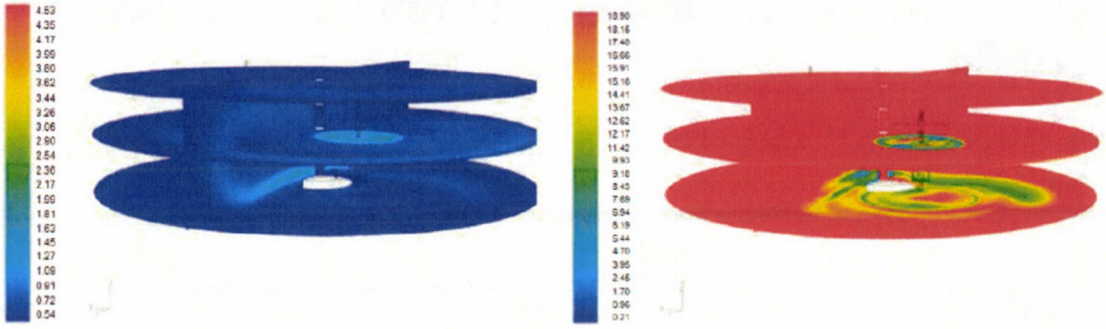

a. b.

Figure 1. The velocity of mass for vertical bladed stirring fans (a) in [m/s], and viscosity contours in [Pas] inside a 300 m^3 tank [2]

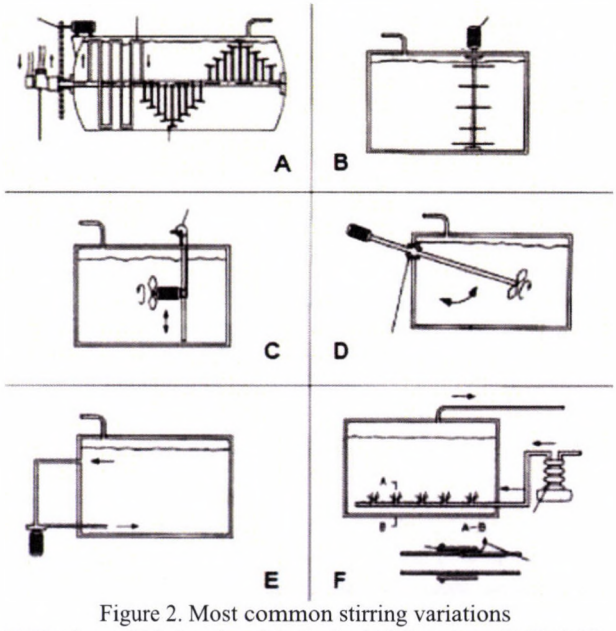

Figure 2. Most common stirring variations
A) Horizontal blade mixer B) Vertical blade mixer C) Variable height / flow propeller D) Propeller installed on a rocker E) Hydraulic stirring F) Air injection stirring

International literature shows that the propeller fan may be the perspectivical one of the various stirring methods, since it has the least hydraulic resistance, its surface can be made the least susceptible to materials' sticking, and the velocity of outbound mass flows can be changed to a significant decree by setting the RPM of the engines. The engines and connection units manufactured with an isolation similar to diving-pumps can be set to different angles within the stirring space, moreover, software programs can be made to conduct this task as well. According to what's been said until now, a universal stirring method does not exist. The actual setting and operations of the stirring machine are determined by the physical and chemical attributes of the materials fed into the tank, and the shape and size of the stirring space are also something to be considered. To satisfy requirements (consistent temperature, physical and chemical attributes in the entire space, and prevention of divergence) knowing the material's momentary attributes is important, for which a software-controlled RPM and rotation direction can be chosen. Various experiments also tried the combination of stirring elements (Figure 3).

Figure 3. Combination of vertical bladed and propeller stirring fans [5].

Figure 4 illustrates the most common stirring element solutions found in literature.

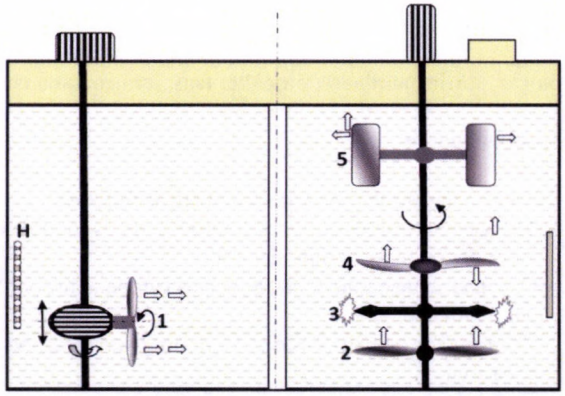

Figure 4. Modelled forms most common in literature.
1 – some propeller axial (possible to set height, direction and RPM), and vertical axis solution variants: 2 – large propeller delivering upwards, 3 – simple turbulent blade, 4 – wing blade, 5 – bladed propeller delivering upwards and sideways

This research considers the propeller stirring method the most efficient, hence we analysed this one. The most common solutions among propeller stirrers were the variable position ones (Figures 5 and 6).

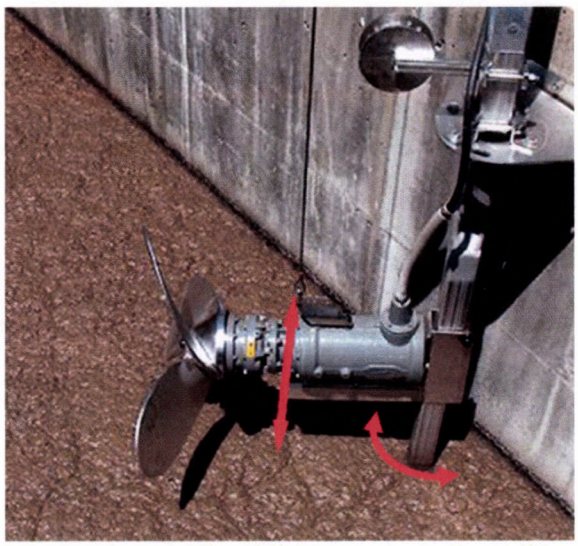

Figure 5. Changing height and direction

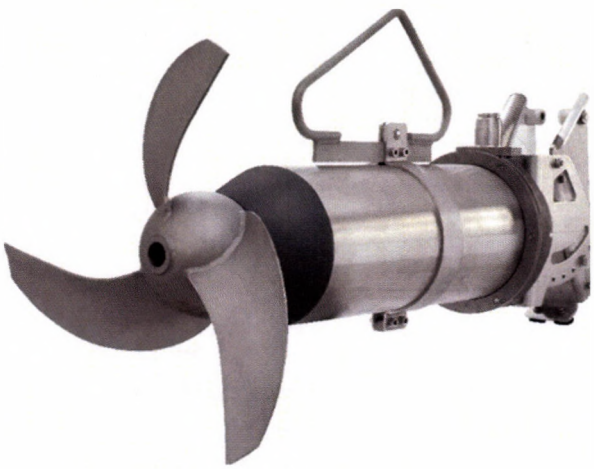

A

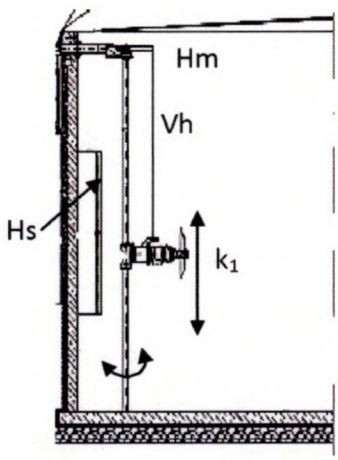

B

Figure 6. Propeller stirrers A – propeller and engine, k_1 – installing the variable stirring fan, Vh – vertical setting, Hm – Horizontal setting, Hs – heat pipes

2. Material and methods

Continuity in case of axial rowing

We evaluated and modelled the stream circumstances of the propeller stirring method considered to be the most efficient by our source literature. The modelling and its results are introduced in the research of Bártfai and his colleagues [9, 10].

- The theoretic equations of the flowing liquid are based on the following assumptions:
- flow in the entire stream tube is stationary,
- the fluid can't be compressed (its density – p – is static),
- the fluid is frictionless,
- we disregard the gravitational field,
- axial speed is constant in each sections,
- radial velocity is zero.

The basis for defining the continuity equation is Figure 7.

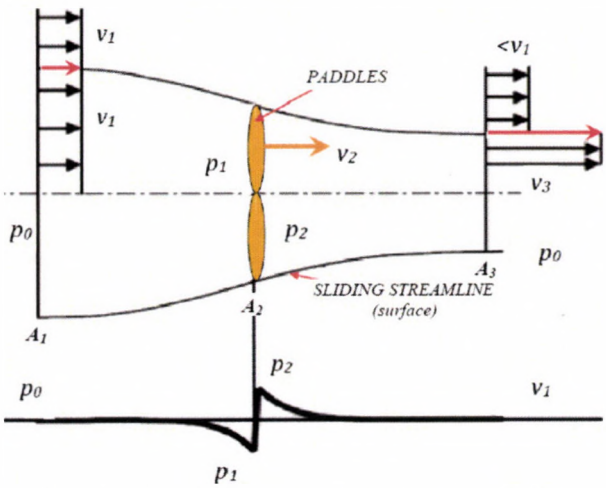

Figure 7. Section curve of the symmetrical current surface bordering the paddles and the medium flowing through their area

Based on these, the equation of continuity:

$$\dot{m}\rho Av = \dot{m}\rho A_2 v_2 = \dot{m}\rho A_3 v_3 = \text{holds true.}$$

With the proper indexes, we can present the equation for each section of the stream tube.

A sudden increase in tangential velocity may be possible on the border-streamline (the so-called sliding streamline). The liquid enters the stream tube on the left with a v_1 relative speed (we can also say that the mixer is advancing towards the left with a $-v_1$ velocity in the freestream). The flow speed of the liquid inside the stream tube and outside of it is equal in this section (see the Figure). The medium gains speed compared to the mixing blades inside the stream tube, and leaves on the right side with a higher ($v_3 > v_1$) velocity, while the relative velocity outside the stream tube is static (v_1). Similarly, pressure is also constant p_0, and while it gains from p_1 to p_2 on the agitator, leaving the stream tube, it recedes to p_0 again.

The thrust signifies the strength of the flow reaction, which presented from the pressure difference is as follows:

$$F = (p_2 - p_1)A_2$$

Bernoulli equations before and after the mixer in the stream tube are as follows:

$$p_0 + \frac{\rho}{2}v_1^2 = p_1 + \frac{\rho}{2}v_2^2$$

$$p_2 + \frac{\rho}{2}v_2^2 = p_0 + \frac{\rho}{2}v_3^2$$

After defining p_1 and p_2, and substituting them into the thrust:

$$F = \frac{\rho}{2}(v_3^2 - v_1^2)A_2 = \rho\frac{v_3 + v_1}{2}(v_3 - v_1)A_2$$

The impulse differences between entering and leaving fluids can only be caused by the force of the propeller blade, impacting the fluid.

$$\dot{m}v_1 + F - \dot{m}v_3 = 0$$

Therefore, force (F) is as follows:

$$\dot{m}(v_3 - v_1) = \rho A_2 v_2(v_3 - v_1) = \boldsymbol{F} = \rho A_2 \frac{v_3 + v_1}{2}(v_3 - v_1)$$

An important provision must be declared – the mass flow in the disk's section can be calculated using the given value for any sections of the stream tube:

$$\dot{m} = A_2 v_2$$

If we substitute this into the equation, then after reduction, it looks as follows:

$$v_2 = \frac{v_1 + v_3}{2}$$

Substituting this into the equation of continuity:

$$\frac{1}{A_2} = \frac{1}{2}\left(\frac{1}{A_1} + \frac{1}{A_3}\right)$$

The increase in velocity inside the stream tube is as follows:

$$\Delta v = v_3 - v_1$$

Meaning the value of v_2 is as follows:

$$v_2 = v_1 + \frac{\Delta v}{2}$$

Hydraulic power is the product of mass flow and change in movement energy value by unit:

$$P_{hy} = \dot{m}\left(\frac{v_3^2}{2} - \frac{v_1^2}{2}\right) = \dot{m}\Delta v v_1\left(1 + \frac{\Delta v}{2v_1}\right)$$

The power consumed for mass transport is the product of velocity before the mixer (v_1) and the movement force (F):

$$P_{fe} = v_1 F = v_1\dot{m}(v_3 - v_2) = v_1\dot{m}\Delta v$$

Resulting in efficiency, which is as follows:

$$\eta = \frac{P_{fe}}{P_{hy}} = \frac{1}{1 + \frac{\Delta v}{2v_1}}$$

Compared to propeller blades, the difference is that the medium is far before the mixer, which makes the v_1 velocity zero, also meaning that A_1 cross section has to be infinite.

Efficiency can usually be 50-65%, which may be further decreased by other mechanical losses.

Usually, the quotient of the axial velocity of the material flowing along the edges of the blades, and the rotation velocity of the blade's end point is almost the same as the tangent of the blade's angle. Therefore, the value which describes this would be:

$$v_2 = tg\alpha Dn$$

In case of parallel and continuous flow of the fluid layers, the internal friction force (F) counter to the direction of movement is proportional to the areas (A) of the surfaces in friction (moving on top of each other), and the velocity gradient(du/dy).

The proportion factor is the constant value defining the fluid's material quality, in other words, dynamic viscosity (η = Pa s):

$$\eta = \frac{A_f}{F_s}\frac{dv_2}{dy_n}$$

Where: v_2 – velocity,

y_n – thickness of the fluid layer

The shear stress can be defined by the physical values of F/A (force/area):

τ, [N/m²]:

$$\tau = -\eta\frac{dv_2}{dy_n}$$

Which makes the velocity gradient, in other words, the shear velocity [s^{-1}]:

$$\dot{\gamma} = \frac{dv_2}{dy_n}$$

Newton's viscosity law states that the shear stress between layers is proportional with the velocity gradient. This doesn't hold true for non-Newton liquids, for which the formula is more complex between the shear stress and the velocity gradient.

Dynamic viscosity (η) can be defined as the quotient of the shear stress (τ = N/m²) and the shear velocity [kg m^{-1} s^{-1}, meaning Pa s] as follows:

$$\eta = -\frac{\tau}{\dot{\gamma}}$$

This means the dynamic viscosity within fluids depends on the shear stress, and the velocity gradient.

If the transport direction of stirring blades is contrary to each other, and they are set in different heights from the ground, the formula can't be defined with functions, which means using modelling which is suitable to displaying the phenomenon happening is required.

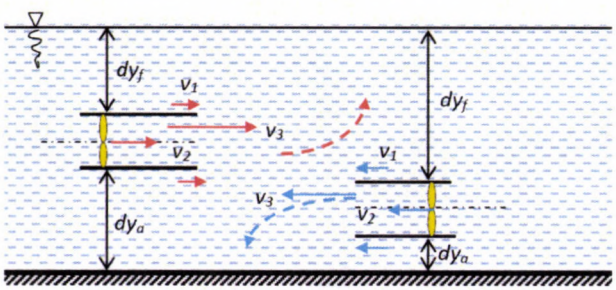

Figure 8. Two counter-rotating blades' interaction results in upwards and downwards streams. dy_f – distance from the surface, dy_a = distance from the ground, v_1 – flow velocity of the fluid inside the fluid body, v_2 – velocity of the fluid leaving the blades, v_3 – velocity of the fluid inside the fluid body, after it left the blades.

Due to this, the axial velocity value of the material flowing on the blade's edge differs in reality, which is why we can consider a C constant instead of the tgα value, which is dependent on the stirring solution (surface area, angle of the blades, etc.), the shape and size of the tank, and the distance between fans and the walls of the tank. The dynamic viscosity of the material is also determined by the Reynolds number of the location (after all, the entire calculation holds true for a single construction and angle), meaning:

$$v_2 = CDn$$

This makes mass flow:

$$\dot{m} = \rho A_2 v_2 = C\rho D^2 Dn$$

And the added (effective) energy:

$$P_{ho} = C\rho D^5 n^3$$

The value of C is inversely proportional for the Reynolds value, but in case the Re value is high, it may become constant

depending on the sizes of the tank. The dissipation of the 'fluid beam' exiting the propeller can be defined the same way as free fluid streams. Taking this, and our prior statements into consideration, modelling can be used to analyse the stirring of reactors from a fluid mechanics perspective, which does take the other elements of the system into consideration. F.e. we can define endless variations if we take any settings of three variable height and direction propeller stirring fans into consideration within a reactor. This is further complicated if their RPM can be varied without set levels. This amount of variations makes it easy to understand, how modelling and simulations are required. These methods may be used to select close-to-best favourable solutions, and choose the ones which seem the most favourable among them to conduct validation experiments on small samples or currently operating machines. The flow attributes which result from changes can be clearly seen on CDF models. As an example, see Figures 9 and 10 and 11.

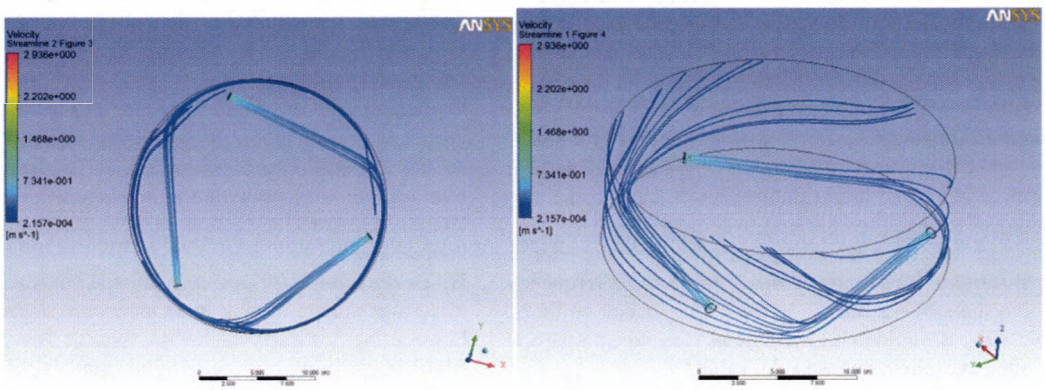

Figure 9. Three stirring fans positioned close to the ground, at the same height, towards the same flow directions.

The figures only show the flow expanding after the fans, which dissipates when it reaches the wall, and since the fans are close to the ground, the flows near the walls can only point downwards and dissipate. The middle section of the fermentation tanks doesn't house substantial movement at all.

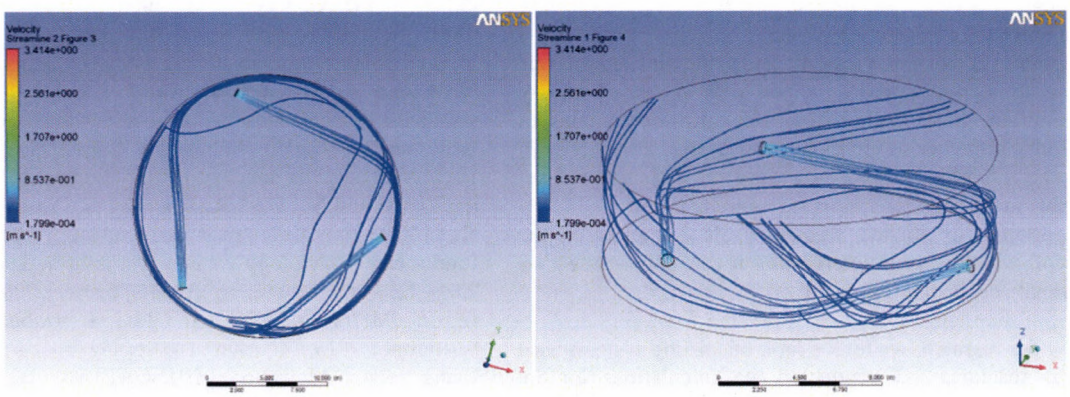

Figure 10. Three stirring fans positioned at different heights from the ground, towards the same flow directions.

This model also shows the flow expanding after the propeller, only dissipating when reaching the walls, but since two fans are farther from the ground, the dissipating flows can be seen flowing both downwards and upwards. Due to this, turbulent elements can also be seen near the walls.

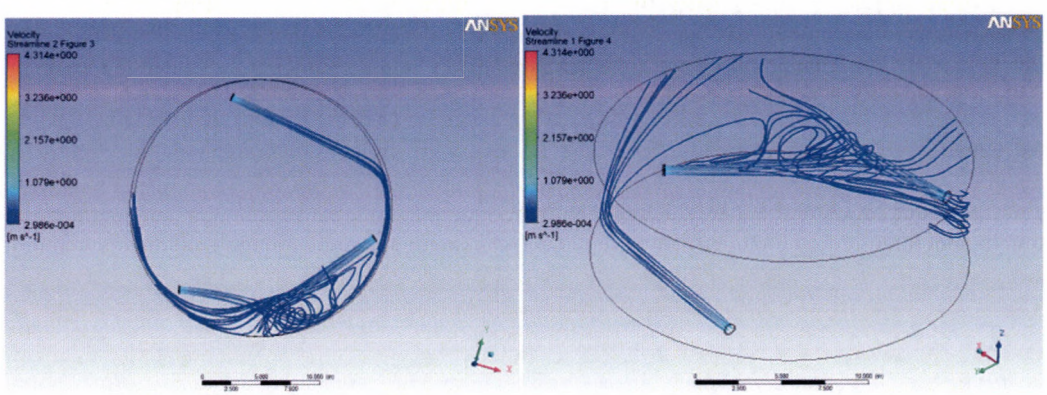

Figure 11. Three stirring fans positioned close to the ground, at the same height; two of them have identical flow directions, while the third has a different flow direction.

The two stirring fans cause intensive turbulence (mass flow), but a third of the wall surface doesn't have any flows whatsoever.

The examples on the figures show how incorrect settings may cause technological errors, which is a detrimental effect on the efficiency of gas yield.

3. Conclusion

- The logic of the fermentation tank-system dictates that feeding the materials should be followed by a more intensive stirring due to the faster heat transport of materials inside and inbound, which can be conducted via increasing the RPM of the stirring fans, in other words, the transport mass flow. However, keeping the increased intensity up for a longer time is not a sound decision, since the increase of shear velocity between material molecules within the fermentation zones causes the life expectancy of methanogen bacteria to decrease.
- Also, a more intensive stirring phase also aids the shorter homogenisation of the material mass. Applying a frequency changer to the stirring fans to achieve this effect would be desirable, since it would make mass flows close to optimal, and a more intensive stirring phase achievable.
- Heat collection during the winter season can only be realised with a higher mass flow for current heat expelling surfaces.
- Masses which aren't moved can develop due to the incorrectly set stirring fans, which makes the validation of favourable settings determined during the modelling process a necessity (f.e. via inserting heat sensors).
- The length, frequency and intensity of stirring cycles can only be validated via evaluating gas yield.
- The increase in dynamic viscosity causes the time required for stirring to increase, which comes with increased energy consumption, most notably when the substrate contains an abundance of higher solidity, inorganic grains. This is why in the case of sewage waste, increasing the efficiency of the transport firms' sand separators is required.
- The optimum of stirring frequency also depends on the material, which is why determining it can only happen via empirically evaluating gas yield.

During our research, we took a look on stirring systems used in biogas reactors, and conducted the calculations for the propeller stirring fan system, which is considered to be the most variable. These calculations define the kinematic effects on the material. The direction, height and RPM – in other words, transport performance – may have to be changed in case of propeller stirring fan systems to achieve results better than any other stirring methods. This statement was supported partially by analyses made public in Issue 2, 2015 of HAE [9]. The setups resulting in the most favourable gas yields can be adapted to the changing conditions (the mass' biological, chemical and physical attributes) the best, and are the most approachable.

Acknowledgement

The study was supported by TÁMOP 4.2.1.C-14/1/KONV-2015-0002.

References

[1.] Tóth L., Beke J., Bártfai Z., Szabó I., Hartdégen G., Oldal I., Blahunk Z.: 2014. Technological Features of Biogas Plants Using Mixed Materials, Hungarian Agricultural Engineering, N° 26/2014 39-46, Published online: HU ISSN 0864-7410 (Print) / HU ISSN 2415-9751(Online) http://dx.doi.org/10.17676/HAE.2014.26.39

[2.] Kamarad L., Pohn S., Bochmann G., Harasek M.: 2013. Determination of mixing quality in Biogas plant digesters using tracer Tests and computational fluid dynamics Cfd Acta Universitatis Agriculturae et Silviculturae Mendelianae Brunensis Volume LXI, 2013 140 Number 5 http://dx.doi.org/10.11118/actaun201361051269

[3.] Schön M.: 2009. Numerical Modelling of Anaerobic Digestion Processes in Agricultural Biogas Plants, Dissertation, Eingereicht an der Leopold-Franzens-Universität Innsbruck, Fakultät für Bauingenieurwissenschaften zur Erlangung des akademischen Grades "Doktor Der Technischen Wissenschaften", Innsbruck, Februar 2009

[4.] Bridgeman J.: 2012. Computational fluid dynamics modelling of sewage sludge mixing in an anaerobic digester Advances in Engineering Software Volume 44, Issue 1, February 2012, Pages 54–62 http://dx.doi.org/10.1016/j.advengsoft.2011.05.037

[5.] Maier C., Schlerka M., Weichselbaum W., Harasek M.: 2010. Development of agitation systems in biogas plants: Investigation of mixing characteristics, improvement of energy efficiency and scale-up using CFD, Chemical Engineering Transactions, Volume 21 Issue 1 Pages 1195–1200. ISSN 1974-9791. http://dx.doi.org/10.3303/CET1021200

[6.] Deglon D. A., Meyer C. J.: 2006. CFD modelling of stirred tanks: Numerical considerations, Minerals Engineering, Volume 19, p 1059-1068. http://dx.doi.org/10.1016/j.mineng.2006.04.001

[7.] Liang Yu, Jingwei Ma, Shulin Chen.: 2012. Numerical simulation of mechanical mixing in high solid anaerobic digester, Bioresource Technology, Volume 102, Issue 2, January 2011, Pages 1012–1018 http://dx.doi.org/10.1016/j.biortech.2010.09.079

[8.] Terashima M., Goel R., Komatsu K., Yasui H., Takahashi H., Li Y. Y.: 2009. CFD simulation of mixing in anaerobic digesters, Bioresource Technology Volume 100, Issue 7, April 2009, Pages 2228–2233 http://dx.doi.org/10.1016/j.biortech.2008.07.069

[9.] Z. Bártfai, L. Tóth., I. Oldal, I. Szabó., J. Beke, N. Schrempf.: 2015, Modelling The Stirring Process of Biogas Plants Using Mixed Materials , HUNGARIAN AGRICULTURAL ENGINEERING, N° 27/2015 Volume 1. In print.

[10.] Karaeva J. V., Khalitova G. R., Kovalev D. A., Trakhunova I. A.: 2015. Study of the Process of Hydraulic Mixing in Anaerobic Digester of Biogas Plant Chemical and Process Engineering. Volume 36, Issue 1, Pages 101–112, ISSN (Online) 2300-1925, http://dx.doi.org/10.1515/cpe-2015-0008

HUNGARIAN AGRICULTURAL ENGINEERING
N° 28/2015 11-14
Published online: http://hae-journals.org/
HU ISSN 0864-7410 (Print) / HU ISSN 2415-9751(Online)
DOI: 10.17676/HAE.2015.28.11

PERIODICAL OF THE COMITTEE OF AGRICULTURAL AND BIOSYSTEM ENGINEERING OF
THE HUNGARIAN ACADEMY OF SCIENCES
and
SZENT ISTVÁN UNIVERSITY
Faculty of Mechanical Engineering

SIMPLIFIED MULTIPLE LINEAR REGRESSION BASED MODEL FOR SOLAR COLLECTORS

Author(s):
R. Kicsiny

Affiliation:
Department of Mathematics, Institute for Mathematics and Informatics, Szent István University, Páter K. u. 1., Gödöllő, H-2103, Hungary

Email address:
kicsiny.richard@gek.szie.hu

Abstract

A recent accurate multiple linear regression (MLR) based collector model is simplified to gain a more easy-to-apply model with still good accuracy. The new model (SMLR model) is validated and compared with the former MLR based model (MLR model) and with a physically-based model used successfully in applications. Based on measurements, the SMLR model is nearly the same accurate as the physically-based one but more easy-to-apply than the physically-based and the MLR models. The computational demand is also lower than in case of any former model. Accordingly, the SMLR model is suggested for fast but relatively accurate collector modelling.

Keywords

solar collectors, mathematical modelling, black-box model, multiple linear regression

1. Introduction

Mathematical modelling is the most widely used and theoretically established tool to investigate and develop solar thermal collectors as environmentally friendly technological heat producers. The two main categories of mathematical models for collectors are physically-based models, which represent exact physical laws (based on theory), and black-box models, which describe empirical correlations (based on experiences or measurements).

Among the most important physically-based models, the Hottel-Whillier-Bliss model [1] may be the earliest, which is frequently used to date. This model determines the collector temperature as a function of time and space. Buzás et al. [2] proposed a simpler model assuming that the collector temperature is homogeneous in space. This model is a linear ordinary differential equation (ODE) validated in [3] and is likely the simplest physically-based model used in the practice (see e.g. [4, 5]), which can still describe the transient collector processes with an appropriate accuracy.

The greatest advantage of black-box models is that it is not needed to know the physical laws of a collector precisely in order to create a model. Nevertheless, the model may be rather precise even if it is simple as in the case of [3]. The most frequent black-box model type is perhaps the artificial neural network (ANN) in the field of collector modelling. Generally, ANNs are accurate tools but rather troublesome to apply because of the so-called training process. The convergence of the algorithm, which indicates the end of a training session, may be also time-consuming. According to Fischer at al. [6], a conveniently usable algorithm ensuring a reliable and fast determination of an appropriate ANN for a collector is still needed to be worked out.

Because of the above problems, a simple and general but still accurate black-box model, which can be applied easily and fast for a wide range of solar collectors, has been recently worked out in [3]. The model is based on the well-known methods of mathematical statistics, more precisely, the multiple linear regression (MLR). Based on the literature, MLR is a rare black-box modelling technique in the field of collectors despite of its simplicity. Considering the high precision (with an error of 4.6%), simple usability and low computational demand of the mentioned MLR-based model (MLR model in short) in [3], it is definitely worth trying to simplify further the MLR model to gain an even more easy-to-apply model with a still good accuracy. Such a simplification (likely the simplest possible MLR based model) is proposed in the present study.

2. Physically-based and MLR models

For the Reader's convenience, the physically-based collector model of Buzás et al. [2], which will be called physically-based model in short, and the MLR model [3] are recalled in this section. The scheme of the studied solar collector can be seen in Figure 1.

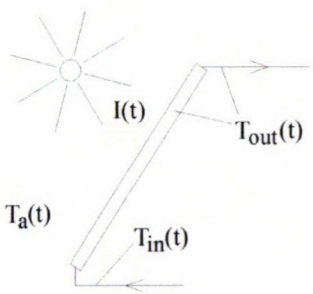

Figure 1. Scheme of the solar collector

Physically-based model

The physically-based model is the following ODE:

$$\frac{dT_{out}(t)}{dt} = \frac{A\eta_0}{\rho c V} I(t) + \frac{U_L A}{\rho c V}(T_a(t) - T_{out}(t)) + \frac{v}{V}(T_{in}(t) - T_{out}(t)) \cdot \quad (1)$$

MLR model

The inputs of the MLR model are from appropriately chosen values of T_{in}, I, T_a and T_{out}. The output is from appropriately chosen values of T_{out}. The flow rate value v is a fixed positive constant or 0.

Because of the boundedness of the flow rate, $T_{in}(t-\tau_1)$can play a role as an input in the MLR model if $T_{out}(t)$ is the output, where the positive constant τ_1 is a time delay. Similar considerations hold for I and T_a as well because of the bounded propagation speed of their effects, so former $I(t-\tau_2)$ and $T_a(t-\tau_2)$ values can play roles as inputs in forming the output $T_{out}(t)$. (The time delays of I and T_a are assumed to be the same (τ_2) for the sake of simplicity.) Naturally, appropriate former value of T_{out} also affects the value of $T_{out}(t)$ and participates as the initial value of the MLR model at time $(t-\tau_2)$ in essence. Considering the collector as a black-box, distinct sub-models as parts of the MLR model were identified for significantly different operating conditions. For example, the collector behaves different if the pump is on (v>0) or off (v=0) permanently. Even, the effect of T_{in} was neglected in permanently switched off case, since there is no flow between the collector inlet and outlet.

Considering a typical day, when the temperature increase of T_{out} is significant, three different operating conditions were distinguished according to Figure 2.

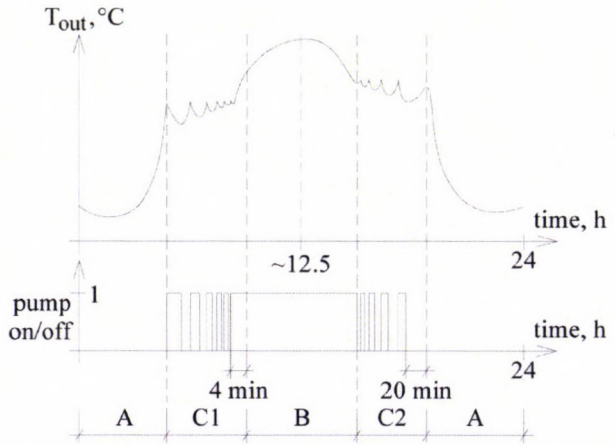

Figure 2. Outlet temperature and pump operation on a typical day

Case A corresponds to permanently switched off pump, Case B corresponds to permanently switched on pump and Case C corresponds to frequent switch-ons and -offs. It can be seen that there are two further significantly different operating cases within Case C: T_{out} basically increases before the solar noon and basically decreases after the solar noon, so Case C is divided into Cases C1 and C2. See [3] for more details.

The MLR model is composed of the following linear equations, which describe the corresponding sub-model of each operating case.

Case A: $$T_{out,mod}(t) = c_{I,A} I(t-\tau_2) + c_{a,A} T_a(t-\tau_2) + c_{out,A} T_{out}(t-\tau_2) + c_A \quad (2a)$$

Case B: $$T_{out,mod}(t) = c_{in,B} T_{in}(t-\tau_1) + c_{I,B} I(t-\tau_2) + c_{a,B} T_a(t-\tau_2) + c_{out,B} T_{out}(t-\tau_2) + c_B \quad (2b)$$

Case C1: $$T_{out,mod}(t) = c_{in,C1} T_{in}(t-\tau_1) + c_{I,C1} I(t-\tau_2) + c_{a,C1} T_a(t-\tau_2) + c_{out,C1} T_{out}(t-\tau_2) + c_{C1} \quad (2c)$$

Case C2: $$T_{out,mod}(t) = c_{in,C2} T_{in}(t-\tau_1) + c_{I,C2} I(t-\tau_2) + c_{a,C2} T_a(t-\tau_2) + c_{out,C2} T_{out}(t-\tau_2) + c_{C2} \quad (2d)$$

$c_{I,A}$, $c_{a,A}$, $c_{out,A}$, c_A, $c_{in,B}$, $c_{I,B}$, $c_{a,B}$, $c_{out,B}$, c_B, $c_{in,C1}$, $c_{I,C1}$, $c_{a,C1}$, $c_{out,C1}$, c_{C1}, $c_{in,C2}$, $c_{I,C2}$, $c_{a,C2}$, $c_{out,C2}$, c_{C2}, are constant parameters.

According to the definition of τ_2, the measurements take place at times t=τ_2,2τ_2,3τ_2,...The modelled value of T_{out} (that is $T_{out\,mod}$) is determined at times t=τ_2,2τ_2,3τ_2...from the measured values of $I(t=\tau_2)$, $T_a(t=\tau_2)$, $T_{out}(t=\tau_2)$and $T_{in}(t=\tau_1)$, based on Equations. (2a)-(2d).

3. SMLR model

The MLR model is simplified in this section in the way of merging Cases A, B, C1 and C2. Thus there is only one operating case with only one mathematical relation (Equation (3) below) in the new model, which will be called SMLR model. The corresponding mathematical relation is the following:

$$T_{out,mod}(t) = c_{in} T_{in}(t-\tau_1) + c_I I(t-\tau_2) + c_a T_a(t-\tau_2) + c_{out} T_{out}(t-\tau_2) + c \cdot \quad (1)$$

c_{in}, c_I, c_a, c_{out} and c are constant parameters to be identified.

Below, the SMLR model (Equation (3)) is identified and validated based on simulation and measured data then it is compared with the physically-based and MLR models in view of precision. The results and figures of the latter models used in the comparison are from. The identification and validation of the SMLR model are based on the same days as in case of the physically-based and MLR models in [3]. The used real flat plate collector field of 33.3 m^2 [7] at the Szent István University (SZIU) in Gödöllő, Hungary (SZIU collector in short) is also the same. T_{out} , T_{in} , I, T_a and v are measured once in every minute at the SZIU collector. The measured value of T_{out} serves only for identification and comparison purposes, the measured value $T_{out}(0)$is fed into the models as initial condition. The technical details of the identification and validation of the SMLR model are very similar as in case of the MLR model in [3], so they are not fully specified below. The needed calculations have been done numerically in Matlab [8] used comprehensively to simulate solar engineering systems (see e.g. [9]).

Identification

Four measured days are selected for the identification in such a way that they cover a wide range of possible operating conditions of a selected season (summer). Since the operating conditions are well characterized with the operating states of the pump (switched on state or switched off state), two measured days (2nd July 2012, 24th June 2012) with relatively few pump switches (smooth operation) and two other days (28th June 2012, 8th June 2012) with relatively many switches (intermittent operation) are selected.

A standard MLR routine is applied based on the measured data to identify parameters c_{in}, c_I, c_a, c_{out} and c. According to the minute-based measuring, τ_2 is set 1 min. V=0.027 m^3 and v=0.98 m^3/h if the pump is on, so $\tau_1 \approx 1.5$ min. The measured value of should be used in the right hand side of Eq. (3) for identification (and for validation). Since =1.5 min is not suitable for the minute-based measuring, $T_{in}(t-\tau_1)$ is substituted for $(T_{in}(t-\tau_2) + T_{in}(t-2\tau_2))/2$ in the identification. The standard MLR routine (based on least squares method) is well-known, available and easy-to-apply in most statistical and spreadsheet programs (SPSS, Excel, etc.) with low computational demand, so it is not detailed here. It can be seen that the SMLR model with a single linear relation (Eq. (3)) has lower computational demand than the physically-based model with an ODE or the MLR model with four relations. The identified parameters of the SMLR model can be seen in Table 1.

Table 2 contains the average of error (time average of the difference between the modelled and measured outlet temperatures) and the average of absolute error (time average of the absolute difference between the modelled and measured outlet temperatures) values for two days (2nd July 2012, 28th June 2012) of the identification of all models. The average of absolute error values

are presented in proportion to the difference between the daily maximal and minimal measured outlet temperature values as well (in %). The mean of these % values with respect to all of the four days of the identification is also presented in Table 2 (6.6 % for the SMLR model).

Table 1. Parameter values of the SMLR model

c_{in}, -	c_l, m²K/W	c_a, -	c_{out}, -	c, °C
-0.0017	0.0019	0.0471	0.9707	-0.2621

Table 2. Average of error and average of absolute error values with the models

			Physically-based model	MLR model	SMLR model
Identification	2nd July (smooth operation)	Average of error	-1.86 °C	-0.47 °C	1.43 °C
		Average of absolute error	4.33 °C; 7.0%	2.79 °C; 4.6%	3.88 °C; 6.3%
	28th June (intermittent operation)	Average of error	-1.26 °C	-0.23 °C	-2.87 °C
		Average of absolute error	4.35 °C; 7.5%	3.01 °C; 5.2%	3.39 °C; 5.8%
	Mean % value for the whole identification (four days)	Average of absolute error	7.8%	4.7%	6.6%
Validation	3rd August (smooth operation)	Average of error	-1.38 °C	-1.31 °C	-0.12 °C
		Average of absolute error	4.70 °C; 7.4%	2.85 °C; 4.5%	3.71 °C; 5.8%
	5th August (intermittent operation)	Average of error	-2.57 °C	-1.58 °C	-1.00 °C
		Average of absolute error	4.66 °C; 8.0%	3.07 °C; 5.2%	3.95 °C; 6.7%
	Mean % value for the whole validation (3rd July – 31st August)	Average of absolute error	7.8%	4.6%	8.0%

Figure 3 compares the modelled and measured outlet temperatures in case of the physically-based and SMLR models for a day of the identification. The operating state of the pump is also shown in the figure.

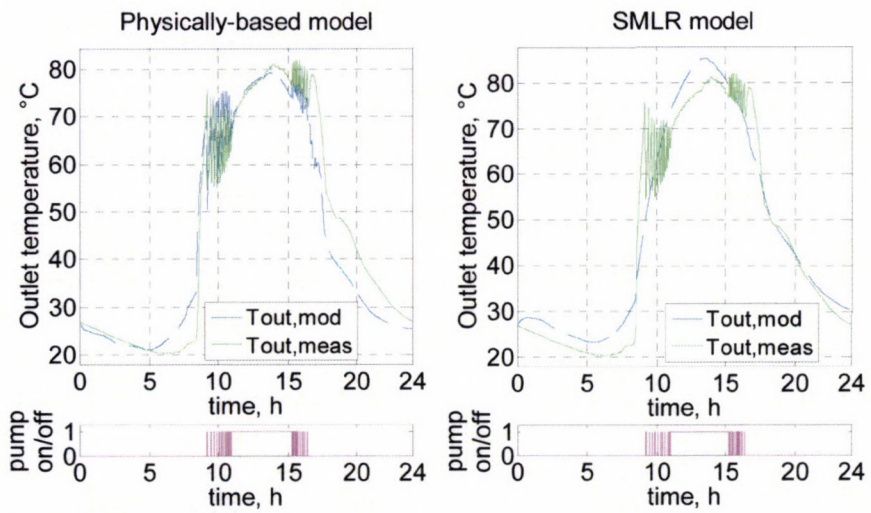

Figure 3. Modelled $T_{out,mod}$ and measured $T_{out,meas}$ collector temperatures on 2nd July 2012 in case of the physically-based and SMLR models

Validation

In the validation, all identified models are applied with the corresponding measured inputs of the remaining two summer months. More precisely, one input is changed in comparison with the identification, namely, the modelled value $T_{out,mod}(t-\tau_2)$ is used as $T_{out}(t-\tau_2)$ in the models (2a)-(2d) and (3) (not $T_{out,mod}(t-\tau_2)$), since the outlet temperature is to be modelled in the validation of course and not to be measured. The modelled days are from 3rd July to 31st August 2012, which are 56 days according to minor technical interruptions.

Table 2 shows the resulted error values (the same as in the Identification section) of each model for two days and for the whole validation. Figure 4 shows the modelled and measured outlet temperatures in case of the physically-based and SMLR models for a day of the validation. The operating state of the pump is also shown in the figure

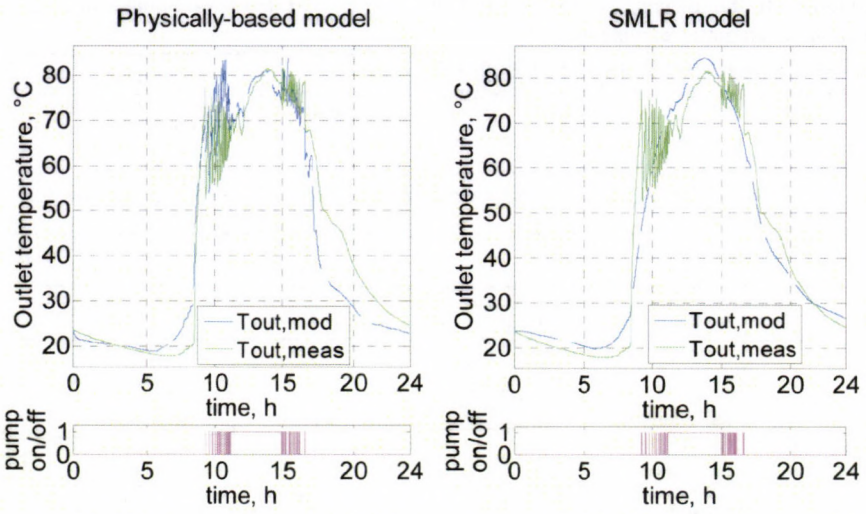

Figure 4. Modelled $T_{out,mod}$ and measured $T_{out,meas}$ collector temperatures on 3rd August 2012 in case of the physically-based and SMLR models

4. Conclusion

Based on the validation, the SMLR model (with an error of 8.0%) is considerably less accurate than the MLR model (with an error of 4.6%) but nearly the same accurate as the physically-based model (with an error of 7.8%), which has been used successfully in the practice. The SMLR model has the lowest computational demand and is much simpler to use than the other models. The SMLR model is easy to identify for any collector with the same inputs and output as above (evacuated tube collectors, parabolic trough collectors, etc.), so the model is general. Thus the SMLR model can be suggested for fast but still relatively precise collector modelling.

It should be mentioned that the collector temperature is measured on the outside surface of the outlet pipe of the SZIU collector and not directly in the collector fluid. Thus the outlet temperature cannot be expected to be modelled perfectly because of the inaccuracy caused by this measuring and that the collector field is charged with significant disturbances (shadowing effect of clouds), which are hard to predict. Also, the rather small volume of the collector field involves high and fast changes in the collector temperature under the influence of the disturbances. These difficulties reinforce that the accuracy of the SMLR model can be called well.

Nomenclature

t – time, s;
T_{out} – homogeneous temperature and also outlet (fluid) temperature of the collector, °C;
I – global solar irradiance on the collector surface, W/m²;
T_a – ambient temperature of the collector, °C;
T_{in} – inlet (fluid) temperature of the collector, °C;
A – collector surface area, m²;
η_0 – optical efficiency of the collector, - ;
ρ – collector fluid density, kg/m³;
c – specific heat capacity of the collector fluid, J/(kgK);
V – collector volume, m³;
U_L – overall heat loss coefficient of the collector, W/(m²K);
v – volumetric flow rate in the collector (assumed to be constant), m³/s;
τ_1 – time of flowing from the collector inlet to the outlet in case of permanently switched on pump, s;
τ_2 – sampling time of the measurements (time between successive measurements of the measured variables), s

Acknowledgements

The author thanks Prof. István Farkas and the Department of Physics and Process Control (SZIU) for the possibility of measuring on the SZIU collector and his colleagues, especially Dr. László Székely, in the Department of Mathematics in the Faculty of Mechanical Engineering (SZIU) for their contribution.

This study was supported by the János Bolyai Research Scholarship of the Hungarian Academy of Sciences.

References

[1.] Duffie J. A., Beckman W. A.: 2013. Solar engineering of thermal processes, 4th ed., John Wiley and Sons, New York.

[2.] Buzás J., Farkas I., Biró A., Németh R.: 1998. Modelling and simulation of a solar thermal system, Mathematics and Computers in Simulation, Vol. 48, pp. 33-46.

[3.] Kicsiny R.: 2014. Multiple linear regression based model for solar collectors, Solar Energy, Vol. 110, pp. 496-506. http://dx.doi.org/10.1016/j.solener.2014.10.003

[4.] Kumar R., Rosen M. A.: 2010. Thermal performance of integrated collector storage solar water heater with corrugated absorber surface, Applied Thermal Engineering, Vol. 30, pp. 1764-1768. http://dx.doi.org/10.1016/j.applthermaleng.2010.04.007

[5.] Buzás J., Kicsiny R.: 2014: Transfer functions of solar collectors for dynamical analysis and control design, Renewable Energy, Vol. 68, pp. 146-155. http://dx.doi.org/10.1016/j.renene.2014.01.037

[6.] Fischer S., Frey P., Drück H.: 2012. A comparison between state-of-the-art and neural network modelling of solar collectors, Solar Energy, Vol. 86, pp. 3268-3277. http://dx.doi.org/10.1016/j.solener.2012.09.002

[7.] Farkas I., Buzás J., Lágymányosi A., Kalmár I., Kaboldy E., Nagy L.: 2000. A combined solar hot water system for the use of swimming pool and kindergarten operation, Energy and the environment, Vol. I. /ed. by B. Frankovic/, Croatian Solar Energy Association, Opatija, 2000., pp. 81-88.

[8.] Etter D. M., Kuncicky D., Moore H.: 2004. Introduction to MATLAB 7, Prentice Hall, 2004, Springer.

[9.] Buonomano A., Calise F., Palombo A.: 2013. Solar heating and cooling systems by CPVT and ET solar collectors: a novel transient simulation model, Applied Energy, Vol. 103, pp. 588-606. http://dx.doi.org/10.1016/j.apenergy.2012.10.023

HUNGARIAN AGRICULTURAL ENGINEERING
N° 28/2015 15-18
Published online: http://hae-journals.org/
HU ISSN 0864-7410 (Print) / HU ISSN 2415-9751(Online)
DOI: 10.17676/HAE.2015.28.15

PERIODICAL OF THE COMITTEE OF AGRICULTURAL AND BIOSYSTEM ENGINEERING OF
THE HUNGARIAN ACADEMY OF SCIENCES
and
SZENT ISTVÁN UNIVERSITY
Faculty of Mechanical Engineering

EXAMINATION THE EFFECTIVENESS OF FLOW CONTROL IN A SOLAR SYSTEM

Author(s):
P. Víg – I. Seres

Affiliation:
Department of Physics and Process Control, Szent István University, Páter K. u. 1., Gödöllő, H-2103, Hungary

Email address:
vig.piroska@gek.szie.hu, seres.istvan@gek.szie.hu

Abstract

The present paper examines the benefits of the flow rate control compared with traditional on-off switch-control in case of solar water heating system. The optimal volumetric flow rate of the solar fluid depending on the radiation and the stored water temperature. This flow rate is realized with controlling the frequency of the pump by an ALTIVAR 31 frequency inverter. The paper presents and summarizes the calculated results based on measurement data obtained during the operation with these regulations.

Keywords

solar energy, solar thermal system, flow rate, control, efficiency

1. Introduction

In the recent times the photovoltaic energy utilization of the solar applications get bigger importance due to the improvement of the photovoltaic technology and to the coming out of cheap PV modules. The guaranteed grid access and the feed-in tariffs help the spreading as well. Due to the spread of the PV technology, the development of the efficiency of the solar thermal systems get smaller significance. The present work is dealing with the improvement of a solar thermal system by examining the efficiency of a flow rate control method.

The dependence of the efficiency of the solar thermal system on the flow rate was investigated by a lot of researcher. In the homepage of the Build it Solar [1] there is an analysis of the efficiency dependence of flat plate collectors as a function of the flow rate. They concluded, that the bigger flow rate cause bigger efficiency, however they stress, that for the bigger flow rate higher pump power and – for keeping the laminar flow – bigger tube diameters have to be used, which increases the installation and maintain costs. Furbo and Shah [2] for SDHW systems determined an 0.2 to 0.3 liter/min/m^2 solar collector ideal flow rate for the optimal operation.

Kar [3] determined the optimal flat-plate collector mass flow rate by maximizing the exergy delivery of the collector as the objective function. Badescu [4] gave an optimal control of flow in solar collector system in case of fully mixed water storage tanks. Yousefi et al. [5] stated, that in case of low flow rates, by increasing the flow rate, the collector and the system efficiency is increased as well.

The control is an important influencing factor from the aspect of the efficiency of a heating system. In the modern heating systems the flow rate control of the heating circuit pump (intelligent pump) is spreading for achieving the optimal heating medium temperature. This indicated the idea, that we should study the effectiveness of the flow control for a vacuum tube system, too.

Víg and Farkas [6] studied the vacuum tube collector efficiency vs the pump flow rate, and they concluded, that the optimal values, which are function of the stored water temperature and the solar radiation not necessarily can be achieved at the maximum flow rate. That is it can be useful to operate a system at optimal flow rate under the given conditions, such as to establish a flow control.

The possible advantages of such a control was studied by Péter Vladár [7] in his diploma thesis by using TRNSYS models. The PID control was calculated to results maximum 20% energy surplus. These reassuring results gave basics for realizing the flow control and checking the theoretical results in practice.

2. System description

The studied system is installed in the Department of Physics and Process Control, Szent István University, Gödöllő, Hungary. On the site of the solar system a meteorological station was installed, too. The collector of the system includes 15 vacuum tubes, the absorber area (noted by A in the model) is 1.22 m^2. The solar fluid collector outlet temperature is noted by Tout. The area of solar loop inside heat exchanger is 1.4 m^2, the specific heat capacity of solar fluid is 3194 J/kgK.

The volume of the solar storage tank is 300 l, it is covered with 5 cm thick insulating layer. The stored water temperature can be measured in 3 layers: bottom (Tsb), middle (Tsm), and top (Tst), the average water temperature is Ts. The measurement of solar radiation is located in the plane of the collector with pyranometer. Figure 1. shows the vacuum tube collector and storage tank of the system.

The flow rate control in the solar loop was realized with control of existing pump of the system by installing an ALTIVAR31 frequency inverter. The regulation is based on the measured data in every 10 s, the data are recorded to the hard drive. The essence of on-off switch-control: if the difference between temperature of solar fluid in the collector outlet and the stored water in the

middle layer of the storage is at least 5 °C, the pump works with maximum power, otherwise switched off, while during the flow rate control, if this temperature difference less than 5 °C, the flow rate decreases linearly.

During the measurement of temperatures Pt100 resistance thermometer and thermocouple were used. The solar fluid is polipropylen-glycol and distilled water in 50-50%. The pump normally working with 3 constant power: 35, 40 and 50 W. The main parts of control system, the pump and the frequency regulator are shown in Figure 2.

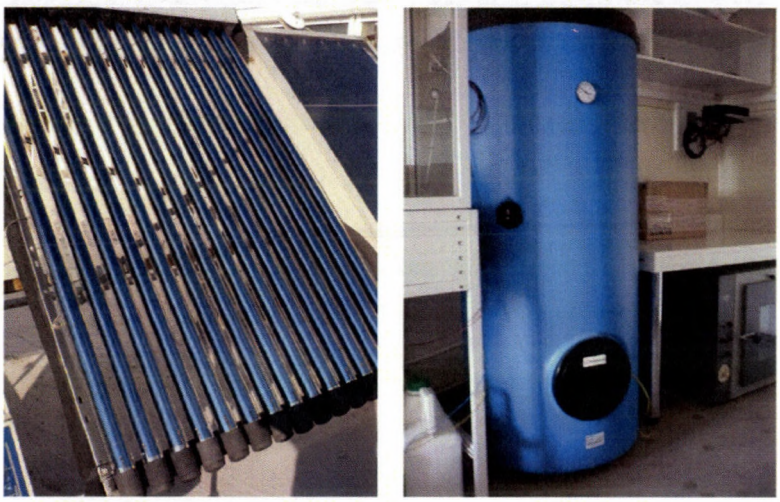

Figure 1. Main parts of the system: collector and storage tank

Figure 2. Pump and frequency regulator

The installation of the regulator in the system, the development of communications with data acquisition ADAM modules and the Labview program which generates the control signal are detailed in another paper.

3. Data gathering

Two system operations are compared: the on-off control and flow rate control. The necessary measurement data were gathered from 1 July 2015. Till August 10 the system worked with on-off control and from August 11 it was operated with flow control.

The flow and heat losses of the collector and the solar tank are negligible due to the good insulation. The heat losses in the long (2 * 25 m) tubing between the collector and the storage are considerable, but as these losses are very similar for the two compared cases, during the comparison they are not important.

It is important to mention for the stratification of the water in the tank, that the warm solar liquid enter in the middle of the tank to the heat exchanger and it exist at the bottom of it. Because of it the temperature of the middle layer temporarily can be higher than the upper layer temperature during continuous operation. The layer temperatures are normalized for the end of the day.

Figure 3 and Figure 4 show typical measurement data rows for the two different control. Figure 3 shows the results of the flow control in case of the variably cloudy day. The upper part of the figure shows the collector outlet temperature (Tout), and the temperatures in the 3 layers of the storage tank. The second graph shows the solar radiation, the third shows the control signal (Tout-Tsm) and forth shows when the pump was on in 7th of September.

It can be seen well, that when the solar radiation is fluctuating, the solar liquid temperature for only short time was higher with 5 degrees than the temperature of stored water in the middle layer. In addition the flow rate control decreased the effect of the fluctuations in the radiation.

Figure 4 shows the graphs of the typical example for the on-off switch-control, the graphs type and markings are similar than Figure 3.

Transient time (tTR) is the sum of minutes, when the pump on-off status changing in the next minute. It can be seen, that, this indicator is short during the flow rate control and remarkable in case of on-off control.

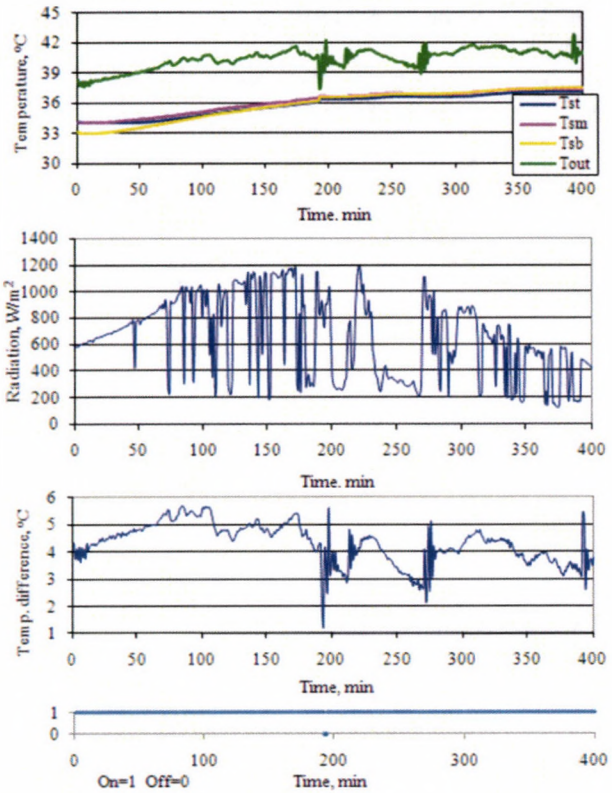

Figure 3. Results with flow rate control

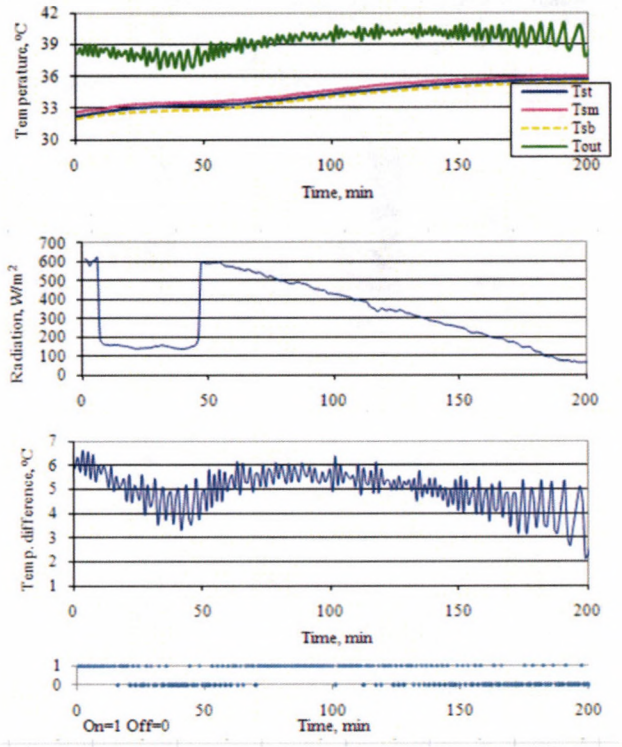

Figure 4. Example for on-off control (2015. 08. 06.)

4. Analysis of the measurement results

For the numerical comparison of the efficiency of the controls, the following concepts and relationships have been used:

Daily working time (t_w) is the time between the first on and last off switch of pump in the day.

Not transient part (noTR):

$$noTR = (1 - \frac{t_{TR}}{t_w}) * 100$$

Daily collected heat energy:

$$Q = c_v * (T_{sE} - T_{sB}) * m + \sum c_v * \dot{m}_L * (T_{st} - T_{sb}) * \tau$$

where c_v is specific heat capacity of water, the stored water average temperature at the end (T_{sE}) and at the beginning (T_{sB}) of day, m=300 kg, the mass of stored water, $\dot{m}_L$ is mass flow of hot water load, τ is unit of time (one minute).

The efficiency of the system is the rate of daily gathered solar energy and energy come from solar radiation (I_t):

$$\eta = \frac{Q}{\sum I_t * A * \tau}$$

For quantifying the thermal stratification the dimensionless quantity (ST) has been introduced where n is the number of time units which the summary applies. This value in case of mixed storage is 0, and growing when improving the stratification.

$$ST = \frac{1}{n} \sum \frac{T_{st} - T_{sb}}{T_s} * 1000$$

Pump daily average power:

$$P_{p,avg} = \frac{1}{n} \sum \frac{\dot{m}}{\dot{m}_{max}} * P_{max}$$

where $\dot{m}$ is the actual mass flow, $\dot{m}_{max}$ is the maximal mass flow in the collector loop.

Results

For the comparison of the two control method, daily periods without hot water consumption were used, and the comparison was made between such intervals, when the average radiation was almost the same (548.3 W/m² ill. 552.5 W/m²) and the temperature of the initial temperature of the stored water was about the same, too. The values are presented in Figure 5.

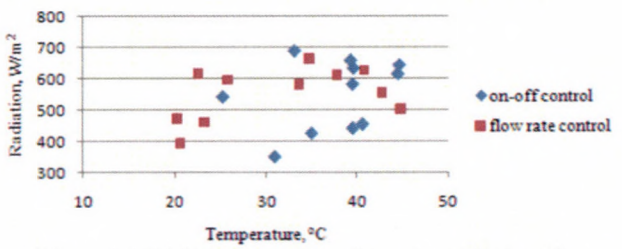

Figure 5. Initial temperatures and average radiations for calculations

In Figure 6. the values of the efficiency, the thermal stratification and the dimensionless ST and the pump working time rate is shown. The numerical values of the graphs are presented in Table 1. For the comparison of the pumps energy need, some data can be seen about ratio of the working time of the pump compared to the total time.

The numerical data show, that in the investigated time period, under the given conditions the system efficiency was 13% higher, and the thermal stratification by 64%, and the length of non-transient periods by 37% was higher under the flow control, compared to the On-Off switch method.

It can be concluded, that the daily working time significantly was increased (by 50 %), but the pump power just went up by 5.3 W.

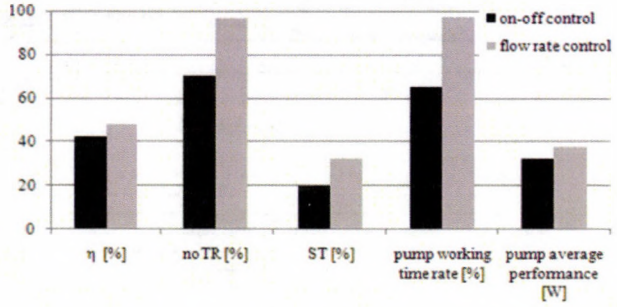

Figure 6. Results for comparison the two controls

Table 1. Calculated results during several controls

	On-off control	Flow rate control	Surplus [%]
η, [%]	42.43	48.03	13.2
ST, [-]	19.87	32.63	64.2
No TR, [%]	70.37	96.72	37.4
Pump working time rate, [%]	65.35	97.45	49.1
Pump average power, [W]	32.66	37.93	16.1

6. Conclusions

It can be stated, that the results, achieved from the measurement data, agree well with the results of the modelling [7]. The advantages of the flow control against the on-off switch can be recognized mainly during the morning system start, during the evening system shutdown and during cloudy conditions or when the water temperature is higher in the tank.

The aim of the paper was to determine if there is measurable difference in the efficiencies for the two control methods. To do this regulation by an intelligent pump can cause high expenses. To reduce the costs we borrowed a frequency inverter, which is a multifunctional, wide range usable device. For a solar system the pump power is relatively low (40 - 50 W), a much simpler and cheaper solution can be done as well, and as in this case the cost of the installation and operation is much lower, so it is worth to install.

As a continuation of our work, the building and the installation of such a circuit is planned.

Acknowledgements

The authors would like to thanks the help of the Schneider Electric Hungária Villamossági Zrt for the free replacement of our faulted frequency regulator, and in this way supporting the research.

References

[1.] Builditsolar, 2014. Determining collector flow rate, http://www.builditsolar.com/References/ColFlowRate.htm

[2.] Furbo S., Shah L. J. 1996. Optimum solar collector flow rates, EuroSun '96, München, DGS Sonnenergie Verlags, pp. 189- 193.

[3.] Kar A. K.: 1989. Exergy optimization of flow rates in flat-plate solar collectors, International Journal of Energy Research, Volume 13, Issue 3, pages 317–326. http://dx.doi.org/10.1002/er.4440130308

[4.] Badescu V.: 2008. Optimal control of flow in solar collector system with fully mixed water storage tanks, Energy Conversion & Management, 49, pp.169-184. http://dx.doi.org/10.1016/j.enconman.2007.06.022

[5.] Yousefi T., Veysi F., Shojaeizadeh E., Zinadini S.: 2012. An experimental investigation on the effect of Al2O3–H2O nanofluid on the efficiency of flat-plate solar collectors, Renewable Energy, Volume 39, Issue 1, March 2012, pp. 293-298. http://dx.doi.org/10.1016/j.renene.2011.08.056

[6.] Víg P., Farkas I.: 2013. Effect of volumetric flow rate on energy production of vacuum tube solar collector, Mechanical Engineering Letters, vol.10, pp. 102-110.

[7.] Vladár P.: 2014. Thesis, Faculty of Mechanical Engineering, Szent Istvan University, Gödöllő, Hungary

HUNGARIAN AGRICULTURAL ENGINEERING
N° 28/2015 19-22
Published online: http://hae-journals.org/
HU ISSN 0864-7410 (Print) / HU ISSN 2415-9751(Online)
DOI: 10.17676/HAE.2015.28.19

PERIODICAL OF THE COMITTEE OF AGRICULTURAL AND BIOSYSTEM ENGINEERING OF
THE HUNGARIAN ACADEMY OF SCIENCES
and
SZENT ISTVÁN UNIVERSITY
Faculty of Mechanical Engineering

THE USE OF BIOMASS FOR ELECTRIC POWER PRODUCTION IN POLISH POWER PLANTS

Author(s):
J. Piechocki – P. Solowiej – M. Neugebauer

Affiliation:
Department of Electrical, Power, Electronic and Control Engineering, University of Warmia and Mazury in Olsztyn, Oczapowskiego 10, 10-736 Olsztyn, Poland

Email address:
jpt@uwm.edu.pl, pit@uwm.edu.pl, mak@uwm.edu.pl

Abstract

More than 95% of electric power in Polish power plants is produced from coal. This results in the emissions of large volumes of CO2 into the atmosphere, hence in some power plant alternative methods of electric power generation are being implemented. One of the many possible solutions is to produce electric power from biomass. There are two biomass options available for the power plants. One is the cogeneration of electricity from biomass and coal, and the second is firing only the biomass in the boilers.

Those solutions may be effectively applied to the production of electric power in north-western Poland, as it is a region with large forest areas and strong agricultural production. One example is the power plant in Białystok which includes a power block that produces energy only from biomass (wood), and the power plant in Ostrołęka with a cogeneration power block. This report compares those solutions from various perspectives.

The material presents a new strategy of use of different energy sources in order to optimise the energy management in the electric power system. The objective of the energy management optimisation strategy in the electric power system is to balance the capacity for the electric power production from biomass with the consumers' demand.

Keywords

biomass, electric power, power plant, cogeneration

1. Introduction

The organisms and their environment enter into a myriad of interactions which lead to the creation of certain ecosystems. A change in the environmental conditions disrupts the functioning of those systems and may result in adverse changes for the entire environment. The changes of the environmental conditions are triggered mainly by human activity. Therefore, the activities of humans, mostly business-related, must be conducted in such way as to minimize its environmental impact. This necessitates the reduction of the volume of pollution related to the production of goods necessary for human needs that is released into the environment. As evident from the experiences thus far and the conducted studies, the highest contributors to the emissions of pollution into the environment are the technologies related to the production of energy in various forms.

The limited conventional energy sources and the problems arising from the nuisance of the energy production with the use of such conventional sources, in particular the environmental hazards related to the combustion of fossil fuels, drive the search for other, alternative solutions. The increasing application of unconventional energy sources, especially the renewable ones, opens up the possibility of avoiding the aforementioned nuisances and hazards. In recent years, research on the use of such alternative energy sources has intensified around the world. The key factor is the rising awareness in the society that ca. 2/3 of the pollution in the environment is directly and indirectly related to the mining and combustion of conventional energy carriers, most of all coal. It should be pointed out here that the global environment pollution has already reached its limit, therefore it is crucial to start cleaning the environment, which can be achieved i.a. by broad application of renewable energy sources. This issue has been discussed on numerous occasions in the reports of international organisations dealing with the philosophy of rational consumption of Earth's energy resources. With state-of-the-art technologies of producing energy from renewable sources, the economic relation is continuously improved as compared to conventional energy sources. That being said, it should be emphasized that the costs of the latter do not include the losses related to environment cleaning.

For environmental reasons, the structure of use of the primary carriers of energy from conventional sources plays an essential role. Compared to Western Europe, Poland is characterised by the dominant position of coal, which amounts to 76% in comparison to ca. 20% in Western European countries. In Western Europe, the structure of use of primary carriers of energy from conventional sources is dominated by oil, which amounts to 45%, with below 15% in Poland. Similarly high are the shares of natural gas and nuclear power. In Poland, the latter is absent altogether from the national energy balance, while the former contributes below 8%.

The result of the structure of use of the primary carriers of energy from conventional and alternative sources is the annual level of emissions into the atmosphere. The data on emissions with respect to the unit of area of the country are provided in Table 1.

The economic losses arising from the emissions caused by the consumption of fuels aggregate to several dozen percent of

the annual national income. The comparison of the economic impacts of the emissions into the atmosphere from the sectors of economy based on the consumption of fuels is provided in Table 2.

Table 1. Annual emissions into the atmosphere per the unit of area of the country [Mg/km^2]

Country	Dust	SO_2	NO_x	CO_2
Poland	7.68	12.61	4.73	1,472
France	0.69	2.80	4.33	184
Japan	1.70	2.87	3.76	641
Germany	2.30	8.19	12.30	824
USA	0.74	2.23	2.13	132
Switzerland	0.55	2.39	5.38	289
Great Britain	0.95	6.02	9.52	664

Table 2. Economic losses arising from the emissions caused by fuel use [%]

Type of pollution	Sector of economy					
	Power industry	Metallurgy	Other industries	Municipal services	Transport	Other technologies
SO_2	25.5	2.0	5.8	11.2	1.2	6.2
NO_x	13.9	11.0	11.0	3.2	10.8	1.8
Dust	2.4	0.5	1.7	2.8	0.0	0.0

Electric power production from biomass in the power plants

Currently, the largest share in the energy production from renewable sources in Poland is generated by biomass which is an alternative, renewable energy source used to produce biofuels. The biomass itself may be used as biofuel, e.g. in the form of hay, wood, etc., or serve as the raw material for the production of other processed biofuels, e.g. rapeseed used in the production of biodiesel, potatoes or sugar cane in the production of bioethanol, or various organic materials, including waste, used to produce biogas.

In the power plants, various types of biomass are used in the production of electric power.

In the combined heat and power station in Białystok, one of the four power blocks with the capacity of 55 MW is fitted with a modernized OP-140 boiler, used solely to fire biomass mainly in the form of wood waste from forest plantations and wood processing, to produce electric power and heat for the city. The annual electric power production capacity is 150,000 MWh. Figures from 1 to 5 illustrate the elements of the power block that uses biomass to produce electric power.

Figure 1. The system of feeding the biomass into the power block

Figure 2. The hopper supplying the system of biomass feeding into the boiler

Figure 3. Power block fed with biomass

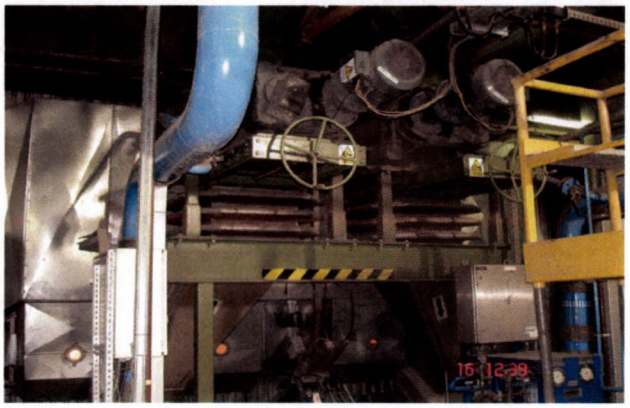

Figure 4. The system of direct feeding of the boiler with biomass

Figure 5. The storage yard for the biomass fed into the system supplying the power block.

In the power plant in Ostrołęka, one of the power blocks with the total capacity of 200 MW is used to cogenerate electric power from co-firing of biomass and mineral coal. The biomass share in the process in 10% and the composition of the biomass is very diverse, including components from the forest plantations, agriculture and food industry, as well as from special energy crops. The system enables the annual additional production of the so-called "green electricity" in the capacity of ca. 86,000 MWh, at the same time reducing the emissions of carbon dioxide from fossil fuels by 60,000 Mg due to the reduction of the coal consumption by 35,000 Mg, and reducing the emissions of sulphur dioxide by 300 Mg; the system uses ca. 65,000 Mg of biomass. Figures from 6 to 9 illustrate the elements of the cogeneration system that uses biomass to produce electric power in the power plant.

Figure 6. The biomass feeding system for the production of coal and biomass mixture for the cogeneration process.

Figure 7. The system of boiler feeding with the coal and biomass mixture

Figure 8. Production of the coal and biomass mixture for the cogeneration process

Figure 9. The storage yard for the coal and biomass for the production of the coal and biomass mixture for the cogeneration process

2. Conclusion

The production of electric power from biomass in the power plants has a number of advantages:

- it is environmentally friendly,
- it reduces the volume of waste, fly ash, slag, etc.,
- it allows the remains and waste from forest and agricultural production, and the food industry to be re-used,
- it increases the availability of energy from renewable sources,
- it drives the development of the market of biomass of plant origin,
- it enables establishing energy crops that are exempt from the crop limits,

– it drives the growth of small businesses in rural areas,
– it provides a steady recipient for the biomass suppliers.

The production of the production of electric power from biomass in the power plants also makes it possible to formulate a new strategy of using diverse energy sources to optimize the energy management in the national electric power system. The optimization of energy management in the electric power system balances the capacity for the electric power production from biomass with the available biomass resources and the consumers' demand.

References

[1.] Piechocki J., Neugebauer M., Sołowiej P.: 2011. „Potencjał energetyczny odnawialnych źródeł energii i możliwości jego wykorzystania dla wybranego regionu województwa warmińsko-mazurskiego"; Inżynieria Rolnicza 3(128); s167-174, ISSN 1429-7264;

[2.] Sołowiej P., Nalepa K., Neugebauer M.: 2008. Analiza energetyczno-ekonomiczna produkcji energii cieplnej w kotłowniach na zrębki drewna. Inżynieria Rolnicza 2 (100) s.263-268, ISSN 1429-7264.

[3.] Piechocki J., Sołowiej P., Neugebauer M.: 2011. „Przewidywane możliwości wykorzystania potencjału energetycznego odnawialnych źródeł energii dla wybranego regiony województwa warmińsko-mazurskiego". Inżynieria Rolnicza 5 (130), s. 237-242. ISSN 1429-7264.

HUNGARIAN AGRICULTURAL ENGINEERING
N° 28/2015 23-24
Published online: http://hae-journals.org/
HU ISSN 0864-7410 (Print) / HU ISSN 2415-9751(Online)
DOI: 10.17676/HAE.2015.28.23

PERIODICAL OF THE COMITTEE OF AGRICULTURAL AND BIOSYSTEM ENGINEERING OF
THE HUNGARIAN ACADEMY OF SCIENCES
and
SZENT ISTVÁN UNIVERSITY
Faculty of Mechanical Engineering

AN ASSESSMENT OF CEREAL STUBBLE BURNING IN TURKEY

Author(s):
Z. Akman

Affiliation:
Suleyman Demirel University Faculty of Agriculture Department of Field Crops 32260 Isparta, Turkey

Email address:
zekeriyakman@sdu.edu.tr

Abstract

In Turkey, cereals are approximately 14 million hectares of sowing area by the 2014 data, about 28 million tons of the total grain production. Four cereal crops are produced on a larger scale: barley, oats, wheat and rye. Leaves, stems and roots of cereal grains, left in the field after grain harvest, is called cereal stubble. Stubble is burned widely in Turkey. Çukurova and Central Anatolian are the regions where the most intense burning stubble. Among the factors that encourage the burning process, soil preparation is difficult for the second crop will be planted after the main product cereals especially in the regions where the second crop of agricultural structures. In this study, it was evaluated the environmental results and the reasons of stubble burning, and it was compared the difference between stubble burning and leaving cereal residues in the field. It was also focused on stubble burning is necessary conditions in Turkey

Keywords

cereal, stubble burning, Turkey

1. Introduction

Turkey is the largest grain producer in the Middle East. Agricultural crops produced in Turkey are mainly wheat and barley. As known, cereal straw is the stem of the plant after the rest of the spike. Leaves, stems and roots of cereal grains, left in the field after grain harvest, comprise from 50 to 75 percent of the total cereal boimass produced by a season's grain crop. This cereal stubble that is left to accumulate on the ground reduces soil erosion by buffering the impact of raindrops and reducing wind speed at the soil surface. Cereal stubble also increases the water available in the soil for plant use by enhancing rainfall infiltration and reducing evaporation losses. Cereal straw accumulation and incorporation in the long term increases organic matter inputs into the soil, reduces the loss of plant nutrients and increases soil biological activity. Each type of residue makes different contributions to this process. However, despite these benefits, stubble burning is applied widely in Turkey. Çukurova and East and Central Anatolian regions are the regions where the most intense burning stubble. In Turkey, recent data showed that about 12.5 million ha area allocated to grain 'is. Sayın [1] and Korucu [2] reported that average of 1.5 - 2 tons / ha of stubble and cereal residues burned and in total 3.7 million hectares burned every year in Turkey.

In these researches, it was evaluated the environmental results and the reasons of stubble burning, and it was compared the difference between stubble burning and leaving cereal residues in the field. It was also focused on stubble burning is necessary conditions in Turkey.

2. Reasons for farmers stubble burning

Among the factors that encourage the burning process, soil preparation is difficult for the second crop will be planted after the main product cereals especially in the regions where the second crop of agricultural structures. Much more labor, energy and time are needed to decompose of the cereals in the soil. However, there is a huge delay even one day delay in the second crop agriculture. Therefore, farmers are becoming more willing to burn. Other reasons for burning stubble in the field can be listed as follows:

1. Easier and less costly removal of cereal stubble and residues in the soil,
2. Controlling or eliminating fungal diseases, weed seeds, and insect pest eggs,
3. Soil processing easier and less frequent.
4. Fire also quickly recycles potassium, phosphorus, and other minerals back to the soil, thereby reducing the quantity of agro-chemicals that are needed on fields.
5. Lack of sufficient information on the results of the farmer's stubble burning
6. The idea that the burning of stubble improve soil fertility

Figure 1. Firefighting efforts, which took place during the burning stubble in Aydin province of Turkey

Also in the moist and cold of soil (eg Black Sea Region), soil organic material decomposition process takes longer. This situation negatively affects their agricultural activities of the farmers, and tillage and seedbed preparation is quite late. Therefore, in regions with cold and humid climate it is becoming mandatory stubble burning (Figure 1).

3. Environmental and agricultural consequences of stubble burning

Anatolia is a land where agriculture first time in the world. Rapid loss of soil due to erosion of this is regrettable. Stubble burning promotes erosion of stubble burning, adversely affect the soil moisture and temperature values. Soil erosion is a very important environmental problem of Turkey. According to statistics, an average of 743 million tons of soil are lost every year. 63% of the national territory is seen severe erosion [3]. One of the main benefits of stubble retention is reduced soil erosion. Retaining stubble decreases erosion by lowering wind speed at the soil surface and decreasing run-off. To minimise erosion approximately 50 % ground cover is required and adequate stubble needs to be maintained for 6–8 weeks following seeding [4].

Grain stubble and crop residues is a major source of soil organic matter in Anatolia. Protecting the stubble in terms of enhancing water retention ability and soil mechanical resistance is important. Cereal growing lands in which organic matter contents were poor even 40 years ago, have been ignored for decades and treated like a "stepchild" in respect to organic material application that generally suggested for vegetables and horticulture production. The long term effects of soil erosion, stubble burning, fallow and mouldboard plough tillage for years have increased the bill of this ignorance and brought the soils into "hungry" and "ill" position for organic matter content. Since soils with low organic matter content can not hold sufficient water, they can not have available conditions for planting, germination and emergence, growth and development. As known, grain stubble and crop residues is a major source of soil organic matter. Protecting the stubble in terms of enhancing water retention ability and soil mechanical resistance is important. Therefore, soils having these unfavorable conditions resist to farmers and production, limit success of cereal research and researchers, and show danger signals for future. Retaining stubble increases the input of carbon to soil. Stubble is approximately 45 % carbon by weight and therefore represents a significant input of carbon to soil. When stubble is retained, the greater inputs of organic carbon to soil increase its biological fertility. Microorganisms in soil require organic carbon to obtain the C, nutrients and energy they need to live. Labile carbon is a particularly important form of organic carbon for soil microorganisms. Management practices that increase inputs of organic carbon to soil, such as retaining stubble, can increase the number of microorganisms in soil and also cause them to be more active. Another advantage of retaining stubble is that it increases soil water content by decreasing run-off and increasing infiltration [5].

When considered in terms of air pollution issues, the scientific literature contains a great amount of information on the emissions of atmospheric pollutants from burning in various vegetation types worldwide. Field burning is a process of uncontrolled combustion during which carbon dioxide (CO_2), the principal product of the combustion, is emitted into the atmosphere along with carbon monoxide (CO), un-burnt carbon (as well as traces of methane i.e. CH_4), nitrogen oxides (NO_x) and comparatively less amount of sulphur dioxide (SO_2) [6].

Figure 2. Stubble fires due to many wild animals are injured or die.

4. Conclusions

Stubble burning is a real environmental problem (Figure 2). Stubble fire on the products in neighboring fields, the orchards, the surrounding trees and fences, telephone poles, nearby settlements and particularly in forests, is particularly damaging to the woods and wooded area. Uncontrolled burning is also the leading cause of the forest fire. Stubble fires due to many wild animals are injured or die. Stubble burning, in addition to air pollution reduces visibility on roads due to the rising smoke from time to time, which leads to traffic accidents. As described above, stubble burning soil physical, chemical and biological impact negatively on the capacity. Also considering that Turkey is poor in terms of soil organic matter, stubble burning is not a rational application. Further increases the risk of erosion because it reduces the physical resistance of the soil stubble burning. To consistently get more product per unit area in both today and for the future, the main purpose of agricultural production must be improve the efficiency of our productive agricultural land and to keep in this condition.

As a result, there is little organic matter in the soil, which is more than the risk of erosion, it is difficult to controlled burning, which rapidly decompose in the field of stubble, stubble should not be burned.

References

[1.] Sayın S., 1989. Çeşitli yönleri ile anızların yakılması. Köy Hizmetleri Ankara Araştırma Enstitüsü Yayın No. 165154.

[2.] Korucu, T., 2002. Çukurova bölgesinde II. ürün mısırın doğrudan ekim olanaklarının araştırılması. Ç.U. Fen Bilimleri Enstitüsü, Kod No. 662, Adana, Türkiye.

[3.] Doğan O.: 2011. Türkiye'de Erozyon Sorunu Nedenleri ve Çözüm Önerileri, Bilim ve Aklın Aydınlığında Eğitim, S. 134, Nisan 2011, ss. 62-69.

[4.] Leonard, 1993. Managing for stubble retention. Bulletin 4271, Department of Agriculture Western Australia.

[5.] Carson J., Flower K.: 2015. Benefits of Retaining Stubble – Western Australia. Soilquality.org., 2015.

[6.] EPA 2003. Cereal-Grain Residue Open-Field Burning Emissions Study. Washington Department of Ecology, Washington Association of Wheat Growers, U.S. Environmental Protection Agency, Region 10. Prepared by: Air Sciences Inc., 421 SW 6th Avenue, Portland. Project No. 152-02, July 2003.

HUNGARIAN AGRICULTURAL ENGINEERING
N° 28/2015 25-29
Published online: http://hae-journals.org/
HU ISSN 0864-7410 (Print) / HU ISSN 2415-9751(Online)
DOI: 10.17676/HAE.2015.28.25

PERIODICAL OF THE COMITTEE OF AGRICULTURAL AND BIOSYSTEM ENGINEERING OF **THE HUNGARIAN ACADEMY OF SCIENCES** and **SZENT ISTVÁN UNIVERSITY** Faculty of Mechanical Engineering

THE COST BENEFIT ANALYSIS OF LOW-CARBON TRANSPORTATION DEVELOPMENT OPPORTUNITIES FOR THE 2020-2030 EU PROGRAMMING PERIOD

Author(s):
Cs. Fogarassy[1] – B. Horvath[1] – A. Kovacs[2]

Affiliation:
[1]Climate Change Economics Research Centre, Szent István University, Gödöllő, Hungary
[2]Department of Operations Management and Logistics, Szent István University, Gödöllő, Hungary

Email address:
fogarassy.csaba@gtk.szie.hu, horvath@carbonmanagement.hu, kovacs.attila@gtk.szie.hu

Abstract

Within the European Union's climate policy, transportation qualifies as one of the most significant sectors since it is responsible for 20% of total GHG (greenhouse gas) emissions. In the 2005-2020 period, the EU is expected to emit a total of 90 MtCO2e. Although this figure qualifies as a 12% decrease in terms of total volume, 80% of it cannot be regarded as cost efficient; in fact, the majority of these emissions fall into the highest CO_{2e} avoidance cost category within the European Union. However, Hungary is in an exceptional situation, as the cheap potential for reducing emissions is significantly higher than the EU average. Hungary is presently one of the countries best performing its 2020 climate policy targets, since its GHG emissions resulting from past years' production is still far behind the "emission baseline" threshold defined on the basis of production in the 1980's. Due to slow and controversial development, Hungary's vehicle park will continue to show a significant dependency on fossil fuels (gasoline, diesel) in 2030. It should be noted that this situation could endanger the long term (2050) commitments for GHG reductions. The aim of the present study was to examine the environmental and financial effects of development projects that contribute to the restructuring of the transport sector and the attaining of climate policy targets as well as implementing these developments in the most cost effective manner possible.

Keywords

low-carbon, green transport, cost-benefit analysis, climate policy, transport strategy

1. Introduction

According to forecasts, Hungary will continue to show a large degree of dependency on fossil fuels (gasoline and diesel) by 2030 [1]. The international studies performed regarding the sector provide a good indication of the fact that the sector's structure does not presently support climate-friendly or low carbon development principles [2]. The reason is that most investments will never enjoy a return (due to under-utilization and the structural defects of the public transport sector), causing possible significant damages and negatively effecting welfare [3, 4]. The present study uncovered the parameters of the possibilities for Hungary's transport sector for 2020 and 2030. Based on the previous analyses performed by the authors, the most important sectoral indicator of the reduction of transport emissions is the change in the ratio of public transportation to private transport [5] as well as the general structure of goods transport [6]. Subsequent studies will therefore deal with the possible tools for maintaining the level of public transportation at its current level of 20-21% despite of decreasing tendencies, and how such measures can provide a financial return [7, 8]. The most important issue in the case of goods transport is identifying the modes of transport that are worth developing in the interest of simultaneously attaining both emissions reduction and increases in cost efficiency without incurring additional costs for society, for example through the amortization of the road system at an increased rate [9, 10]. It can be established based on previous analyses that the cost effectiveness of large investments within the sector is often questionable [11, 12]. Using the developments implemented in Western Europe, the present study attempts to outline development concepts that build on a greater degree of social activity but emphasize smaller technological investments. An example is the inclusion of electric mopeds in personal transport, which would result in decreasing both GHG emissions and the use of vehicles.

2. Materials and methods

The fundamental aim of the study was to develop a system that is suitable for the multipurpose assessment of the effects of interventions at the national economy level. One of the bases of the model is the cost-benefit analysis; the other is multi-targeting. There are several solutions available for managing the latter, but in general they trace decisions back to a simple, single-target decision [13]. The simplest solution for managing multi-targeting is selecting one target from the available targets while considering the remaining targets to be given in the future and to then run the model. The model results are saved and the above steps are repeated for each of the targets previously considered given. This results in a set of solutions which, if illustrated and analyzed, enables the selection of the solution or set of solutions.

Based on the above, the study is based on the following cost-benefit analysis equation (1) [14]:

$$AI_{pv} = -\underbrace{(IC - DI)}_{\text{Decision on development}} + \underbrace{(AS - AC)}_{\text{Effects of operations}} \pm \underbrace{IE \pm GHG_i)_{pv}}_{\text{Indirect effects}} \quad (1)$$

where:

AI_{pv} – the present value of additional income
IC – the additional investment cost of the equipment to be purchased (EUR)
DI – possible support and discounts (EUR)
AS – the additional sales revenue resulting from the additional yield or increase in quality attributed to using the given technology (EUR/year)
AC – the balance of the given technology's additional costs and its possible savings (EUR/year)
IE – the indirect economic impacts (environmental effects, effects on society) of using the given technology (EUR/year)
GHG_i – the indirect effects on emissions of using the given technology, based on the value of the decrease in GHGs as per the EU ETS quota forecast (HUF/year)
pv – present value

The essence of the CBA model developed by the authors can be found in the point entitled "Indirect effects." Similarly to the COWI model, this denotes the value of the quantified externalities generated by the project. Since the aim of the study and the target of the model is to decrease the rate of GHG emissions, the benefits arising from these effects are calculated by integrating them into this part. The basis of this is the forecast of EU ETS quota prices issued for the period ending with 2030 and prepared by the European Union, which was used to quantify the degree to which the CO_2 balance changed [15].

In order to be able to perform a credible analysis, the initial technological composition for the given sector (BAU) as included in the basic formula has to be defined. The CBA pertaining to the structural changes can then be performed on the basis of the scenarios compiled for the various periods.

The model is comprised of the following main units:
- Historical datasets
- Scenarios
- Forecasts
- Cost-benefit tables
- Results, vulnerability study

The database used in the study

The TREMOVE model developed by the Belgian organization called Transport & Mobility Leuven was used to examine the transport sector from the aspect of climate policy. Their methodology is based on a trend calculation ending with 2030, which analyses the European Union Member States' transport structure and its cost-benefit relationship. The database of the newest version (3.4) is publically available and provides enough information to effectively be applied in the cost-benefit mechanism created by the study.

3. Research results

Scenario 1: Maintaining the share of public transportation

The authors assumed two fundamental cases in their scenarios: in one, processes continue as per the present political and support systems, which literature refers to as "Business As Usual" (hereinafter BAU). In the other case, significant resources were allocated to the sector in the form of a project in the interest of achieving decreases in carbon dioxide emissions. Figure 1 shows that according to the basic scenarios (BAU), the increase in the population's kilometer demands will be accompanied by a proportionate increase in private transport, causing the percentage of public transport to fall as low 15%. Scenario 1 wishes to present the investment needs and development expectations that maintaining the present share of public transport at present levels and increasing it later on entails until 2030. The following Figure shows that public transport will not lose its share within the transport structure (in the Project version) as a result of the developments.

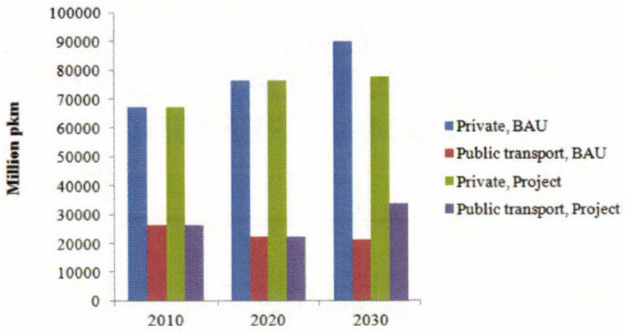

Figure 1. The structure of the transport system
Note: Own calculation based on TREMOVE 3.4 model data, 2015

Evaluation of Scenario 1

The carbon orientation matrix (Figure 2.) presents a summary of the study performed in Scenario 1. It shows the processes that took place within the sector after project implementation, during the studied period. Project placement is indicated by the grey bubble, depending on whether the return curve turned around and whether the results led to a decrease in emissions or to a surplus within the sector. The Figure precisely shows that although the emissions values were decreased, the project run by the study still ended up in the left lower quadrant. This means that the achieving of the set goals requires investments in the transport sector that will not provide a return even over the long term.

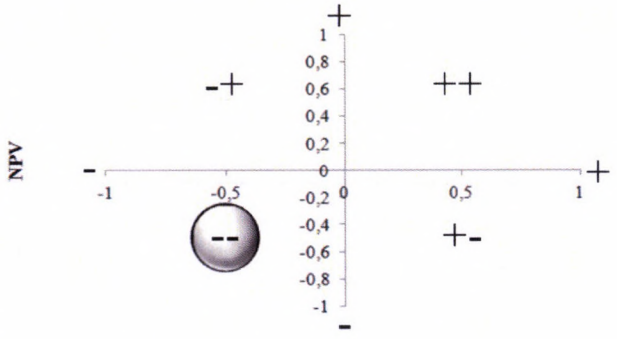

Figure 2. Scenario 1 carbon orientation matrix

Explanation
(1)- + : A project is implemented that increases emissions and the investment does not provide a return within the lifecycle.
(2)+ + : A project where the invested costs show a tendency of providing a return, but the activity itself was not suitable for decreasing GHG emissions.
(3)- - : Emissions can only be decreased with high costs on which there will be no return.
(4)+ - : Acceptable scenarios that enable CO_{2e} decreases to be attained while also providing a return on investments over a longer period of time. (Investments that are recoverable even after their lifecycles, with externalities that can change in line with political preferences.)

Scenario 2: Rerouting heavy goods transport (over 16 tons) from public roads to electric freight trains

The trend of an increasing need in the amount of kilometers travelled was applied in the case of both goods transport and passenger transport (Figure 3.); however, this case attempted to examine the changes in the shares of the various vehicles. It has been clear for some time now that decision makers are using various regulative measures in an attempt to remove transport vehicles with greater capacities (over 16 tons) from the roads as much as possible (by traffic restrictions, introducing combined transport, tolls, etc.) and that they prefer vehicles with smaller payloads [16]. However, the figure below presenting the structure of goods transport clearly shows that in regards to shipped weight, these vehicles, besides to electric freight trains, still make up the majority of this sector. That is why Scenario 2 examines what would happen if the goods they transport would not only be rerouted to vehicles with smaller capacities, but rather towards railway freight traffic. Compared to the BAU version, the project regrouped 20% of the activity of vehicles exceeding 16 tons to electric freight trains using low carbon technologies by 2030.

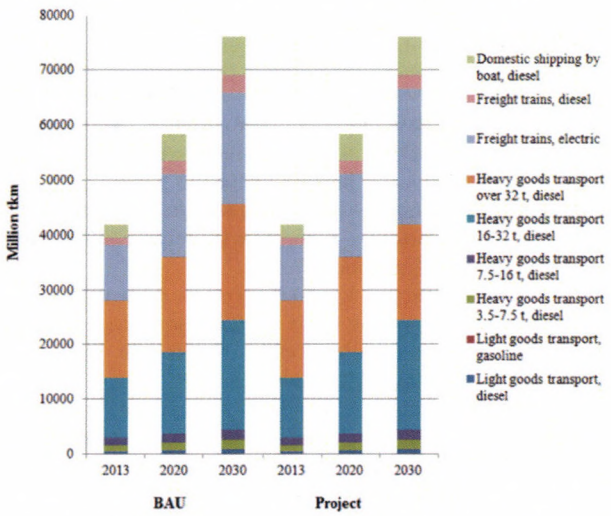

Figure 3. Breakdown of the structure of goods transport according to vehicle types and fuels; Note: Own calculation based on TREMOVE 3.4 model data, 2015

Evaluation of Scenario 2

As a summary of the above conclusions, it is worth illustrating the results in a carbon orientation matrix (Figure 4.), which shows that, similarly to Scenario 1 the present Scenario is also one that is disadvantageous for Hungary. Its location in the lower left quartile means that GHG reductions could only be attained with serious effort and – as shown by the financial indices – they would not provide a return.

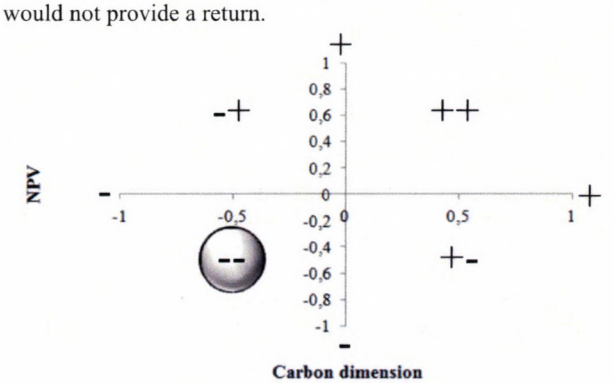

Figure 4. Scenario 2 carbon orientation matrix

Scenario 3: Increasing the share of transport by moped

In the last scenario, the study examined what would happen if, instead of orientating the BAU variation towards a sectoral approach (as in the case of public transport and goods transport), the study merely increased the rate of a new mode of transport (the moped) within individual transport. The essence of this approach is keeping the trend of the increase in the demand of number of kilometers travelled similarly to the example set by BAU, but decreasing the ratio of passenger vehicles by 5% and replacing them with mopeds (Figure 5.). Previous experience has shown that the ratio of urban to long distance traffic is one of the main areas requiring development. Urban transport is responsible for the main emissions load in this relationship [17]. Public transport naturally continues to play an important role in this scenario as well; however, it has been shown above that resources should not be invested in public transport, as investments do not provide a return in the sector. Scenario 3 was imagined within the framework of a project in which the populace replaces their passenger vehicles with mopeds, for which the state provides financial support in the form an organized program.

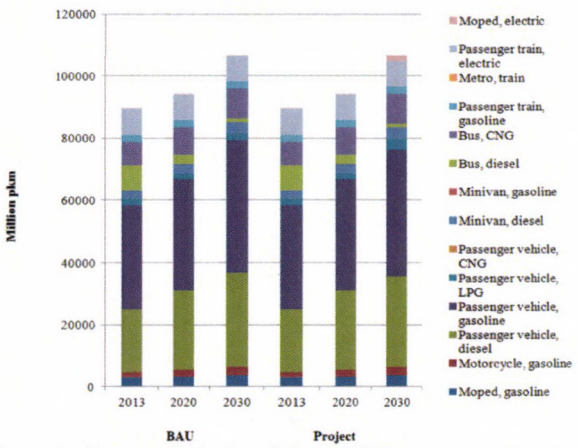

Figure 5. Changes in the breakdown of the passenger transport structure according to vehicle types and fuels until 2030
Note: Own calculation based on TREMOVE 3.4 model data, 2015

Evaluation of Scenario 3

The project implemented in Scenario 3 holds the ideal position in the carbon orientation matrix (Figure 6.), as it had positive values in both aspects (GHG reduction and financial return). Although the emissions results were not as convincing as the results attained regarding its finances, it has to be taken into account that this approach still presents a better overall picture for solving the problem of urban traffic than the public transport version studied in Scenario 1.

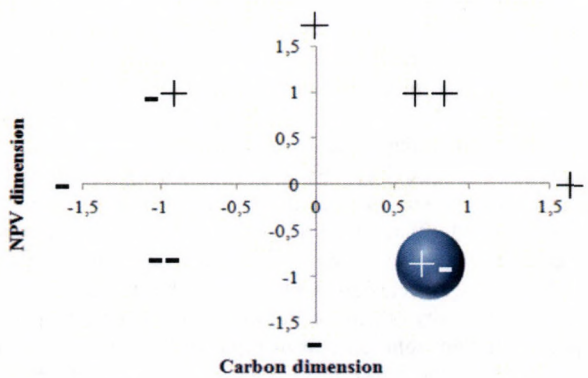

Figure 6. Scenario 3 carbon orientation matrix

As already described above, the cost and GHG effectiveness of electric mopeds can be further increased by increasing the number of kilometers they are used every day or by expanding the length of time they are used each year (6-7 months instead if 5).

4. Conclusion

The analysis consisted of running three projects that aimed at intervening in those areas of the transport sector that, based on previous experience, were considered to be the most important from the aspect of development. The introduced "carbon orientation matrices" fundamentally aim at presenting the financial and carbon reduction aspects of various developments simultaneously. The "relative carbon cost" figure (Figure 7.) was created in order to compare the various scenarios; in it, the three scenarios can be compared to each other. The logic of their placement essentially remained unchanged; however, the sizes of the bubbles play an important role in this figure. Bubble size indicates the resource requirements of the given project: what amount is equal to a savings of 1 t of CO_{2e} in the period between 2020 and 2030 (if the carbon change is negative) or to the emission of 1 t of CO_{2e} in the same period (if the carbon change is positive).

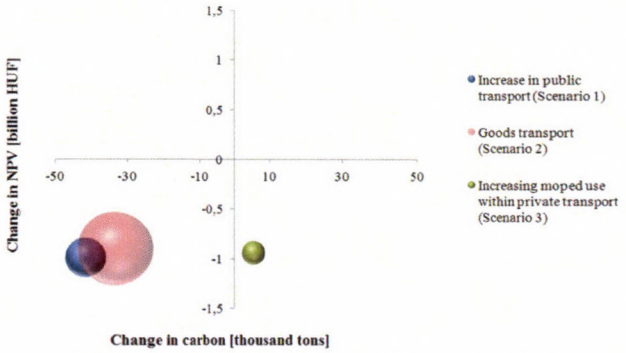

Figure 7. The relative carbon costs of the scenarios included in the analysis

The first goal (Scenario 1) was to maintain the share of public transport at its present value (20%), which the BAU forecast shows would significantly decrease until 2030 (to 15-17%). However, the cost-benefit analysis showed that the cost structure of developing the public transport system in question is not at all efficient and all invested assets are characterized by an NPV curve that does not provide a return. The summary figure also shows that although the large investment requirement is paired with actual emissions reductions, the project would still not provide a financial return within its planned lifecycle.

The second main aspect is the possible development of the goods transport system (Scenario 2), the restructuring of which has been a topic of discussion amongst professional and political decision makers for some time now. Based on the results of the CBAs, it is apparent that replacing heavy vehicles with railway transport is the worst possibility of those included in the study. Surprisingly, Scenario 2 shows a possibility where moving towards a low-carbon solution not only fails to provide a financial return, it is also less effective in reducing emissions than expected. Based on the data, the correct direction that development should take is not using the more expensive (requiring great investments and developments) method of railway freight transport to ship goods, but to continue to use smaller capacity but more mobile vehicles for transport that provide a safe solution and to replace those with low-carbon technologies (i.e. CNG or electric vehicles). An example is the practice of large European multinational companies, which use heavy goods transport vehicles (exceeding 16 tons; around 20-40 tons) to ship goods to a center and then use smaller vehicles (between 3.5-7 tons) for distribution.

During the elaboration of the electric moped sample project (Scenario 3), the authors wished to establish how the fundamental characteristics of private transport can be affected by the introduction of a relatively simple but environmentally friendly mode of transport. This clearly shows that, compared to previous scenarios, an investment that provides a return (and reduces GHGs) can be made even with the inclusion of significantly less resources. The study included a macro-level examination of the spreading of the selected technology. In the interest of better efficiency, it would be more expedient if the decision makers of large cities could consider the implementation of various large volume developments at the micro level. Based on the results of Scenario 3, it can basically be established that the maintenance and operation issues of the transport sector can be solved in a low-carbon manner (low-energy use and GHG reduction) with the use of sector-level regulations and the initiation of smaller volume projects primarily in the private sector rather than with the help of large, central investments.

References

[1.] Forster D., Okamura S., Wilkins G., Morris M., Scott P., Kuikman P., Lesschen J. P., Gardiner A., Boermans T., Grözinger J., Eichhammer W., Reichardt, K.: 2012. Next phase of the European Climate Change Programme: Analysis of Member States actions to implement the Effort Sharing Decision and options for further community-wide measures. AEA group, Harwell, United Kingdom.

[2.] Leduc G., Blomen E.: 2009. Sectoral Emission Reduction Potentials and Economic Costs for Climate Change (SERPEC-CC), Transport – Passenger cars, road freight and aviation. Ecofys, London, United Kingdom.

[3.] Hill N., Brannigan C., Smokers R., Schroten A., Essen H., Skinner I.: 2012. Developing a better understanding of the secondary impacts and key sensitivities for the decarbonisation of the EU's transport sector by 2050. Final project report. AEA group, Harwell, United Kingdom.

[4.] Borocz M., Horvath B., Herczeg B., Kovacs A.: 2015. Greener cement sector and potential climate strategy development between 2015-2030 (Hungarian case study). Applied Studies in Agribusiness and Commerce – APSTRACT Volume 9. No. 4. pp. 65-74. http://dx.doi.org/10.19041/APSTRACT/2015/4/9

[5.] Fiorello D., De Stasio C., Köhler J., Kraft M., Newton S., Purwanto J., Schade B., Schade W., Szimba E.: 2009. The iTREN-2030 reference scenario until 2030. Deliverable 4 of iTREN-2030 (Integrated transport and energy baseline until 2030). Fraunhofer ISI, Karlsruhe, Germany.

[6.] Coussy P., Portenart P., Afriat M., Alberola E.: 2014. Greenhouse gas emissions in the road transport sector: moving towards inclusion in the European system of CO_2 allowances? Energies nouvelles, Lyon, France.

[7.] Dobers K., Klukas A., Lammers W., Laux M., Mauer G., Schneider M.: 2013. Green Logistics: Optimisation Approaches for Resource-Efficient Logistics Services, 2013. pp. 149-161. http://dx.doi.org/10.1007/978-3-642-32838-1_17

[8.] Nemry F.: 2011. Contribution of the transport sector to the objective of the Effort Sharing Decision on non Emission Trading System sectors greenhouse gas emissions. European Commission – Joint Research Centre Notes, Brussels, Belgium.

[9.] Mattila T., Antikainen, R.: 2011. Backcasting sustainable freight transport systems for Europe in 2050. Energy Policy, Volume 39, Issue 3 pp. 1241-1248. http://dx.doi.org/10.1016/j.enpol.2010.11.051

[10.] Tsapakis I., Schneider W. H., Nichols, A. P.: 2013. A Bayesian analysis of the effect of estimating annual average daily traffic for heavy-duty trucks using training and validation data-sets, s, Transportation Planning and Technology, 36:2, 201-217. http://dx.doi.org/10.1080/03081060.2013.770944

[11.] Borkent B., O'Keeffe S., Neelis M., Gilbert A.: 2012. Costs and Effectiveness of Domestic Offset Schemes, Final report. Ecofys, London, United Kingdom.

[12.] Fogarassy Cs., Bakosne B. M.: 2014. Externality analysis of sustainable cattle breeding systems. Hungarian Agricultural Engineering Volume 26, pp. 5-10. http://dx.doi.org/10.17676/HAE.2014.26.5

[13.] Szanyi-Gyenes X., Mudri Gy., Bakosne B. M.: 2015: New tools and opportunities in growth and climate friendly greening for small and medium enterprises in the European Union. Applied Studies in Agribusiness and Commerce – APSTRACT Volume 9. No. 4 pp. 25-32. http://dx.doi.org/10.19041/APSTRACT/2015/4/3

[14.] Kovacs A.: 2014. A mezőgazdasági vállalatok tervezése a környezeti kölcsönhatások figyelembevételével. Szent István Egyetem, Gödöllő.

[15.] Gohar L. K., Shine K. P.: 2007. Equivalent CO2 and its use in understanding the climate effects of increased greenhouse gas concentrations. Weather, 62: 307–311. http://dx.doi.org/10.1002/wea.103

[16.] Caris A., Macharis C., Janssens G. K.: 2008. Planning in Intermodal Freight Transport: Accomplishments and Prospects , Transportation Planning and Technology, 31:3, 277-302, http://dx.doi.org/10.1080/03081060802086397

[17.] Schade W., Krail M.: 2012. Aligned R&D and transport policy to meet EU GHG reduction targets. Final Report. Deliverable 7.1 of GHG-TransPoRD (Reducing greenhouse-gas emissions of transport beyond 2020: linking R&D, transport policies and reduction targets). Fraunhofer ISI, Karlsruhe, Germany.

HUNGARIAN AGRICULTURAL ENGINEERING
N° 28/2015 30-33
Published online: http://hae-journals.org/
HU ISSN 0864-7410 (Print) / HU ISSN 2415-9751(Online)
DOI: 10.17676/HAE.2015.28.30

PERIODICAL OF THE COMITTEE OF AGRICULTURAL AND BIOSYSTEM ENGINEERING OF
THE HUNGARIAN ACADEMY OF SCIENCES
and
SZENT ISTVÁN UNIVERSITY
Faculty of Mechanical Engineering

MODELLING OF A HYBRID CLIMATE SYSTEM

Author(s):
G. Bércesi[1] – K. Petróczki[1] – J. Beke[2]

Affiliation:
[1]Department of Metrology, Process Engineering Institute, Szent István University, Páter K. u. 1., Gödöllő, H-2103, Hungary
[2]Department of Energetics, Process Engineering Institute, Szent István University, Páter K. u. 1., Gödöllő, H-2103, Hungary

Email address:
bercesi.gabor@hallgato.szie.hu, petroczki.karoly@gek.szie.hu, beke.janos@gek.szie.hu

Abstract

In Hungary a large part of consumed energy is spent on heating and cooling buildings. Utilization of renewable energy sources is spreading in this sector, but because of their disadvantages, they are mostly used as a part of hybrid climate systems. The paper deals with setting up a mathematical model of a hybrid climate system of an educational building, in order to examine its dynamical behaviors and research conditions of optimal operation and design principles of such systems. The building equipped with multiple types of heat sources and radiators, and to help research and education, its climate system is equipped with a high accuracy measuring system.

Keywords

hybrid climate system, modelling, heat pump

1. Introduction

In Hungary more than 60% of the annual energy use of buildings is spent on heating and if the climate system is supplemented with a cooling system in the summer, this ratio can increase further. This ratio is expected to persist longer. Thus special attention should be paid on saving energy – and mostly fossil fuels – on energy supply of heating, cooling and air conditioning systems of buildings. So because of increasing environmental awareness utilization of renewable energy sources is growing. However due to their disadvantages, like higher costs and limited availability, they are often used as a part of a hybrid energetic system supplemented with heat sources using fossil fuels. In stand-alone renewable energy using systems biomass firing is used most often, however in hybrid systems heat pumps with different heat sources (e.g. ground heat, groundwater, surface water, air), together with gas boilers are mostly utilized. One of the advantages of heat pump systems is that usually they can be used also for heating and cooling purposes. Caused by dependence of their performance on environmental parameters, there is an optimal range of conditions for using renewable energy sources or switch to conventional ones. There should also be an optimal capacity of heat buffer tanks in the heating system of each building using conventional and renewable energy sources together, in order to damp dynamic changes in heat energy demand on the heat source side properly in a cost effective way. In development and optimization of a process, first step is understanding the operation and the dynamical behaviors of the system that can be done by construction of a mathematical model of the system [1, 2]

This paper is based upon a PhD research. Its aim is construction and identification of the system model of building under investigation using the measurement data provided by the installed complex measuring system. Then using the model and numerical simulation methods, examination of effect of design and operational parameters on the efficiency of multiple source hybrid climate systems. This paper deals with measurement and modelling objectives of the topic.

2. Measurement

The experimental building with its climate system placed under investigation is situated on the Campus of Szent István University, Gödöllő, Hungary. Due to its recent renovation became a two-floor building with the Museum of the History of Agricultural Tool- and Machine Development on the basement and lecture halls, classrooms, laboratories and offices on the top floor. Its name is Knowledge Transfer Centre (TK). It has 3805 m^2 area and 15880 m^3 heated volume. The main part of its climate system is a ground-source water to water heat pump and 10 pcs of 100 m deep borehole heat exchangers. They can provide about 68 kW heating and 50 kW cooling power. As supplementary heat source in the heating season there are installed 2 pieces of 100 kW and 1 piece of 80 kW nominal power condensing gas boilers, in the cooling season a 407 kW water chiller (air – water heat exchanger) can be operated in the night. The lecture halls, classrooms, offices and laboratories are installed with fan-coil systems, on the corridors there are flat radiators, and the greatest lecture hall with 350 seats is completed with an air handler unit. In the heating system there is a 1000 liter capacity buffer tank. Figure 1 shows the photo of the frontage of the building and the schematic drawing of its hybrid heating system.

Within the project TÁMOP-4.2.1.B-11/2/KMR-2011-0003 project with title "Increase of the level of the education and research" together with the subproject in the Faculty of Mechanical Engineering: "Energy production based on renewable energy sources" a complex measuring system had been installed on the climate system of the building, that works independently form its own direct digital control (DDC). It operates almost

continuously since the May of 2013. It measures temperatures on 26 points of the climate system including forward and returning temperatures of borehole heat exchangers, heat pump, fan-coil and radiator circuits, buffer tank temperature, heated room and ambient temperatures. The temperature sensors are Pt-100 RTDs connected to an Agilent 34970A type measuring amplifier. In addition the electric energy consumption of the heat pump is also measured with the same amplifier. Through a measuring computer the data collected with one minute sample period is saved and can also be viewed online. The most difficult task is measurement of flow rates because the measuring system was installed on the completed and working climate system in which the piping could not be disrupted. But we suppose the inverter driven circulating pumps of the system are operating at approximately constant flow rates, so it is not needed to measure them constantly, and we can use for example a snap-on ultrasonic flow sensor for single measurements and record only the on/off state of pumps [3]. Figure 2 shows an example data series collected by the measuring system, plotted in function of time.

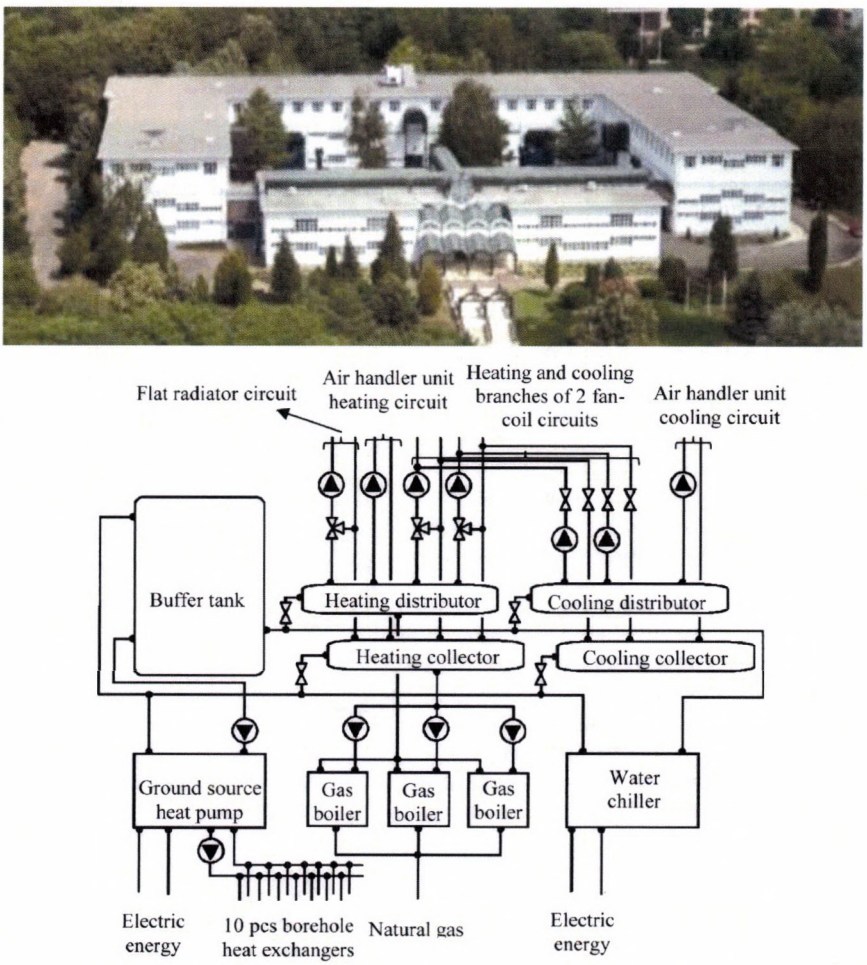

Figure 1. The frontage of the building and the schematics of its climate system

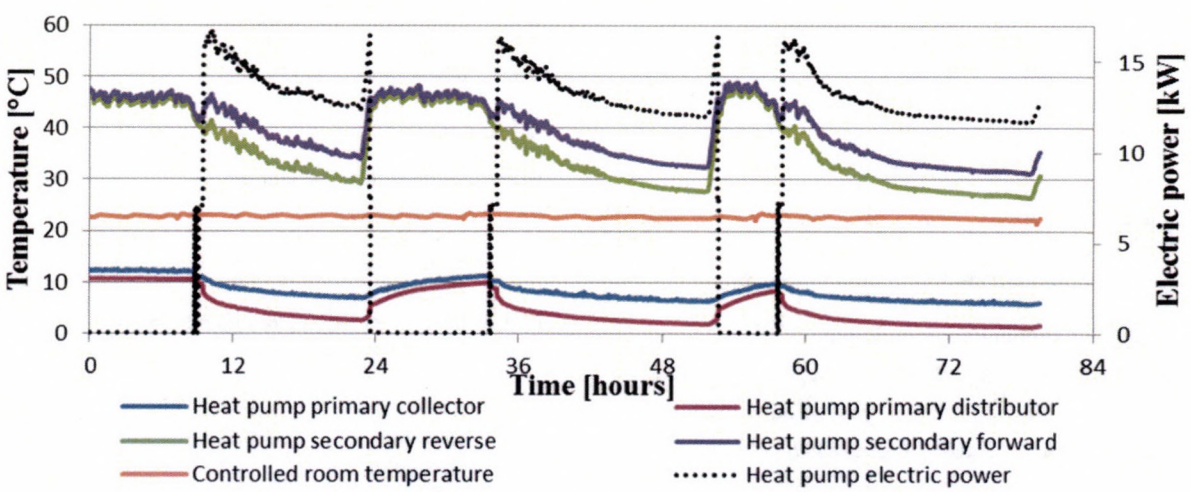

Figure 2. Example of visualization of data collected by the measuring system

3. Modelling

The aim of heating/cooling/air conditioning of buildings is to set the parameters of the thermodynamical equilibrium to the desired value. Thus in modelling of the heating system the heat balance of the building should be analyzed with examination of heat losses, heat storage elements and heat sources [4, 5]. All the factors of these processes can be identified using measurement data and characteristics of the used materials.

The energetic systems are usually distributed parameter systems. A basic model of them can be easily made with reducing to lumped element modelling using heat current network analog model. This is built from specific connection of models of each part of the system. The lumped element heat current network analog model is built from thermal resistances, heat capacitances, voltage generators representing temperature difference and current generators representing heat current (flow). The model can be used for the investigations about dynamics of the system and the heat buffer tanks. The main simplifications of the this model are approximating the ground heat source model as infinite capacity heat container (with constant temperature, but if the forward temperature falls below 0 °C – because of the freezing of the soil - they produce zero temperature difference) and the heated spaces are handled as one with no difference between fan-coil, radiator and air-handler units.

An improved modelling method is directly writing down the energy balance equations for each component that results a system of ordinary differential equations. This differential equation model can be supplemented with representations of real possibilities of manipulation elements (e.g. on/off state of pumps, valve/mixer valve positions) and thereby can be used for examination of real control strategies. So in this model these possibilities of manipulation are the input parameters. The output parameters are the process values for the control, like forward and returning temperatures of fan-coil and radiator circuits. This model is also built up with connection of mathematical model of each part. In this model ground source works similarly to the heat current network model, but heated space is divided to two parts: one heated with flat radiators and another one heated with fan-coils and air handler units. The equations for the heating system:

The heat from the borehole heat exchangers:

$$\dot{Q}_{BHE} = c_{BHE} \cdot \dot{m}_{BHE} \cdot (T_{BHEr} - T_{BHEf})$$

$$T_{BHEr} = \begin{cases} T_{BHEf} + 3°C, \text{if } T_{BHEf} \geq 0°C \\ T_{BHEf}, \text{if } T_{BHEf} < 0°C \end{cases}$$

The heat pump – with heat storage:

$$p_{HP} \cdot (\dot{Q}_{BHE} + P_e) - P_{HP} = \dot{Q}_{HP}$$

The buffer tank:

$$P_{HP} - P_{Hd} = \dot{Q}_P$$

$$c_w \cdot \dot{m}_{HP} \cdot (P_{HPf} - P_P) - c_w \cdot (\dot{m}_H - \dot{m}_G) \cdot (T_P - T_{Hd}) = c_w \cdot m_P \cdot \frac{dT_P}{dt}$$

$$\dot{m}_H = s_R \cdot \dot{m}_R + s_{FC1} \cdot \dot{m}_{FC1} + s_{FC2} \cdot \dot{m}_{FC2}$$

The heating distributor and collector:

$$P_{HP} + \varphi_G \cdot P_G = s_R \cdot P_R + s_{FC1} \cdot P_{FC1} + s_{FC2} \cdot P_{FC2} + s_{AHU} \cdot P_{AHU} = c_w \cdot \dot{m}_H \cdot (T_{Hd} - T_{Hc})$$

Corridors (spaces heated with flat radiators):

$$s_R \cdot P_R - P_{R-e} = \dot{Q}_R$$

$$s_R \cdot c_w \cdot \dot{m}_R \cdot [\varphi_R \cdot (T_{Hd} - T_{Rr}) + T_{Rr}] - -\kappa_R \cdot A_R \cdot (T_R - T_a) = c_R \cdot m_R \cdot \frac{dT_R}{dt}$$

Spaces heated with fan-coils and air handler unit:

$$e_{FC1} \cdot P_{FC1} + e_{FC2} \cdot P_{FC2} + s_{AHU} \cdot P_{AHU} - P_{FC-a} = \dot{Q}_{FC}$$

$$e_{FC1} \cdot c_w \cdot \dot{m}_{FC1} \cdot [\varphi_{FC1} \cdot (T_{Hd} - T_{FC1r}) + T_{FC1r}] + +e_{FC2} \cdot c_w \cdot \dot{m}_{FC2} \cdot [\varphi_{FC2} \cdot (T_{Hd} - T_{FC2r}) + T_{FC2r}] + + s_{AHU} \cdot c_w \cdot \dot{m}_{AHU} \cdot (T_{Hd} - T_{AHUr}) - -\kappa_{FC} \cdot A_{FC} \cdot (T_{FC} - T_a) = c_{FC} \cdot m_{FC} \cdot \frac{dT_{FC}}{dt}$$

The conditions are, the DDC unit – according to the heat demand depending on difference between ambient and desired internal temperatures - controls valves and pumps of the radiator, fan coil and AHU circuits and operates heat sources defining temperature relation. On this basis a block diagram can be built up for numerical solution of the system of equations and running simulations with varying parameters.

4. Conclusion

Due to the complex data acquisition network installed on the examined hybrid climate system, the data important in terms of its operation and modelling is collected continuously. The mathematical model of the system has been constructed, which can be identified based upon the measurement data, the design parameters and knowing of actually operating controller system. Then it can be numerically simulated in order to analyze control strategies. If necessary for investigations, additional further goals can be clarification of model of the borehole heat exchangers, the heat pump and the heated spaces and their relations.

Nomenclature

Q	heat energy	J
P	power	W
T	temperature	K
m	mass	kg
t	time	s
$\dot{m}$	mass flow	$kg \cdot s^{-1}$
c	specific heat	$J \cdot kg^{-1} \cdot K^{-1}$
κ	heat conductivity	$W \cdot m^{-2} \cdot K^{-1}$
A	surface area	m^2
pHP	heat pump power level	0%, 50%, 100%
s	state of circulating pump	0 – off, 1 – on
e	state of shut off valve	0 – close, 1 – open
φ	position of mixing valves	0 – 100%
φG	power level of gas boilers	0 – 100%

Subscripts

BHE	borehole heat exchanger
HP	heat pump
H	heating
P	buffer tank
R	radiator circuit
FC1,2	fan-coil and air handling unit circuit
AHU	air handling unit circuit
w	water
r	returning
f	forward
d	distributor
c	collector
a	ambient

References

[1] Caraman S., Barbu M., Minzu V., Badea N. Ceanga E.: 2010. Modelling and control of an autonomous energetic system obtained through trigeneration, Bul. Inst. Polit. Iaşi, 56-60 (4), pp. 61-72.

[2] Cho H., Luck R., Eksioglu S. D., Chamra L. M.: 2009. Cost-optimized real-time operation of CHP systems, Energy and Buildings, 41(4), pp. 445-451. http://dx.doi.org/10.1016/j.enbuild.2008.11.011

[3] Gergely Z., Tóth L., Petróczki K., Bércesi G.: 2013. Renewable energy assisted air conditioning system instrumentation, Hungarian Agricultural Engineering, 25/2013, pp. 13 - 16

[4] Hámori S.: 2008. Épületgépészeti irányítástechnika, Debreceni Egyetem, 119 p.

[5] van Schijndel A. W. M., de Wit M. H.: 2003. Advanced simulation of building systems and control with simulink. Eindhoven, Netherlands, Eighth Inernational IBPSA Conference, University of Technology, Eindhoven, pp. 1185 - 1192.

HUNGARIAN AGRICULTURAL ENGINEERING
N° 28/2015 34-38
Published online: http://hae-journals.org/
HU ISSN 0864-7410 (Print) / HU ISSN 2415-9751(Online)
DOI: 10.17676/HAE.2015.28.34

PERIODICAL OF THE COMITTEE OF AGRICULTURAL AND BIOSYSTEM ENGINEERING OF
THE HUNGARIAN ACADEMY OF SCIENCES
and
SZENT ISTVÁN UNIVERSITY
Faculty of Mechanical Engineering

COMPARING EXAMINATION OF ELECTROMAGNETIC FIELD LEVELS IN DOWNTOWN APARTMENT HOUSES WITH FLATS IN HOUSING ESTATES

Author(s):
G. Vizi[2]

Affiliation:
Institute of Architecture, Szent István University Ybl Miklós faculty of architecture and civil engineering, Thököly street 74., Budapest, H-1143, Hungary

Email address:
vizi.gergely.norbert@ybl.szie.hu

Abstract

In Budapest the housing stock mainly consists of old apartment buildings and housing estates from prefabricated reinforced concrete slabs. This paper gives a comparing examination on the electromagnetic field levels measured in these homes. The results show that average value in electric fields and magnetic fields in flats in housing estates are half of the values measured in apartment houses. Power flux density in flats in housing estates is ten-twenty times greater than in old apartment houses. However, values in the above mentioned flats are below the limits set by ICNIRP, the difference is interesting and can be explained by architectural reasons.

Keywords

electromagnetic field levels, measurement, comparison, standards, protection

1. Introduction

I have heard many times somebody complaining that the cell phone is not receiving signal in every corner of the apartment. Most of these people were living in downtown Budapest in an old apartment building. Previously I have experienced that the electric and magnetic radiation levels on extremely low frequency (ELF) are higher in old apartment buildings.

Buildings built in Budapest before 1946 gives 80-100% of the housing stock in the inner districts and 60-80% in the middle districts. The result of building housing estates from prefabricated reinforced concrete slabs beginning in 1970 is that today these types of flats give the 24% of the housing stock in Budapest, and the flats built after 2000 which are present in different proportions in different districts, give about 20% of the housing stock. From these numbers it is clear that the housing stock contains mainly old apartment buildings, and the other great number of flats is in housing estates from the '70s and '80s. For the above mentioned reasons I have decided to take measurements in these two types of flats, and find out the major differences, and the possible reasons what can cause different electromagnetic levels in the same city.

2. Measurements

The measuring tool I used for low frequency is Gigahertz Solution NFA 1000. This is a 3D analyser between 5 Hz and 1000 kHz. I performed two rounds of measurements in each apartment, first I measured the electric field levels, then the magnetic field levels, walking round in the room first by the walls, then in the middle. I placed particular attention on the beds, since this is the place where a person stays still for the longest time trying to relax. In this measurement series the focus was on radiation levels from wiring and household appliances so the frequency was fixed on 50/60 Hz both when measuring electric and magnetic field levels. I draw a floorplan in advance for each flat and noted the measured values on the spot where the measurement was taken.

I have used Gigahertz Solution HF59B High frequency analyser with a triangular antenna for 800MHz-2,5GHz. With this tool I walked slowly around the room turning around many times to observe what the direction of the highest irradiation is. I marked the directions with red arrows on the floorplan and noted the value next to it. Since my main interest was on the effect of outside or uncontrollable sources I always asked the owner to turn off the wifi router if there was one present. In most cases the direction of the irradiation was towards the façade wall, and in some cases towards a neighboring wifi router.

When evaluating I separated the values into minimum, main, and maximum values. Main value means the average of the most frequent values. In extremely low frequency (ELF) the median of the electric fields measured at the Living room of the 10 old apartment buildings is 16.5, 32, 101 V/m (minimum, main, max). The median in the block of flats buildings is 0.65, 12.88, 51 V/m (minimum, main, max). The median of the magnetic fields is 36, 44, 63nT, while in the block of flats 19.64, 22.4, 32.7nT. The median of the electric fields measured at the Bedroom of the 10 old apartment buildings is 20, 43, 111 V/m (minimum, main, max). The median in the block of flats buildings is 1.82, 7.57, 27.93 V/m (minimum, main, max). The median of the magnetic fields is 41, 42, 61nT, while in the block of flats 16.2, 19.5, 24.1nT. All values in the old apartment buildings are at least the double of the values in the block of flats buildings (Table 1).

The evaluation of the high frequency (HF) measurements gave the opposite results. In this frequency the medians of the electromagnetic levels in the Living rooms are 2.2, 3,9 $\mu W/m^2$ (main, max) in the old apartment buildings while 11.5, 96.34 $\mu W/m^2$ (main, max) in block of flats buildings. In the bedrooms these values are 1.05, 4.24$\mu W/m^2$ and 12.5, 59.36 $\mu W/m^2$ respectively. In the old apartment buildings the power flux density is basically the tenth of the power flux density in flock of flats buildings (Table 2).

Table 1. The measured electric and magnetic field levels

	Electric field levels in Old apartment houses										Block of flats in housing estates					
	1	2	3	5	6	8	9	10	11	Med	1	2	3	4	5	Med
Living	19	30	14	7,8	8,8	40	10	31	23	**16,5**	6.2	0.2	0.3	0.6	0.7	**0.65**
	34	30	15	21	19	75	80	45	33	**32**	30	12	1,7	2,1	23	**12.88**
	82	151	97	115	72	208	104	98	67	**101**	48	12,5	111	28	71	**51.05**
Bed room	20	17,3	22	5,7	16	5,4	26	54	26	**20**	3,6	0	0	8	1,1	**1.82**
	33	36	68	20	24	47	85	123	43	**43**	7,4	7,2	1,1	10	13	**7.57**
	61	245	200	72	99	485	103	310	111	**111**	9,3	32	30	13	45	**27.93**
	Magnetic field levels in Old apartment houses										Block of flats in housing estates					
	1	2	3	5	6	8	9	10	11	Med	1	2	3	4	5	Med
Living	59	20	36	48	17	59	22	8	10	**36**	8	16	27	56	9,4	**19,64**
	65	40	42	52	28	77	33	14	18	**44**	14	19	27	56	13	**22,4**
	82	60	66	57	36	134	36	19	28	**63**	18	24	83	67	15	**32,7**
Bed room	56	42	28	41	26	52	58	8	27	**41**	12	14	19	36	11	**16,2**
	56	42	33	42	32	52	94	10	31	**42**	14	16	19	36	20	**19,5**
	79	74	55	64	38	188	192	10	41	**64**	16	29	20	44	22	**24,1**

Table 2. The measured Power flux density

	Old apartment houses										Flats in housing estates					
	1	2	3	5	6	8	9	10	11	Med	1	2	3	4	5	Med
Livi	2,2		30	2	2,4	4,6	2,8	1,02	0,38	**2,2**	0,4	5	68	1,8	18	**11,5**
	4,6		108	3	3,8	8	4,9	2,67	0,93	**3,9**	0,4	90	176	109	98	**96,34**
Bed			30	12	5	0	0,4	1,05	0,79	**1,05**	2,9	13,9	12	13	18	**12,5**
			93	20	10	1,6	6,5	1,98	0,86	**4,24**	9,6	32	110	190	42	**59,36**

3. Reasons

Structural reasons

There are some major structural differences between an old apartment building, and a block of flats building. First of all the material of the walls are different. The old apartment buildings are made of solid bricks, the block of flats building is made from prefabricated reinforced concrete slab panels. I have made simulations using CST Microwave Studio to observe the difference in behavior in these situations. CST Microwave Studio is a tool that rigorously solves the governing equations of electromagnetism, Maxwell's equations, for any situation given. It does that by making use of powerful numerical techniques, in this case the Finite Integration Technique. The characteristics used for this material in the simulations are coming from the material library in the electromagnetic simulation software used: CST's "one year old concrete", and "brick". The real part of the permittivity for concrete is 5.608 the imaginary part is 0.217, for brick the permittivity is4.64 the conductivity is 0.02 S/m which is in agreement with the values in literature [1, 2]. Simulations were performed on a small room with outer dimensions 5.0 m x 3.6 m x 3.3 m. Results show that the electromagnetic level inside a room where the walls are made of bricks is lower than the same room with concrete walls (Figure 1).

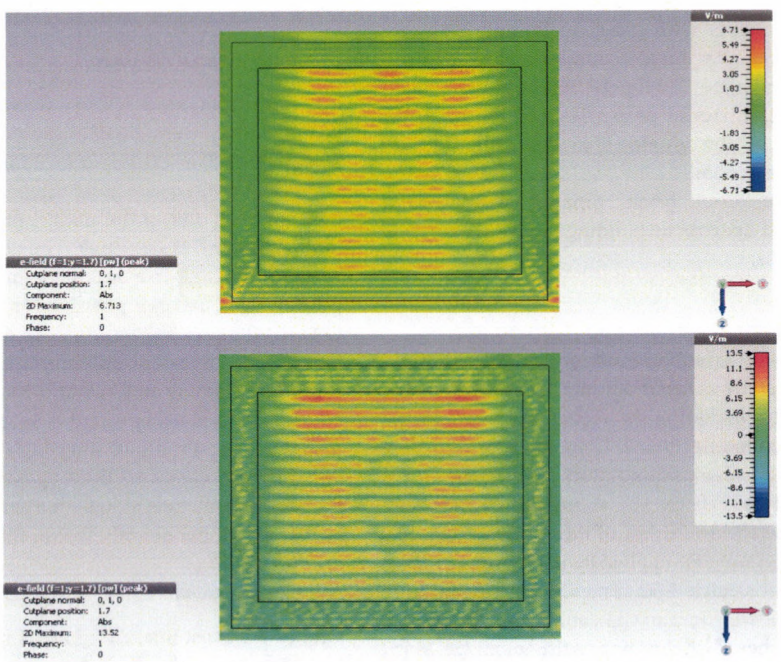

Figure 1. Field levels in a simulated room made from brick (top) and concrete (bottom)

The second difference is that not only the material, but the thickness of the walls is different. It is common that the wall of an old apartment building is 51-64 cm thick, while the thickness of a concrete panel is only 25-30 cm. These panels include mineral or polystyrene insulations, but for simplified simulations I have only considered homogenous walls with different thicknesses. Results show that thicker walls have higher attenuation (Figure 2). Attenuation is expressed in shielding effectiveness (SE) as the ratio of the external field to the internal one in decibels:

$$SE = 20Log\frac{|E_{ext}|}{|E_{\text{int}}|}$$

Attenuation was found in the simulations 4.73 dB and 10.17 dB by 30 and 50 cm thick solid brick wall respectively.

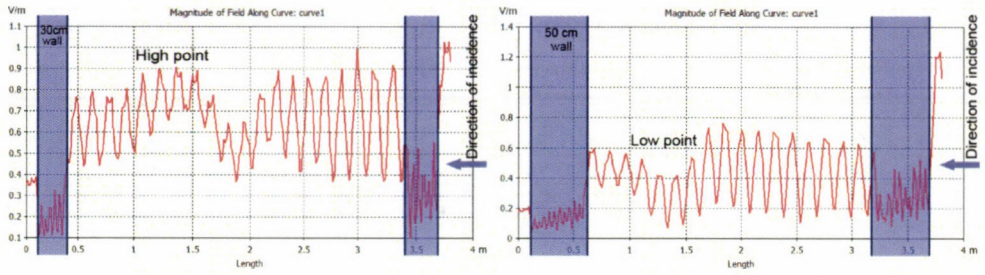

Figure 2. Magnitude of field in the section of the simulated rooms with 30 (left) and 50 right cm thick wall

The third major difference is in the size of the windows, and the proportion of the windows and the wall. Since the inner height of these old apartments is around 3.80 meter, the shape of the windows is a horizontal rectangle. The width of these windows is usually 1.20 the height is 2.30 meter. The proportion of the opening (window) to the wall is 20-29%. The inner height of a flat in a housing estate is around 2.70. The windows are located in the centre of the panel, or the windows (almost) fill the whole width of the room. The width of the windows differ, the height is usually 1.50 meter. The proportion of the windows and the front wall in these flats is 32-44% which is 62-65 percent bigger than in old apartments (Table 3).

Table 3. Proportion of wall and windows in a façade wall of a room

Location	Room width	window size	Proportion of the wall and windows
Old apartment house, Bedroom	3.6	1.20 x 2.30	20%
Old apartment house, Living room	5	2 x 1.20 x 2.30	29%
Block of flats, Bedroom	2.6	1.50 x 1.50	32%
Block of flats, Living room	3	(0.9+1.50)x1.50	44%

I have run simulations were the material properties of the glass were: permittivity 4.82 and tangent delta 0.0054. The tangent delta is the parameter describing the losses in the material. These tests verified that the results with glass or without glass are essentially the same. Thus non-shielded windows behave as just openings. Conclusion is since "common" window glass itself doesn't shield due to its material properties and thinness, the greater the proportion of the windows to the wall, the less attenuation is given to the room.

Thicker walls made from brick, smaller window-wall proportion make the old apartment buildings more resistant to high frequency radiations.

Local reasons

In ELF the spatially most extended outdoor sources are high-voltage overhead power lines used for the transmission and distribution of electricity, including the feeder lines for electric vehicles like trams and commuter trains. There are approximately 360,000 km of overhead transmission power lines in the EU at voltages of between 110 - 750 kV [3]. A smaller country like Hungary has approximately 3,800 km of these lines. Very few electric power transport system is supplied by underground cables (2%), against the fact that electric field is negligible and magnetic fields are significantly lower next to the cables, but on the line itself the field can be higher [4] According to the actual GKM [5] decree the clearance from a 120kV power line should be 13 m in Hungary. In buildings in a 25m distance I have measured 830nT which is approximately 15 times greater than in other buildings where there are no power lines around.

Urban structural reasons

For mobile communication networks the lowest power flux density values were found at ground floor, and the highest values were detected in category above the second floor [6]. One reason is that higher floors are more often in line of sight to mobile phone base stations and in the main lobe of the antenna resulting in higher power flux densities. The other reason is that the distance between the high-rise buildings -due to fire security reasons- are greater, what makes it possible for the antenna to radiate directly towards the opposite building. In downtown the buildings are in most cases three-four maximum five story high. The height of these buildings is equivalent with the height of 4-5 story high building in a housing estate. These buildings are not just lower than the in most cases 10 story high buildings in a housing estates, but they are closer to the opposite buildings in this case the transmitter antennas radiate in a certain angle to cover more area of that street, not directly facing the building.

Near future technologies

One of the most interesting news in last year that might bring a big change in the ELF was the announcement of wireless

electricity [7]. The technology uses a coil of electrical wire that generates a magnetic field, and if another coil is brought close electrical charge will be generated. The developers now work on increasing the distance so that power can be transferred efficiently. If this technology is used all over the house that will possibly raise the level of the magnetic field in it.

As for the HF, studies have shown already that the median of mobile phone downlink signals doubled from 2006 to 2009, and continued to increase due to further growth mainly in UMTS base stations [6, 8]. New types of network architectures based on small cells will be needed to offload traffic. 5G wireless systems are in the doorstep. This will lead to more access points and transmitters radiating from more directions, and it will bring the access point closer to the user. In frequency usage, there are networks which already work on 5 GHz, instead of 2.4 GHz, Scientists are facing many changes! New architectural, urban structural studies have to be made, to examine the changes in reflection, absorption and power density levels.

4. References and recommendations

For each frequency domain, the ICNIRP have limited the exposure levels. Regarding 50 Hz fields, the ICNIRP reference level for the electric field is 5000 V/m and the reference level for the magnetic field is 200μT [9]. The EU issued a recommendation in 1999 concerning restrictions on the exposure of the general public to electric and magnetic fields. Restriction is 100μT for magnetic fields [10]. In many EU countries, these values are recognized, but some national or local governments have issued their own stricter exposure guidelines, like in Belgium the restriction for magnetic fields is 10μT. The values from measurements are below these levels, however, the Building biology standards recommend even stricter limits, saying "any risk reduction is worth achieving. Nature is the ultimate standard". They recommend less than 5 V/m, and 20nT in ELF (sbm2008) If one wants to meet these recommendations, there are some simple steps that can be done.

The main ELF sources of exposure for the general public are from household and similar electric appliances. In ELF-EFs and ELF-MFs can be reduced the easiest by distance keeping, because exposures from these devices are localized and strongly depend on the distance from the appliance. In existing buildings, reorganizing the room, changing the position of the bed, or removing alarm clocks with radio, metallic lamps, and extension cables from under and around the bed will significantly reduce the level of electric and magnetic fields. Renewing the whole electric system is an expensive choice, but it is strongly advised in old flats, where in most cases the electric system is not grounded. By changing the electric wiring to modern shielded (foil or braid) cables will reduce the electric fields. One of the outcomes in the measurements taken in different homes is that electric and magnetic fields in homes with not grounded electric wiring were 3-4 times higher than in homes with grounded electricity (Table 4).

Table 4. Examples for electric and magnetic field levels in grounded and not grounded homes

	Location	magnetic field	electric field
Not grounded	Dohány u 84	77-157 nT	68-88 V/m
	Brody Sándor u 36	45-90 nT	56-116 V/m
	Brody Sándor u 17	33-40 nT	98-150 V/m
Grounded	Hunyadi tér 1	18-28 nT	23-33 V/m
	Zoltán utca	20-21 nT	5,1-6,1 V/m
	Garay tér 11	19-26 nT	19-29 V/m

As for the high frequency, the power density limitation is 10 W/m2 for the general public [9, 10] The measured values are way below this level but again, if we take the building biology recommendations into consideration, the numbers are not so satisfying. There are some other recommendations like EU-Parlament STOA: 100μW/m^2, or in Salzburg the indoor limit is 1μW/m^2.

Since 2008 it is possible to buy cordless telephones with LR mode, which only emits radiation during active telephone calls. This option is not activated by default, but activating this mode the median of DECT radiation can decrease by 24% [6].

Checking for the available wifi networks on the mobile phone showed many times that six or more networks are present with different signal strengths, which mean that the flat is irradiated from more directions. Using wifi routers with sleep mode would turn off the signal at night when nobody uses the network. There are options to shield our flat from outside sources, for example carbon based wall paints. My simulations have shown that if only the walls are shielded the power density from radiation through the windows can be even higher inside than it was before. Therefore shielding the windows is one important step.

5. Conclusion

Architectural design has effect on the inside electromagnetic levels. Thoughtfully designed buildings where the electromagnetic effects are taken into consideration can reduce field levels, and help propagation. There are simple steps that the resident can do to make the flat harmonized. The wireless communication technology improves rapidly, architects, scientists working in the field of electric engineering and wireless communication have to be aware of the effect of their profession on the other disciplines, and have to work together to build the city of the future.

Acknowledgements

I would like to thank for those who made it possible for me to make measurements in their home.

References

[1.] Shah M. A., Hasted J. B., Moore L.: 1965. Microwave absorption by water in building materials: Aerated concrete. British J. of Applied Physics, Vol. 16, pp. 1747-1754

[2.] Sou C. K., Landron O., Feuerstein M. J.: 1992. Characterization of electromagnetic properties of building materials for use in site-specific propagation prediction, Mobile Portable Radio Res. Grp. (MPRG) Tech. Rep. 92-12, Virginia Tech.

[3.] ENTSO-E Statistical Yearbook.: 2009.

[4.] ICF Consulting.: 2003. Overview of the Potential for Undergrounding the Electricity Networks in Europe, Final Report for the DG TREN-EC.

[5.] GKM.: 2011. 122/2004. decree (X.15)

[6.] Tomitsch J., Dechant E.: 2015. Exposure to Electromagnetic Fields in Households – Trends from 2006 to 2012, Bioelectromagnetics, Vol. 36, pp.77-85 http://dx.doi.org/10.1002/bem.21887

[7.] CNN.: 2014. Wireless electricity? It's here by Nick Glass and Matthew Ponsford. CNN, 2014.
[8.] Kurz T., de Ridder M., Becker C.: 2013. EMF –Monitoring in Bayern 2011/2012. Bavarian Environment Agency
[9.] ICNIRP.: 2010. Guidelines for Limiting Exposure to Time-Varying Electric and Magnetic Fields (1 Hz TO 100 kHz), International Commission on Non-Ionizing Radiation Protection. Health Physics, 99:818-836.
[10.] EU Council.: 1999. European Union, Council Recommendation, of 12 July 1999 on the limitation of exposure of the general public to electromagnetic fields (0 Hz to 300 GHz) (1999/519/EC), Off. J. Europ. Comm., L 199/59.

HUNGARIAN AGRICULTURAL ENGINEERING
N° 28/2015 39-43
Published online: http://hae-journals.org/
HU ISSN 0864-7410 (Print) / HU ISSN 2415-9751(Online)
DOI: 10.17676/HAE.2015.28.39

PERIODICAL OF THE COMITTEE OF AGRICULTURAL AND BIOSYSTEM ENGINEERING OF
THE HUNGARIAN ACADEMY OF SCIENCES
and
SZENT ISTVÁN UNIVERSITY
Faculty of Mechanical Engineering

TEMPORAL AND SPATIAL VARIATIONS OF GROUNDWATER LEVEL AND SALINITY: A CASE STUDY IN THE IRRIGATED AREA OF MENEMEN PLAIN IN WESTERN TURKEY

Author(s):
N. Korkmaz[1] – M. Gündüz[1] – Ş. Aşık[2]

Affiliation:
[1]International Agricultural Research and Training Centre, Camikebir Mah., Çavuşköyyolu Sok., No:9, 35660 İzmir, Turkey
[2]Ege University Faculty of Agriculture Dept. of Farm Structures and Irrigation, 35100 Izmir-TURKEY

Email address:
nil_korkmaz@yahoo.com, gunduz.mehmet@gthb.gov.tr, serafettinasik@gmail.com

Abstract

The aim of the study was to determine the temporal and spatial variations in the level and salinity of groundwater. In 2011 and 2012, in the rainy season, before the irrigation season, during the irrigation season and after the irrigation season the depth of groundwater was measured and at the same time groundwater samples were taken from each well. According to the results obtained, groundwater salinity was high in the years of the study, and its level was high in the rainy period and the irrigation period, but low before irrigation and after the irrigation period.

Keywords

ground water level, ground water salinity, spatial, temporal, Gediz

1. Introduction

It is a prerequisite of sustainable irrigated agriculture that irrigation should be done in such a way as to be effective and productive without damaging the environment. The most important role in meeting the world's need for food is played by areas of irrigated agriculture. It is a prerequisite of sustainable irrigated agriculture that it should be done in such a way as to be effective and productive without damaging the environment. Agricultural irrigation, especially when it is done with unsuitable techniques and in unsuitable amounts, can cause problems of salinity and alkalinity related to rising groundwater levels, especially in areas with topographic insufficiencies. Saline groundwater causes a reduction in the uptake of water from the soil by roots because of an increase of osmotic pressure in soil solutes, giving rise to a decrease in crop yield and quality. Soil productivity is affected by soil physical properties that play a crucial role in planning drainage systems. Improper planning of drainage systems can create high water table problems, and in turn, an unsuitable environment for plant growth. Therefore, drainage systems should be well planned and monitored regularly. It is labor-intensive and time-consuming to determine the spatial and temporal changes in drainage parameters such as ground water level, elevation, hydraulic gradient and salinity by conventional methods over large areas. Geographical information systems (GIS) and geostatistical analysis can be used to assess the spatial and temporal changes efficiently and rapidly [1].

Uninformed and uncontrolled irrigation in the Menemen Plain area, low efficiency of field irrigation practices and leaking from the canal network have caused the groundwater level to rise. In July, the month of the most intense irrigation, groundwater levels in the left bank irrigation area of the Menemen Plain do not fall below 101-150 cm in the 80.4% of the area close to the sea, and in 1.7% they do not fall below 51-100 cm [2]. Before management of the system was handed over to the irrigation association, average groundwater depths were approximately 186 cm and salinity was 2.65 dSm^{-1}, while after the handover, these figures were 148 cm and 3.14 dSm-1 [3]. The aim of this study is to determine temporal and spatial variation in the level and salinity of groundwater in the part of the Izmir-Menemen Plain left bank irrigation area which is close to the Aegean Sea with the use of the Geographical Information System and geostatistical methods.

2. Material and method

The Menemen Irrigation System is situated in the Gediz River basin in the west of Turkey, between 38°26'-38°40' north and 26°40'-27°07' east. The basin's alluvial base is divided into two by a narrowing at Emiralem, to the west of the city of Manisa. The part between this point and the sea is the Menemen plain. It lies at 10.3 m above sea level. At the site of the study, the soil has a fine loam texture, and is insufficiently to poorly drained and salty-alkaline, over the Gediz alluvial base. Cotton and grain are grown on most of the land [4]. The Menemen plain has a Mediterranean climate, with hot dry summers and cool wet winters. According to data collected over many years, total annual precipitation is 539.8 mm. Average temperature is 16.90C. In the two years of the study, 2011 and 2012, total precipitation was 812 mm and 624 mm respectively [5].

The catchment area of the Gediz basin is 17 000 km^2, and the surface water potential is 2.0 $km3yr^{-1}$ [6]. The main source of water of the Lower Gediz basin, including the Menemen Left Bank irrigation system, is the Demirkopru Dam, fed by the Gediz River, and the Marmara Lake. The Menemen Left Bank irrigation system consists of the left main canal which is connected to the Emiralem regulator, and six secondary canals. The system was constructed in 1944, and irrigates an area of 16 585 ha. The area of the present study covers 2560 ha at the end of the Menemen Left Bank Irrigation area and is 7 km from the Aegean Sea. In this area, 67 groundwater observation wells were dug based on

1/25000 digitised soil series maps. The wells were dug so that there was one for each 100 ha. Groundwater observation wells were located at 100, 300, 600 and 1000 m intervals in two of the 100 ha areas whose soil series showed little or great variation (Figure 1). The wells were generally opened to a depth of 3.80 m, but at some points they were dug shallower due to pebbles. In the wells, PVC pipes were used with a diameter of 63 mm and with holes of 2 mm diameter spaced at intervals of 5 cm. The locations of the observation wells were recorded with the Global Positioning Systems. In January, April, June, August and October of 2011 and 2012, groundwater (GW) levels were measured and water samples were taken from the same wells to measure electrical conductivity (EC). January and April represented the period affected by rain, June the pre-irrigation season, August the irrigation season, and October the post-irrigation season. EC (dSm-1) was established according to Standard Method 2510 B with the use of an electrical conductivity device [7].

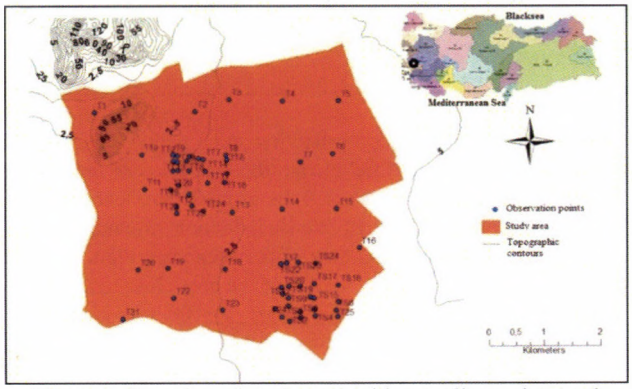

Figure 1. Location of study area with sampling points and topographic contours at 2.5 m intervals. Surface elevations are in meters above sea level.

The program ArcGIS 10.2 CBS was used for geostatistical modelling [8]. Using this program, groundwater level and EC maps were created for each period from the original data. Data were analyzed in three steps: (i) normality tests were conducted to test the hypothesis which assumes that each property is normally distributed (Kolmogorov-Smirnov); (ii) descriptive statistics including arithmetic mean, standard deviation and coefficient of variation, CV, were calculated, and (iii) semivariogram analysis and complementary kriging interpolations were conducted for each variable. A proper transformation (log-transformation) was applied based on the result of the normality tests conducted using JMP 5.0.1 [9]. Geostatistical software (GS+7.0, [10]) was used to construct semivariograms and spatial structure analysis for variables. One of spherical, gaussion, exponential, and linear models was fitted to the experimental semivariograms by the least square fitting technique. Root mean squared error, coefficient of determination, and visual fitting were considered in selecting the models. Nugget variance expressed as the percent of total semivariance was used to judge the spatial dependency of variables. If the rate was equal or lower than 25%, variables were considered as strongly dependent, between 25 and 75% moderately dependent, and greater than 75% weakly dependent [11].

3. Results and discussion

Ground water level

Tables 1-3 show the descriptive statistics, the semivariogram model and its parameters and the cross validation results for groundwater depth values measured in 2011 and 2012.

Table 1. Descriptive statistics for the ground water level by seasons (cm)
aStandard deviation, b Coefficient of variation

Year	Seasons	Mean	Minimum	Maximum	SD[a]	CV[b]	Skewness	Kurtosis
2011	January	***91***	***0***	214	55	***60.2***	0.16	-0.80
	April	141	73	222	40	31.7	0.31	-0.90
	June	145	29	310	48	33.4	0.55	0.80
	August	133	76	201	33	***25.0***	-0.03	-1.04
	October	***186***	70	***313***	51	27.6	0.16	0.05
2012	January	140	***10***	256	55	***39.5***	-0.20	-0.49
	April	144	75	247	43	30.0	0.47	-0.75
	June	156	69	310	44	28.4	0.70	1.49
	August	***128***	17	248	45	35.1	-0.23	-0.13
	October	***197***	129	***313***	35	***17.9***	0.40	0.80

In 2011, groundwater levels showed a variability of 0-313 cm, monthly averages 91-186 cm, and coefficients of variation 25.0-60.2%. In 2012 these values were 10-313 cm, 128-197 cm and 17.9-39.5% respectively. Groundwater levels rose in the rainy period (January) and the irrigation period (August), and fell in the pre-irrigation (June) and post-irrigation (October) periods. This shows that rain and irrigation both cause the groundwater level to rise.

In all periods of the study years, groundwater levels showed a normal distribution, and the model which best fitted the data was the spherical isotropic semivariogram model. Range values varied in 2011 from 1100 to 2723 m, and in 2012 from 1000 to 4570 m. This model was also used in an evaluation in Turkey of groundwater levels of the Mustafakemalpaşa irrigation area and the Bafra Plain [12, 13]. Degrees of spatial dependence varied between 13.6% (June) and 50.0% (August) in 2011 and 15.8% (June) and 42.4% (August) in 2012. In April and June 2011 and April and October 2012, spatial dependence was classed as strong, and in the other months as moderate. Groundwater levels were classified as strong in spatial dependence classification in April and June 2011 and April and October 2012 and moderate for the other months.

The proportion of areas where the groundwater levels were above 90 cm was 40.5% in January 2011, 1.4% and 1.5% in April and June 2011, 4.7% in January 2012, and 5.2% in August 2012. The proportion of areas where the two-year average was over 180 cm was found to be, in order of periods, 92.7, 88.6, 85.5, 97.6 and 60.1% (Figure 2). From the point of view of drainage and salinity, a groundwater depth of up to 2 m is seen as risky [14].

Table 2. Parameters of isotropic best fit semivariogram models of ground water level by seasons

Year	Seasons	Nugget (C_0)	Sill (C_0+C)	Range (m)	C/C_0+C	r^2	Spatial Dependency		Model
							%	Class	
2011	January	1186	3380	***2723***	0.649	0.626	34.8	moderate	Spherical
	April	378	1587	1819	0.762	0.608	23.8	strong	Spherical
	June	389	2845	2668	0.863	0.927	***13.6***	strong	Spherical
	August	512	1025	1702	0.500	0.637	***50.0***	moderate	Spherical
	October	1000	2300	***1100***	0.565	0.642	43.5	moderate	Spherical
2012	January	1050	3796	2690	0.723	0.820	27.7	moderate	Spherical
	April	357	1991	2000	0.820	0.610	17.9	strong	Spherical
	June	945	2258	***4570***	0.581	0.652	41.8	moderate	Spherical
	August	865	2036	2060	0.575	0.589	***42.4***	moderate	Spherical
	October	185	1172	***1000***	0.842	0.735	***15.8***	strong	Spherical

Table 3. Results of cross-validation for ground water level

Year	Seasons	ME	RMS	MS	RMSS	ASE
2011	January	-0.803	40.0	-0.0099	0.89	43.4
	April	-0.498	29.7	-0.0088	0.91	29.9
	June	-0.436	33.5	-0.0033	0.99	31.9
	August	0.154	29.1	0.0029	1.05	27.6
	October	0.417	48.5	0.0045	1.08	47.4
2012	January	-0.091	46.8	0.0003	1.05	42.9
	April	-0.420	29.2	-0.0085	0.90	30.4
	June	-0.210	42.4	-0.0018	1.10	37.3
	August	-0.198	35.3	-0.0023	0.92	36.7
	October	0.907	27.7	0.0181	1.00	26.7

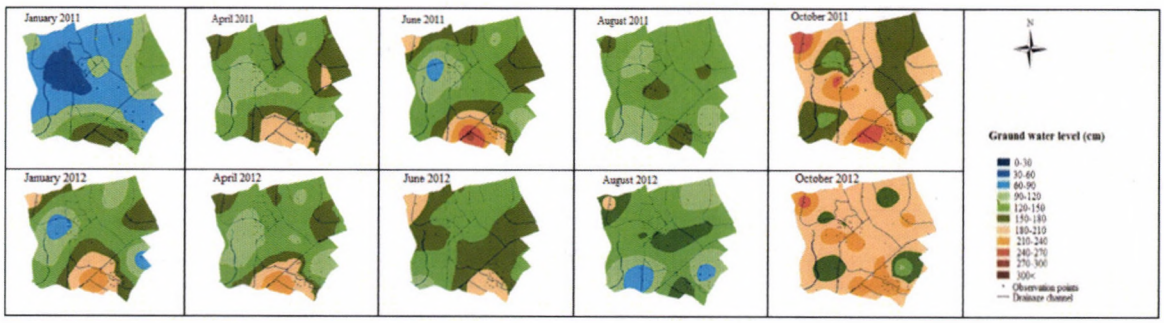

Figure 2. Spatial and temporal variation in groundwater levels for 2011and 2012

Ground water salinity

Tables 4-6 show the descriptive statistics, the semivariogram model and its parameters and the cross validation results for groundwater EC values measured in 2011 and 2012.

Because groundwater salinity values showed log-normal distribution, transformation was applied before calculating the semivariogram. EC values showed consistency with the isotropic characteristic and the spherical semivariogram model. Range values varied between 3345 and 3790 m in 2011, and 2388 and 3049 m in 2012. Degrees of spatial dependence varied between 15.5% (January) and 45.9% (August) in 2011, and 21.5% (August) and 41.8% (October) in 2012. January 2011 and August 2012 were classed as strong regarding spatial dependence, and the other months as moderate.

Table 4. Descriptive statistics for the ground water salinity by seasons, (dSm^{-1})
[1]Standard deviation, [2]Coefficient of variation

Year	Seasons	Mean	Minimum	Maximum	S.D.[1]	C.V.[2]	Skewness	Kurtosis
2011	January	7.58	0.78	33.72	7.5	98.8	1.76	2.85
	April	6.66	0.54	43.83	7.6	114.7	2.85	9.61
	June	7.69	1.06	38.25	7.7	101.9	1.87	3.39
	August	7.24	0.73	29.09	7.0	97.0	1.63	2.09
	October	7.58	1.06	30.83	7.9	103.9	1.58	1.54
2012	January	6.89	0.72	58.18	8.6	125.2	3.71	18.20
	April	7.01	0.64	29.60	6.8	97.1	1.62	1.96
	June	6.90	0.76	24.46	6.7	96.7	1.40	0.77
	August	7.47	0.64	46.36	8.5	114.3	2.40	6.67
	October	7.00	0.90	42.45	8.1	115.7	2.45	6.66

Nowhere in the study area was groundwater salinity found to be in the low or moderate classes. In terms of groundwater EC content classification, it was found that in 2011, proportional field quantities varied between 2.4% (August) and 9.0% (April) in class

III, between 3.7% (August) and 6.5% (October) in class IV, and between 84.3% (October) and 94.8% (August) in class V. The equivalent values for 2012 were 2.0% (October) – 5.6% (August), 3.8% (April) – 11.2% (August) and 83.2% (August) –94.4% (June). It can be seen that no water of class I and II salinity was found in the study area, but that class V water was widespread (>80%). Areas with class III and IV salinity were generally in the south-east of the area. Spatial distribution of groundwater salinity was similar in the two years of the study, with no great differences between the years (Figure 3). In similar studies carried out in Turkey, it was found that groundwater salinity on the Lower Seyhan Plain was 28.8, 18.4 and 24.9 dSm^{-1} in May, July and September 2006 respectively [15], and greater than 2 dSm-1 on only 5-7% of the area in Tokat-Kazova [16], in the right bank irrigation area of the Bafra Plain, which has a sea water entry, it varied between 1.36 and 11.9 dSm^{-1}, with an average of 4.18 dSm^{-1} [17].

Table 5. Parameters of isotropic best fit semivariogram models of ground water salinity by seasons

Year	Seasons	Nugget (C_0)	Sill (C_0+C)	Range (m)	C/C_0+ C	r^2	Spatial Dependency		Model
							%	Class	
2011	January	0.168	1.086	3410	0.845	0.624	15.5	strong	Spherical
	April	0.473	1.278	***3790***	0.805	0.852	37.0	moderate	Spherical
	June	0.360	1.049	3554	0.689	0.886	34.3	moderate	Spherical
	August	0.477	1.040	3680	0.541	0.897	45.9	moderate	Spherical
	October	0.344	1.101	***3345***	0.688	0.700	31.2	moderate	Spherical
2012	January	0.406	1.009	3018	0.598	0.804	40.2	moderate	Spherical
	April	0.366	0.938	2538	0.610	0.824	39.0	moderate	Spherical
	June	0.393	0.977	2948	0.598	0.829	40.2	moderate	Spherical
	August	0.247	1.147	***2388***	0.785	0.625	21.56	strong	Spherical
	October	0.442	1.057	***3049***	0.581	0.614	41.8	moderate	Spherical

Table 6. Results of cross-validation for ground water salinity

Year	Seasons	ME	RMS	MS	RMSS	ASE
2011	January	-0.011	6.71	-0.118	1.24	6.05
	April	0.184	7.15	0.009	0.93	7.63
	June	-0.230	7.49	-0.118	1.22	6.99
	August	0.055	6.63	-0.048	0.94	7.69
	October	-0.136	7.01	-0.084	1.03	7.36
2012	January	-0.017	8.10	-0.060	1.07	7.24
	April	0.020	6.65	-0.089	1.11	7.20
	June	-0.009	6.25	-0.065	1.04	6.94
	August	-0.144	7.83	-0.121	1.19	7.68
	October	-0.162	6.97	-0.003	0.85	7.35

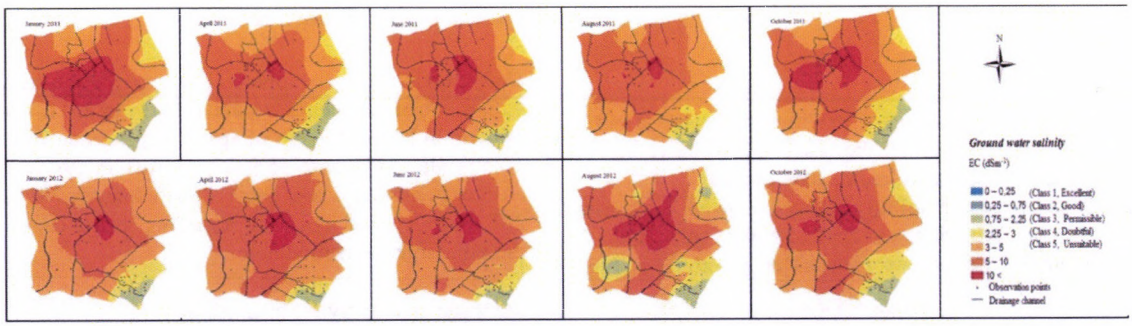

Figure 3. Spatial and temporal variation in EC of groundwater in 2011 and 2012

4. Conclusion

Spatial dependence in groundwater levels before and after the irrigation season was strong; in groundwater salinity values it was generally moderate. Geostatistical range values for ground water level were 1000 m and 2350 m for groundwater salinity, which, when evaluated together, must be taken as 1000 m. The nugget effects of ground water level and ground water salinity were generally high. Sea effects and drainage differences were found in the study area. Groundwater levels rose in the rainy (January) and irrigation (August) periods, and fell in the pre-irrigation (June) and post-irrigation (October) periods. During the irrigation season, groundwater levels of 90-150 cm were found in 80% of the area. After the irrigation season, groundwater levels in 70% of the area fell to below 180 cm. Groundwater salinity was greater than 3.00 dSm^{-1} in 90% of the study area. Furrow irrigation was practiced in the study area. Collecting water charges by land area irrigated rather than by water volume causes a fall in water application ratio of 50-60%. The mistaken practices of farmers in soil and water management cause the groundwater to rise and its salinity to increase. The performance of the existing drainage system in the study area in face of the high level and salinity of the groundwater should be evaluated, effective work should be carried out, and the

practice of blocking drainage canals in order to collect water for use in irrigation should be stopped.

References

[1.] Cetin M., Diker K.: 2003. Assessing drainage problem areas by GIS: A case study in the eastern Mediterranean region of Turkey. Irrig. And Drain. Volume 52, pp. 343-353.

[2.] Çamoğlu G., Ölgen K., Karataş B. S. ve Aşik S. 2006. Menemen sulama sisteminde taban suyunun zamana ve mekana göre değişiminin değerlendirilmesi: Maltepe ana kanalı örneği, 4. Coğrafi Bilgi Sistemleri Bilişim Günleri, Fatih Üniversitesi. İstanbul.

[3.] Kıymaz S.: 2006. Gediz Havzası örneğinde sulama birliklerinin sorunları ve çözüm yolları, (Doktora Tezi), Çukurova Üniversitesi Fen Bilimleri Enstitüsü, Tarımsal Yapılar ve Sulama Bölümü, Adana.

[4.] Topraksu.: 1971. Menemen Ovası temel toprak etüdü, TOPRAKSU Genel Müdürlüğü Toprak ve Etüd Haritalama Dairesi Raporları, Seri No: 24. Ankara.

[5.] Utaem.: 2014. Uluslararası Tarımsal Araştırma ve Eğitim Merkezi Müdürlüğü Menemen hidrometeorolojik rasat verileri, İzmir.

[6.] Baran T., Durnabaş İ., Özış Ü., ve Gül A.: 1999. Ege Bölgesinin yerüstü su potansiyeli, İzmir Su Kongresi, 4-5 Haziran 1999, İzmir, pp.57- 73

[7.] Apha-Awwa-Wpcf.: 1998. Standard methods for the examination of water and wastewater, 20th edition, American Public Healty Association, Washington D.C.

[8.] Esri.: 2014. Using ArcGIS geostatistical analyst. environmental systems research institute, Redlands, CA, USA, 300 pp.

[9.] SAS Institute.: 1989. JUMP 5.0.1. A Business Unit Of SAS Copyright, 1989 – 2002.

[10.] Robertson G. P.: 2000. GS+ : Geostatistics for the environmental sciences. Gamma Design Software.

[11.] Camberdella C. A., Moormann T. B., Novak J. M., Parkın T. B., Karlen D. L., Turco R. F., Konopka A. E.: 1994. Field-Scale Variability Soil Properties in Central Lowa Soils, Soil Sci. So. Am. J. Vol 58, pp.1501-1511.

[12.] Gündoğdu K. S.: 2004. Sulama proje alanlarındaki taban suyu derinliğinin jeoistetistiksel yöntemlerle değerlendirilmesi, Uludağ Üniversitesi Ziraat Fakültesi Dergisi, 18(2):85-95. Bursa.

[13.] Cemek B., Demir Y., Erşahin S., Aslan H., Güler M.: 2006. Spatial variability of groundwater depth, soil salinity in irrigated of Bafra Plain in Northhern Turkey, International Symposium on Water and Land Management for Sustainable Irrigated Agriculture, Adana-Turkey.

[14.] Shegena Z.: 2012. Mappıng of soil salinity in sego irrigation farm, southern Ethiopia using geospatial tools, Master of Science.

[15.] Çetin, M., Kırda, C., Efe, H. ve S. Topçu (2008), düşük kaliteli suların sulamada kullanılmasının neden olabileceği olası tuzluluk sorununun coğrafi bilgi sistemi ortamında irdelenmesi, TMMOB 2. Su Politikaları Kong, Volume 2, pp. 471-481, Ankara.

[16.] Akbaş F., Ünlükara A., Kurunç A., İpek U., Yıldız H.: 2008. Tokat-Kazova'da taban suyu gözlemlerinin CBS yöntemleriyle yapılması ve yorumlanması, Sulama ve Tuzlanma Konf., 12-13 Haziran, Şanlıurfa.

[17.] Arslan H., Cemek B., Demir Y., ve Yıldırım D.: 2011. Deniz suyu girişiminin belirlenmesinde çevresel izotopların kullanılması, Tarım Bil. Arş. Der.. Volume 4 (2), pp. 59-64.

HUNGARIAN AGRICULTURAL ENGINEERING
N° 28/2015 44-47
Published online: http://hae-journals.org/
HU ISSN 0864-7410 (Print) / HU ISSN 2415-9751(Online)
DOI: 10.17676/HAE.2015.28.44

PERIODICAL OF THE COMITTEE OF AGRICULTURAL AND BIOSYSTEM ENGINEERING OF
THE HUNGARIAN ACADEMY OF SCIENCES
and
SZENT ISTVÁN UNIVERSITY
Faculty of Mechanical Engineering

CORRELATION BETWEEN DIELECTRIC PROPERTIES AND AEROBIC BIODEGRADABILITY OF MEAT PROCESSING SLUDGE

Author(s):
S. Beszédes[1] – P. Veszelovszki[2] – B. Lemmer[1] – L. Ludányi[1] – G. Keszthelyi-Szabó[1] – C. Hodúr[1]

Affiliation:
[1]Department of Process Engineering, Faculty of Engineering, University of Szeged, Moszkvai blvd. 9, Szeged, H-6725
[2]Technical Institute, Faculty of Engineering, University of Szeged, Moszkvai blvd. 9, Szeged, H-6725, Hungary

Email address:
beszedes@mk.u-szeged.hu, veszelov@mk.u-szeged.hu, lemmer@mk.u-szeged.hu ludanyi.lajos@gmail.com, szabog@mk.u-szeged.hu, hodur@mk.u-szeged.hu

Abstract

The dielectric properties, namely the dielectric constant and the dielectric loss factor are important for predicting the behavior of materials during microwave processing, because both of them determine the interaction between the molecules with the oscillating electromagnetic field. Because the dielectric properties are not known for food industry sludge, our main aim was to measure the dielectric constant and dielectric loss factor for meat industry sludge, and to investigate the correlation between the dielectric parameters and the biodegradability indicators. Our experimental results show, that despite of the high moisture content of sludge, temperature depending behavior of ε' was different that of can be known for water. Sludge had a decreasing tendency in the temperature range of 20-60°C, but over a critical value of the temperature increasing induced an increment in the value of ε'.

Our experimental results verified that the change of sCOD/tCOD has a good linear correlation with the dielectric loss factor. Similar to the trends determined for the solubility change, a good correlation was found between the dielectric loss factor and the change of biodegradability measured by the BOD/tCOD parameter. Our experimental results verified that the change in the value of dielectric loss factor correlate with the disintegration degree and the biodegradability of sludge, as well Correlation between the electrical parameters and biodegradability indicators enable to develop a real-time and in-line measuring and control system for batch and continuous flow microwave sludge conditioning technology.

Keywords

dielectric properties, microwave, sludge, biodegradability

1. Introduction

Nowadays the renewable energy generation can be often connected to waste management technologies. For example, since an effective utilization of food industrial biomass waste has desired, the establishment and optimization of an efficient biogas production process from these waste materials is very important from perspectives of both energy and environmental issues. Food industry generates a huge amount of liquid and solid organic waste and by-products. Beside the considerable environmental risk of waste, it has a good potential to indirect bio-energy production for example in anaerobic digestion (AD) process. Biofuel production from agri-food wastes can also contribute to make waste management more socially acceptable, sustainable and cost effective.

Wastewater sludge originated from food processing has high organic matter content, but the biodegradability is limited due to the structure and the low level solubility of organic matters. Degree of hydrolysis is one of the key issues for the whole efficiency of the sludge utilization processes. In hydrolysis the polymeric, insoluble compounds, such as proteins, fats carbohydrates and their derivatives are decomposed into less molecules, such as amino acids, monosaccharaides, alcohols or fatty acids. Due to the complex particle structure and the presence of strong cell membranes sludge is difficult to bio-degrade under aerobic or anaerobic conditions, as well. The main aim of sludge pre-treatment technologies is to disrupt the cell membranes, thus lysis of the cells of microorganisms, and to accelerate the hydrolysis of macromolecular components.

Among the different sludge handling methods, microwave irradiation is successfully applied in the process of hygienization, dewatering, drying and pre-treatment stage of anaerobic digestion (AD). A microwave method is suitable to increase the degree of conversion of organic matters contained in the sludge flocks into easily accessible compounds for fermentative microorganisms. Disruption of cell membranes led to release of the protoplasm-enzymes responsible for the increasing of ammonia and phosphate concentration in sludge liquor [1]. The major advantage of MW heating over conventional thermal methods is the volumetric heating, which leads to faster heat and mass transfer and shorter process time. Application of MW irradiation combining with the oxidation process, such as ozonation, can also be considered to be promising technology as pre-treatment before AD of high organic matter containing but less degradable sludge [2].

Energy transfer carried by microwave irradiation affect the biodegradability of materials in two ways. Thermal effect is expressed in the increase of internal pressure of intracellular liquor caused by internal heating and rapid evaporation, which altogether can lead to cell wall disruption [3]. The non-thermal effect of high frequency electromagnetic field contributes to alter the structure of macromolecules with polarization of side chains and breaking of hydrogen bounds [4, 5]. High efficiency of MW treatments in the biomaterial processing and also on the rate of

chemical reactions is often explained by the non-thermal effects of microwaves due to the direct interaction of electromagnetic field with molecules [6]. MW irradiation has been successfully adopted as pre-treatment method via the high energy dissipation of polar compounds of sludge.

The most used method to characterize the change in the efficiency of disintegration is the measure of the soluble to total chemical oxygen demand (SCOD/TCOD). Lysis of microbial cell walls and disintegration of sludge flocks is determined by hydrogen bindings, hydrophobic interactions and also by the concentration of divalent cations. Increment of Ca^{2+} and Mg^{2+} as a component of phospholipids is due to the disruption of cell walls [7]. Therefore the measurement of divalent ion concentration in liquid phase can be an indirect method to follow the degree of disintegration. Additionally, the strong effect of microwave irradiation on the cell wall disruption and sludge flock disintegration was confirmed by microscope observations [8].

Results of preliminary studies established that organic matter releasing is mainly influenced by the final temperature and temperature ramp of sample during the process and the length of microwave irradiation. If the final temperature is higher than 80°C a partial conversion of NH^{4+} into gas phase as NH^3 can be observed, decreasing the organic matter concentration of liquid phase [9]. Furthermore if the temperature of sample reach the boiling point a slight decrease of COD concentration occurred [8]. Because the heat stress is influenced by the temperature ramp which is depended on the strength of electromagnetic field, the power of microwave irradiation can be also determinative process parameter [10].

Numerous reports concluded that microwave pre-treatment is suitable to enhance the efficiency of anaerobic digestion process, what manifested in higher biogas product and accelerated biogas production rate [11, 12]. The increment of biogas production and utilization value of biogas (calorific value and quality determined mainly by the methane, carbon dioxide and hydrogen sulfide concentration) is affected by the type of processed sludge [13].

Microwave heating depends on the ability of electromagnetic (EM) field to polarize the molecules or atoms. Depending of the frequency of EM field the dipoles and ions in solutions and suspensions is moving with time lead to energy dissipation. The behavior of molecules of the material in EM field is characterized by the dielectric parameters. The measurement of dielectric properties is widely used in many field of researches. The value of permittivity or dielectric constant provides information about the polarization and relaxation response of molecules in the electromagnetic field. Dielectric loss factor indicate the transmission loss of electromagnetic waves in the material [14].

The dielectric properties, namely the dielectric constant (ε') and the dielectric loss factor (ε") are important for predicting the behavior of materials during microwave processing, because both of them determine the interaction between the molecules with the oscillating electromagnetic field [3]. Dielectric constant measure the ability of material to store the irradiated energy, the value loss factor relate to the ability of material to convert electric energy into heat [15].

The value of dielectric parameters are depend on the frequency and the physical and chemical properties of irradiated sample, such as moisture content, temperature, chemical composition, the form of water bounding, the migration ability of polar and dipole components and the chemical or structural change during the microwave treatment [16]. The dielectric loss factor significantly increases with increasing concentrations of dissolved ions. But dielectric loss factor decrease with increasing of temperature at the most widely used 2450 MHz frequency. The relaxation time of bound water molecules is longer than that of free water [17]. Because the bound water is associated by with proteins and carbohydrates in cell membranes and sludge flocks, the disruption and structural change cause change in dielectric properties, as well.

The sludge pretreatments aim to modify the sludge structure, disrupt the cell walls causing liberation of intracellular components [7, 18] what affect the biodegradability and the dielectric parameters, as well. Therefore the measurement of the change of dielectric properties induced by the pre-treatments, or the real-time measurement of them during the microwave and/or chemical and oxidation procedure enable to develop novel process control and optimization method for laboratory and industrial scale application.

Because the dielectric properties are not known for food industry sludge, our main aim was to measure the dielectric constant and dielectric loss factor for meat industry sludge, and to investigate the correlation between the dielectric parameters and the biodegradability indicators.

2. Materials and methods

Investigated wastewater sludge was originated from meat industry with a total solid (TS) content of 9.7 %, initial total COD of 105.9 kgm^{-3}, and soluble COD of 20.1 kgm^{-3}. The chemical oxygen demand of sample was measured triplicated using colorimetric standard method.

COD in supernatant was determined after separation by centrifugation (12,000 rpm for 10 minutes) and prefiltration (0.45 μm Millipore disc filter).

The biochemical oxygen demand (BOD5) measurements were carried out in a respirometric BOD meter (BOD Oxidirect, Lovibond, Germany), at 20 °C for 5 days

Dielectric constant (ε') and dielectric loss factor (ε") were determined in a tailor made dielectrometer equipped with a dual channel NRVD power meter (Rohde & Schwarz). Magnetron of dielectrometer operates at a frequency of 2450 MHz. ε' and ε" was calculated from the reflection coefficient (Γ), phase shift (ϕ), incident (P_i) and reflected power (P_r).

$$\delta = arc\ tg\left(\frac{|\Gamma|\sin\varphi}{1-(|\Gamma|\cos\varphi)}\right) - arc\ tg\left(\frac{|\Gamma|\sin\varphi}{1+(|\Gamma|\cos\varphi)}\right)$$

$$\varepsilon'' = tg\delta \cdot \varepsilon'$$

$$\varepsilon' = \sqrt{\frac{P_r}{P_i}}$$

3. Results and discussion

In the first series of our experiments the dielectric constant (ε'), the dielectric loss factor (ε") and temperature dependency of them were determined. For the analysis two sludge sample were used with different dry matter content (SL1=9,7 w%; and SL2=14,8 w%). SL2 sludge was prepared from SL1 sludge by addition of concentrated sludge fraction to achieve higher dry matter content.

The temperature range of measurements was 20-80°C to avoid boiling, because bubbles containing vapor disturb the analysis of dielectric parameters in the measuring cell of dielectrometer used in our experiment. Fluctuation of dielectric parameters can occur when boiling point is reached during the heating, or air bubbles are arisen in the fluid.

Our experimental results show, that despite of the high moisture content of sludge, temperature depending behavior of ε' was different that of can be known for water. SL1 sludge had a decreasing tendency in the temperature range of 20-60°C, but over a critical value of the temperature increasing induced an

increment in the value of ε'. SL2 sludge with higher dry matter content had a different behavior as a function of temperature, because over the temperature of 60°C increment of ε' was not significant.

Change of dielectric loss factor, as the function of temperature, has a similar tendency to ε' for SL1 sludge. Contrary to the different behavior of ε', tendency of the change in the value of ε" for SL1 was similar to that of measured for SL2 (Figure 1). The temperature depending breaking point for ε" was different for the two type of sludge with different dry matter content.

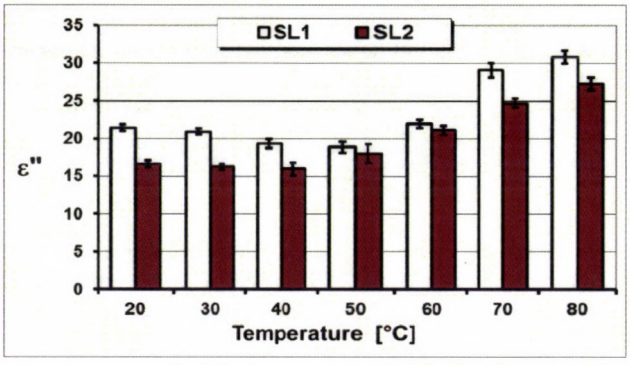

Figure 1. Change of dielectric loss factor with temperature

After decreasing phase the value of ε" starts to increase at 50°C and 40°C for SL1 and SL2 sludge, respectively. Therefore, it can be concluded, that the value of dielectric loss factor was influenced by the temperature moisture content of sludge, as well. Because the quantity of sample and the water content was not changed during the measurement the special behavior of ε" was assumed to the structural change of sludge.

In order to find explanation for the change of ε" and to confirm our hypothesis on structural change, in other experimental series the ratio of soluble chemical oxygen demand (sCOD) to the total chemical oxygen demand (tCOD) was determined, which correlate the disintegration degree and the solubility of sludge organic matters. Our experimental results verified that the change of sCOD/tCOD has a good linear correlation with the dielectric loss factor (Figure 2).

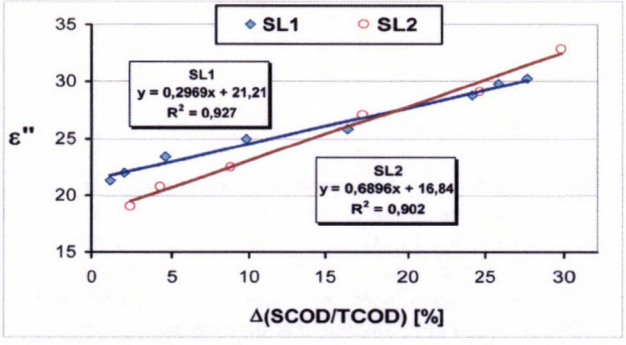

Figure 2. Correlation of dielectric loss with the change of organic matter solubility

The thermal treatments resulted in the disruption of cell wall and disintegration of sludge structure what has an increasing effect of the ratio of fee water content to the bounded water in the sludge. On the other hand, the degraded cell walls led to the liberation of intracellular substances and the hydrolysis of macromolecules resulted in a higher concentration and enhanced migration ability of ions and polar compounds. Above a certain temperature, when sludge disintegration reach a critical value, the change of dielectric parameters are more influenced by the ionic migration than the dipole rotation [6].

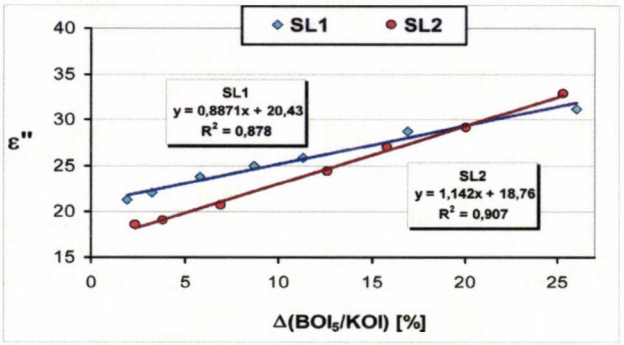

Figure 3. Relationship between dielectric loss factor and BOD/TCOD

On the other hand, the change in solubility of organic matter has also effect on biodegradability. The correlation between solubility and biodegradability given as the ratio of BOD to COD has been verified earlier [2]. Similar to the trends for the solubility change, a good correlation was found between the dielectric loss factor and the change of biodegradability measured by the BOD/tCOD parameter (Figure 3).

4. Conclusion

In our work the dielectric constant (ε') and the dielectric loss factor (ε") was measured for a meat processing wastewater sludge. There was found, that ε' and ε" decreasing with increasing temperature, but over a certain value of temperature (depending on the dry matter content of sludge) start to increase. This behavior of dielectric parameters is in a relationship with the structural change of sludge, which was characterized by the sCOD/tCOD ratio and the biodegradability of organic matter content of sludge, which was given by the ratio of BOD_5 to tCOD.

Our experimental results verified that the change in the value of dielectric loss factor correlate with the disintegration degree and the biodegradability of sludge, as well. Correlation between the electrical parameters and biodegradability indicators enable to develop a real-time and in-line measuring and control system for batch and continuous flow microwave sludge conditioning technology.

Acknowledgements

This project was supported by the János Bolyai Research Scholarship of the Hungarian Academy of Sciences.The members of research group are thankful for the financial support provided by the Hungarian Scientific Research Fund (OTKA), under contract number K105021. This research was realized in the frames of TÁMOP 4.2.4. A/2-11-1-2012-0001 „National Excellence Program – Elaborating and operating an inland student and researcher personal support system convergence program" The project was subsidized by the European Union and co-financed by the European Social Fund.

References

[1.] Appels L., Houtmeyers S., Dereve J., van Impe J., Dewil R.: 2013. Influence of microwave pre-treatment on sludge solubilization and pilot scale semi-continuous anaerobic digestion. Bioresource Technology Vol. 28, pp. 598-603. http://dx.doi.org/10.1016/j.biortech.2012.11.007

[2.] Beszédes S., László Zs., Szabó G., Hodúr C.: 2009. Examination of the effect of microwave irradiation on the biodegradable and soluble fraction of organic matter of sludge. Annals of Faculty of Engineering Hunedoara-International Journal of Engineering, Vol. 7(4), pp. 87-90

[3.] Géczi G., Horváth M., Kaszab T., Alemany G. G.: 2013. No major differences found between the effects of microwave-based and conventional heat treatment methods on two different liquid foods. PLOS ONE Vol. 8(1), pp. 1-12 http://dx.doi.org/10.1371/journal.pone.0053720

[4.] Park B., Ahn J. H., Kim J., Hwang S.: 2004. Use of microwave pretreatment for enhanced anaerobiosis of secondary sludge. Water Science and Technology, Vol.50, pp.17-23

[5.] Lakatos E., Kovács A. J., Neményi M.: 2005. Homogenious microwave field creation. Hungarian Agricultural Engineering, Vol. 18, pp. 80-81

[6.] Leonelli C., Mason T. J.: 2010. Microwave and ultrasonic processing: Now s realistic option for industry. Chemical Engineering and Processing, Vol. 49, pp. 885-900. http://dx.doi.org/10.1016/j.cep.2010.05.006

[7.] Ahn J. H., Shin S. G., Hwang S.: 2009. Effect of microwave irradiation on the disintegration and acidogenesis of municipal secondary sludge. Chemical Engineering Journal Vol. 153, pp. 145-150. http://dx.doi.org/10.1016/j.cej.2009.06.032

[8.] Bohdziewicz J., Sroka E.: 2006. Application of hybrid systems to the treatment of meat industry wastewater. Desalination, Vol. 198, pp. 33-40. http://dx.doi.org/10.1016/j.desal.2006.09.006

[9.] Eskicioglu C., Kennedy K. J., Droste R. L.: 2006. Characterization of soluble organic matter of waste activated sludge before and after thermal pretreatment. Water Research Vol. 40, pp. 3725-3736

[10.] Beszédes S., László Zs., Szabó G., Hodúr C.: 2011. Effects of microwave pretreatments on the anaerobic digestion of food industrial sewage sludge. Environmental Progress and Sustainable Energy, Vol. 30, pp. 486-492 http://dx.doi.org/10.1002/ep.10487

[11.] Park W. J., Ahn J. H., Hwang S., Lee C. K.: 2010. Effect of output power, target temperature, and solid concentration ont he solubilization of waste activated sludge using microwave irradiation. Bioresource Technology Vol. 101, pp. 13-16 http://dx.doi.org/10.1016/j.biortech.2009.02.062

[12.] Toreci I., Kennedy K. J., Droste R. L.: 2009. Evaluation of continuous mesophilic anaerobic sludge digestion after high temperature microwave pretreatment. Water Resource Vol. 43, pp.1273-1284

[13.] Sólyom K., Mato R. B., Perez-Elvira S. I., Cocero M. J.: 2011. The influence of the energy absorbed from microwave pretreatment on biogas production from secondary wastewater sludge. Bioresource Technology Vol. 102(23), pp. 10849-10854. http://dx.doi.org/10.1016/j.biortech.2011.09.052

[14.] Komarov V.: 2012. Handbook of dielectricand thermal properties of materials at microwave frequencies. Artech House, US, 2012, 169 p.

[15.] Zheng J., Kennedy K. J., Eskicioglu C.: 2009. Effect of low temperature microwave pretreatment on characteristic and mesophilic digestion of primary sludge. Environmental Technology, 2009:Vol. 30,pp. 319-327. http://dx.doi.org/10.1080/09593330902732002

[16.] Clark D. E., Folz D., West J. K.: 2000. Processing materials with microwave energy. Materials Science and Engineering A287, pp. 153-158 http://dx.doi.org/10.1016/S0921-5093(00)00768-1

[17.] Wang S., Tang J., Cavalierai R. P., Davis D.: 2003. Differential heating of insects in dried nuts and fruits associated with radio frequency and microwave treatments. Transaction ASAE Vol 46, pp. 1175-1182.

[18.] Cho S. K., Shin H. S., Kim D. H.: 2012. Waste activated sludge hydrolysis during ultrasonication: two-step disintegration. Bioresource Technology Vol. 44, pp. 480-483. http://dx.doi.org/10.1016/j.biortech.2012.07.024

HUNGARIAN AGRICULTURAL ENGINEERING
N° 28/2015 48-52
Published online: http://hae-journals.org/
HU ISSN 0864-7410 (Print) / HU ISSN 2415-9751(Online)
DOI: 10.17676/HAE.2015.28.48

PERIODICAL OF THE COMITTEE OF AGRICULTURAL AND BIOSYSTEM ENGINEERING OF
THE HUNGARIAN ACADEMY OF SCIENCES
and
SZENT ISTVÁN UNIVERSITY
Faculty of Mechanical Engineering

TEST RESULTS OF A PYROLYSIS PILOT PLANT IN HUNGARY

Author(s):
P. Korzenszky[1] – K. Lányi[2] – P. Simándi[3]

Affiliation:
[1]Szent István University, Faculty of Mechanical Engineering, 2100 Gödöllő, Páter K. u. 1.,
[2]Szent István University, Faculty of Veterinary Science, 1078 Budapest, István u. 2.
[3]Szent István University, Faculty of Economics, Agriculture and Health Studies, Tessedik Campus, Institute of Environmental Sciences, 5540 Szarvas, Szabadság u. 1-3.,

Email address:
korzenszky.peter@gek.szie.hu, lanyi.katalin@aotk.szie.hu, simandi.peter@gk.szie.hu

Abstract

Experiences obtained in the pyrolysis pilot plant during the Szent István University's pyrolysis research project are described. Eight different raw wastes were treated in a pyrolysis pilot plant in Mezőberény. Test results obtained are suitable as reference in connection with the quality of end products. It is also useful in examining how the environmental emission values of this kind of plants can comply with national legal requirements. By using the objective test results and experiences from operating model conditions, our research group is able to analyze and evaluate test results of a similar system in the following.

Keywords

thermolysis, pyrolysis, waste recycling, secondary raw materials, waste to energy

1. Introduction

This paper gives an account of the experiences obtained during the test operation of the EE-MBPT/01 equipment designed, constructed and operated by the Environ-Energie Kft. in Mezőberény, Hungary within the framework of Szent István University's pyrolysis pilot plant research project. The aim of the project was to serve as basis for comparison regarding the pyrolysis technologies / plants operating in Hungary and obtain comparable experiences. The used low-temperature (450°C) pyrolysis technology is a non-series industrial equipment of the Environ-Energie Kft, which was offered by them (as a cluster member) in the framework of the "Cluster for the Environmentally Conscious Development" cooperation to another member of the cluster, the Szent István University for testing.

The composition of the raw materials processed is monitored continuously. The end-products are stored, and their physical and chemical properties are recorded and analysed separately. The system is monitored continuously regarding both the physical / chemical parameters and the main parameters of the thermolytic process. During the process, temperature and pressure values are measured and registered.

The pilot equipment is capable of neutralizing various raw materials (e.g., wastes) by thermolytic degradation meeting both waste management and environment protection criteria.

2. Literature background

The pyrolysis technology has a wide range of literature throughout the world. The process has many opponents, but also illustrious representatives. At the same time, a need to reduce the quantity of wastes accumulated on the Earth urges for a solution. As it is known, in case of using pyrolysis one ton of tire is comparable with one ton of high-quality hard coal that is proportional to the substitution of almost 750 kg of crude oil.

In the general knowledge there are many conflicting opinions based often on questionable grounds regarding thermal waste recovery, within that especially the thermolysis-based solutions, which could not have been supported for the time being by operating experience of sufficient number.

Several authors study the most general aspects of the impacts by pyrolysis technology and green economy on the society, the regional development policy of waste management as well as the green energetics and its spatial aspects. "Green electricity", reduction of oil imports, reduction of garbage collection fee and job creation could be the great advantage of a newly created pyrolysis plant [1].

Many laboratory methods apply to the analysis of thermolysis residues, such as UV-VIS spectrum that may be a rapid analytical method of the technology in the future. The essence of the rapid methods is to obtain accurate information as soon as possible from the materials generated in due course during the several-hour process [2].

Scientific workshops study the further usability of solid by-products generated during pyrolysis. By mixing bio char into soil, we can return the carbon bound in the biomass to the soil, and the quantity bound this way will not get back to the atmosphere [3].

Many equipment of various sizes have been made throughout the world. In many places there is a continuous production technology set to one type of raw material. However, the joint behaviour of the pyrolysis raw materials arriving as a mixture of various wastes has not been an investigated subject, yet. Some authors report on new opportunities for innovation [4, 5].

The research results of a pyrolysis pilot plant may open new prospects for popularizing energy from waste. There are two ways to view the materials that cannot be used in other ways: we can consider and dispose them as wastes or we can see the potential inherited in them for the further processing and utilizing. The procedures using the energy in the wastes, such as the pyrolysis

technologies are critical in order to speed up the deflection of waste flows from final dumping.

3. Materials and methods

The first step of installing the technology is to clarify and specify the plant dimensions based on the plans and documentation prepared. With the knowledge of the technology, after examining the conditions for building up the equipment, selecting the potential locations is one of the fundamental questions of the project. After having organized the delivery of the ordered and procured equipment, machines and equipment, the arrangement of the acceptance on the premises was also a substantial and important task. With the knowledge of the site plan and the technology, the appropriate infrastructure (lighting, water, electricity, IT) must be developed in accordance with local characteristics. After designing the place of the machinery and equipment based on the technology plan as well as finalizing all of them, the assembly of the system and then the placement of the linked auxiliary plants will follow.

The essence of the pyrolysis procedure is that from the raw materials fed in, utilizable liquid, gaseous and solid products are generated in a double-walled reactor, in a temperature range of 400-600 °C, by means of agitation, at atmospheric pressure, under oxygen-free conditions. The first step of technology serves generally to treat the various raw materials thermally in order that the various compounds disintegrate suitably, the inert substances would evacuate and the utilizable materials could be recovered.

In this technology, during the pyrolysis taking place in the reactor, the raw material to be processed will be gasified, and the gaseous material created as a result of this demolition phase of the technology consists of oil vapours and flammable gases. Heavy oil is unbound from the steam-gas mixture by skimming, and wins its final end product phase by a number of subsequent technological phases (e.g. cleaning). In the closed cycle technology, combustible gases produced during the gasification of raw waste induced by the heat degradation are returned to the burner of the reactor following various separation and cleaning procedures. Thus, the gas needed for the operation of the burner can be provided at least partly from own source. Sulphur recovery from the gas can be necessary depending upon the pyrolysed raw waste; the technology does not require provision of plus water. The second step is connected to the steam production or other energetic utilisation. Pre- and post-treatments belong to the technology, covering for example the preparation of raw materials, treatment of the remains, water treatment, or flue gas treatment. Figure 1 shows the simplified schematic diagram of this rather complex process.

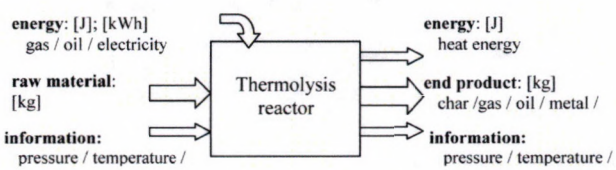

Figure 1. Schematic diagram of the thermolysis process

Technology No. EE-MBPT/01 operating in the Mezőberény plant is suitable for conducting comparative studies with similar thermolytic systems. Figure 2 shows the 3D sketch of realised equipment.

Almost every notable points of the technology are monitorable or suitable for sampling. Monitoring points were determined in the equipment not to interfere with the process, but to provide direct information about the measured parameters. The most important parameters characterising the technology – like the temperature, or pressure – are monitored and recorded by every second on the computer placed in the control room. A PLC system provides simple and fast data communication for the slowly changing thermolysis process. Code system assists the identification of monitoring points, which contains the site of measurement, the measured parameter, and the number of given technological step.

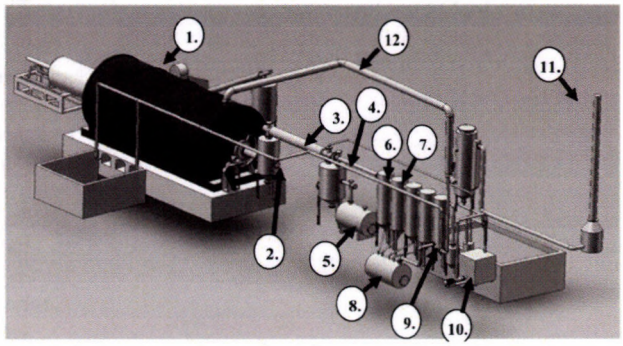

Figure 2. The pyrolysis technology in 3D presentation
1 – Reactor, 2 – Gas holder, 3 – Gas cooler,
4 – Oil-water separator, 5 – Heavy oil tank,
6 – Capacitor I, 7 – Capacitor II, 8 – Light oil tank,
9 – Scrubber tank, 10 – Vacuum pump,
11 – Gas flare, 12 – Combustion gas piping

As an example, the monitoring point No. PT012 measures the pressure of gas exiting the rotary kiln (reactor). Table 1 gives assistance in identifying the monitoring points.

Table 1. Identification of measuring points (PT012)

P		T	01	2
L – fluid level P – pressure	T – temperature Q – gas	T – technology	Serial number of technological step	1 – input data 2 – output data

The process control and visualisation system covers the graphical visualisation, operator's control, interventions, controls, communication, network handling, database handling, and data collection. Information arriving from the process is visualised on high-resolution colour graphic figures in vector graphical form. Process figures can contain various animations, graphs, trends, histograms, and even tables. Unlimited scalability of the system allows for developing new variable-types and components. List of technological monitoring sites, parameters to be measured and the individual measuring limits are given in the Table 2.

Sampling points for raw material, end-products and scrubber water were determined by the trial plans following the detailed analysis of technology. Carry-out of sampling was determined separately. Measurement and sampling points are seen in the Figure 3.

Data of pyrolysis of various raw wastes were recorded by the trial plans, covering also the operation of pilot plant. The most important data of the technology were summarized in table format, namely the following: date, raw waste to be pyrolysed, sampling date of raw material, starting and end-time of pyrolysis process, starting and end-time of gas- and oil-formation, the maximum temperature and pressure values during the process, the ambient temperature. Energy-type values used during the pyrolytic process were also summarised in the table, as well as, time of sampling of raw waste and the end-products, point of sampling, sampling temperature, and other parameters of sampling.

Table 2. Identification of measuring point, measured parameters and measuring ranges

Sign	Equipment unit	Measured parameters	Measuring ranges	Type of measuring
LT080	Light oil tank	Oil level	min / max levels	L
LT230	Cooling water tank	Cooling water level	min / max levels	L
PT012	Rotary kiln	Outlet gas pressure	0-100 mbar	P
PT041	Oil / gas separator	Inlet gas pressure	0-100 mbar	P
PT061	Still capacitor	Inlet gas pressure	0-100 mbar	P
PT100	Water seal	Tank pressure	0-100 mbar	P
PT102	Water seal	Gas outlet pressure	0-100 mbar	P
QT010	Gas danger at the rotary kiln	Hydrocarbon meter and gas danger warning	Signal processing / digital	Q
QT100	Gas danger at the scrubber	Hydrocarbon meter and gas danger warning	Signal processing / digital	Q
TT012	Rotary kiln	Outlet gas temperature	0-600 °C	T
TT034	Tube capacitor	Cooling water outlet temperature	0-100 °C	T
TT041	Oil / gas separator	Inlet gas temperature	50-500 °C	T
TT044	Oil / gas separator	Cooling water outlet temperature	0-100 °C	T
TT061	Still capacitor	Inlet gas temperature	50-500 °C	T
TT064	Still capacitor	Outlet cooling water temperature	0-100 °C	T
TT080	Light oil tank	Oil temperature	0-100 °C	T
TT102	Water seal	Gas outlet temperature	0-100 °C	T
TT131	Dust separator	Flue gas inlet temperature	100-800 °C	T
TT132	Dust separator	Flue gas outlet temperature	100-800 °C	T
TT233	Cooling water tank	Cooling water temperature	0-100 °C	T

Monitoring tools were used in multiple steps in order to reach the research results and as set in the trial plans. For the pyrolysis pilot runs, temperature measurements were carried out at 11 points, pressure measurements at 5 points, liquid level measurement at 2 points, hydrocarbon level measurement at 2 points. The primary consideration was to assure safe, troubleproof, and stable operation of the equipment for carrying out the research measurements.

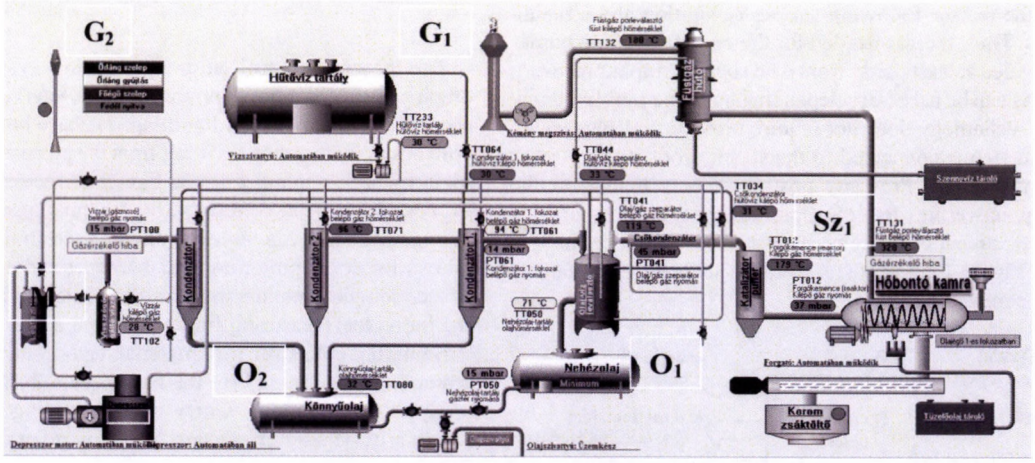

Figure 3. Measuring and sampling points
G_1 – outlet flue gas; G_2 – synthesis gas; O_1 – heavy oil; O_2 – light oil; MV – scrubber water; Sz_1 – residual pyrolysis char

4. Results and evaluation

Several different raw wastes were pyrolysed in the Mezőberény pilot plant of the project according to the trial plans in order to study the thermolytic process in the EE-MBPT/01 technology. The raw wastes to be pyrolysed were tyres, wood shreds (biomass), PET bottles, shredded tyres, industrial plastic waste, mixed plastic waste, municipal solid waste and coal-dust. Origin of the raw materials was known and recorded in every case. In the case of every raw material, two parallel pyrolyses were carried out, which could be characterised by the parameters shown in the Table 3.

Following the feeding of raw waste the system was closed and the heating-up phase initiated, which changed depending upon the characteristics of the waste to be pyrolysed. One of the notable points during the process was the start of gas formation, therefore

its exact time was also recorded. Measured values were visualised directly in the monitors of the operation personnel. Sampling for the environmental analytical chemical measurements was carried out by the experts of external laboratory being in charge of the whole task. Due to the research aims of the project, we measured temperature and pressure values at more points than it was necessary in order to gain more detailed information. By increasing the measurement points the given sub-units of the monitored system can be operated better, truer, and safer. Increasing the number of temperature measurement points improved the determination of efficiency of technology sub-units and energetic optimization of the process, which both influenced the productivity indices.

Table 3. Parameters of pyrolyses of different raw wastes

	1st pyrolysis experiment		
Raw material	**mass (kg)**	**duration (min)**	**max. temperature (°C)**
tyres	500	320	380
wood shreds (biomass)	400	230	270
PET bottles	400	270	350
shredded tyres	600	385	380
industrial plastic waste	350	240	220
mixed plastic waste	500	600	320
municipal solid waste	300	380	245
coal-dust	300	360	265
	2nd pyrolysis experiment		
Raw material	**mass (kg)**	**duration (min)**	**max. temperature (°C)**
tyres	500	295	390
wood shreds (biomass)	400	260	270
PET bottles	400	570	370
shredded tyres	600	385	375
industrial plastic waste	350	355	210
mixed plastic waste	500	465	325
municipal solid waste	300	305	265
coal-dust	300	365	265

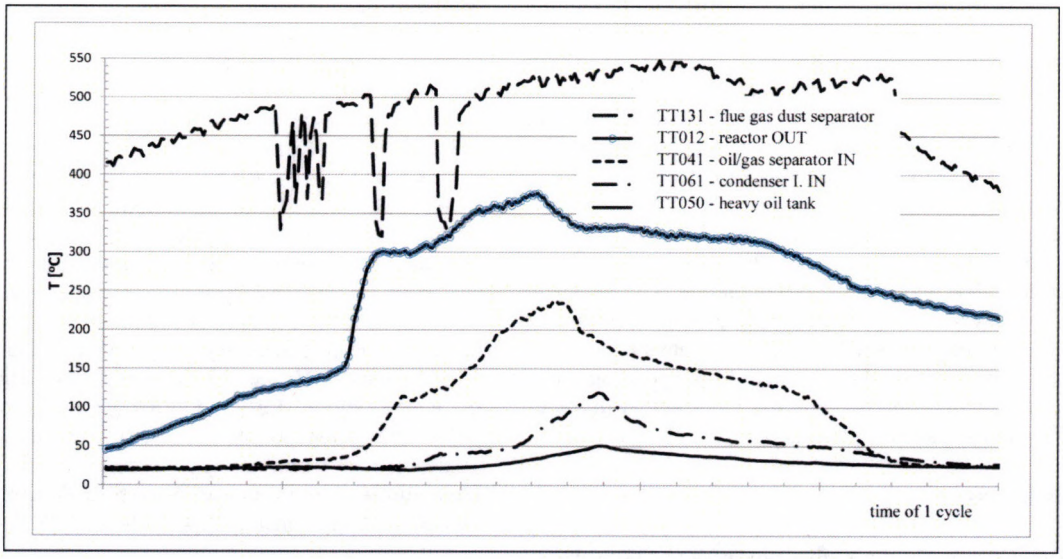

Figure 4. Pyrolysis temperature values for a hypothetic cycle

Figure 4 shows a possible way of visualisation of measured temperature data – in this case this is an edited version.

In order to enable examination of coherent technological parameters during the real-time analysis of technological process simultaneous visualisation of temperature and pressure values was necessary.

Figure 5 shows a possible way of visualisation of measured pressure data – in this case this is an edited version.

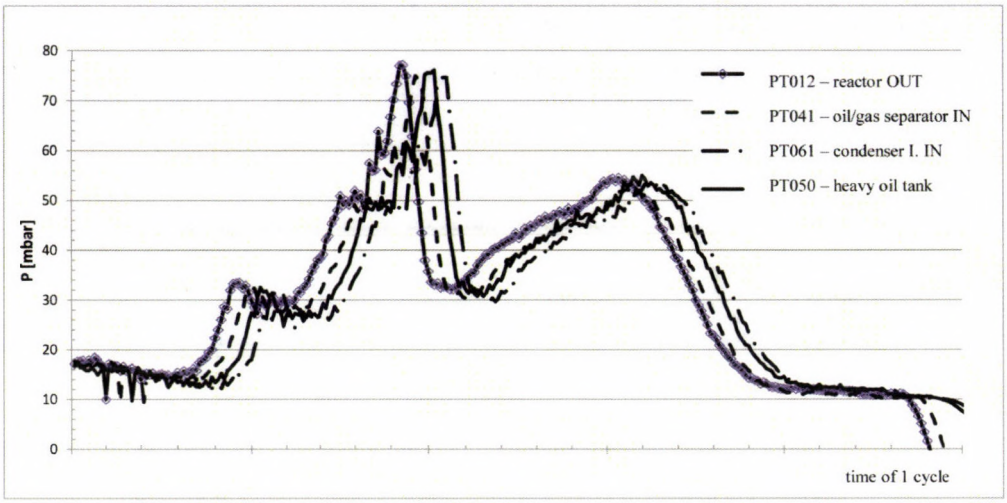

Figure 5. Pyrolysis pressure values fora hypothetic cycle

5. Conclusion

Research aims of the projects were realised through the involvement of Environ-Energie Kft. The EE-MBPT/01 plant in Mezőberény having 3 tons/day nominal capacity can serve as reference plant and is suitable for discontinuous thermolytic recycling of various raw (waste) materials in accordance with both the waste management and environmental considerations. The technology can provide a sustainable alternative for wastes that would be anyway dumped or treated in other less-sustainable way. The obtained end-products can be used as secondary raw materials for chemical industry or as secondary energy resources, fitting in the European Union's waste management approaches. The equipment operates in a well-controllable and troubleproof way by the help of its process control and visualisation system. Every moment of the technology can be handled even by remote control due to the continuous monitoring. The measured data can be visualised immediately, even in real-time in the control display. The plant and the equipment are suitable for conducting comparative examinations and the documented follow-up of the processes.

The plant of Environ-Energie Kft. in Mezőberény is suitable for monitoring and examining pilot and operational experiments under controlled conditions as well as collecting measured data. During the operation of pilot plant and subsequently analysing the results, researchers obtained insight into the details of thermolysis process.

Test results from the project are suitable as reference in connection with the quality of end products in the case of each raw material studied under operating conditions. It is also useful in examining how the environmental emission values of this kind of plants can comply with national legal requirements. By using the objective test results and experiences from operating model conditions, our research group is able to analyse and evaluate test results of a similar system in the following.

Acknowledgements

This research was supported by the Hungarian Government and the European Union, with the co-financing of the European Social Fund, within the framework of the TÁMOP-4.2.2.A-11/1/KONV-2012-0015 project.

The authors would like to express their gratitude to the whole staff of the ENVIRON-ENERGIE Energy Developer and Investor Kft. (ENVIRON-ENERGIE Kft. EE-MBPT/01 equipment) for their kind contribution to our results.

References

[1.] Duray B., Csengeri E., Egri Z.: 2013. "Zöld területfejlesztés" - egy pirolízis alapú vidékfejlesztési modell lehetőségeinek feltárása [In: Buday-Sántha Attila, Danka Sándor, Komlósi Éva (szerk.) Régiók fejlesztése 2013/2: TÁMOP-4.2.1B-10/2KONV-2010-0002 Projekt kutatászáró konferencia Pécs, 2013. május 23-24. 364 p.] Pécsi Tudományegyetem Közgazdaságtudományi Kar, pp. 25-32. 2. kötet(ISBN: 978-963-642-530-2)

[2.] Vágó I., Czinkota I., Simándi P., Rácz I., Tolner L.: 2013. Analysis of Pyrolysis Residues' UV-VIS Spectrums In: International Symposia "Risk Factors for Environment and Food Safety": Natural Resources and Sustainable Development., Oradea, Románia, 2013.11.08-2013.11.09. Anale Universitatii din Oradea, Fascicula Protectia Mediului 21 pp. 765-773.

[3.] Gulyás M., Fuchs M., Rétháti G., Holes A., Varga Zs., Kocsis I., Füleki Gy.: 2014. Szilárd pirolízis melléktermékekkel kezelt talaj vizsgálata tenyészedényes modellkísérletben, AGROKÉMIA ÉS TALAJTAN 63, pp. 341-352.

[4.] Lányi K., Molnár E., Vanó I., Korzenszky P.: 2014. Looking behind the process of pyrolysis in waste management: questions on the composition and quality of end-product and their answers by means of analytical chemistry, Hungarian Agricultural Engineering 26, ISSN 0864-7410, http://dx.doi.org/10.17676/HAE.2014.26.25

[5.] Korzenszky P., Puskás J., Mozsgai K., Lányi K., Mák Z.: 2014. Innovation possibilities of a thermolysis plant to be established in Hungary [In: Marianne Bell (szerk.) 20th International Symposium on Analytical & Applied Pyrolysis: Pyro2014.] Birmingham, 2014.05.19-2014.05.23. Paper B143.

HUNGARIAN AGRICULTURAL ENGINEERING
N° 28/2015 53-55
Published online: http://hae-journals.org/
HU ISSN 0864-7410 (Print) / HU ISSN 2415-9751(Online)
DOI: 10.17676/HAE.2015.28.53

PERIODICAL OF THE COMITTEE OF AGRICULTURAL AND BIOSYSTEM ENGINEERING OF
THE HUNGARIAN ACADEMY OF SCIENCES
and
SZENT ISTVÁN UNIVERSITY
Faculty of Mechanical Engineering

FORECASTING SHARE PRICE MOVEMENTS USING NEWS SENTIMENT ANALYSIS IN A MULTINATIONAL ENVIRONMENT

Author(s):
S. Molnár[1], M. Molnár[2], Zs. Naár-Tóth[2], T. Tímár[1]

Affiliation:
[1]Faculty of Mechanical Engineering, Institute of Mathematics and Informatics, Szent István University
[2]Faculty of Economics and Social Sciences, Institute of Economics, Business Law and Methodology Szent István University, Páter K. street 1., Gödöllő, H-2103, Hungary

Email address:
molnar.sandor@gek.szie.hu, molnar.mark@gtk.szie.hu, toth.zsuzsanna@gtk.szie.hu, timar.tamas@gek.szie.hu

Abstract

Using a common definition we can define news analysis as the measurement of the various qualitative and quantitative elements of textual news stories. These elements include sentiment, relevance and novelty. By quantifying news stories we can gain a useful way to manipulate and use everyday information in a mathematically concise manner. In this article a framework for news analytics techniques used in finance is provided. Various news analytic methods and software are discussed, and a set of metrics is given that may be applied to assess the performance of analytics. Various directions for this field are discussed. The proposed methods can help the valuation and trading of securities, facilitate investment decision making, meet regulatory requirements, or manage risk.

Keywords

textual news stories, finance, alternative metrics, software, investment decision making

1. Introduction

Quantitative analysis of text (news, tweets, articles, etc) can provide additional information for financial analysis. First of all text contains an additional emotional content (called sentiment) which provide valuable input for further conjectures on a given topic. Another important factor is the opinions and links found in the text to other sources. Third the quantification of some intrinsically qualitative information can be difficult and results in „signal loss". Fourth, textual information contains some additional value over aggregated and composite quantitative information [1].

Evolution of computer hardware, computing power and storage capacity allowed for the birth and fast evolution of data mining. In addition to the vast amount of data generated every day and every hour it is possible to rely on large databases for analysing information. Dictionaries are used for providing a quick assessment of sentiments found in an article by quickly comparing the contents of the respective text with the built-in words and developing a score. One example is the Harvard Inquireer which allows for deciding on the optimistic or pessimistic nature of an article. Associative dictionaries are also a novelty, they basically function as a thesaurus and allow for establishing the proper context of a text. To visualise context some webpages offer online graphics to provide an eycatching clue, see e.g. Visuwords or other pages.

Advantage of using such dictionaries is that they provide an unbiased fundament for evaluation, an objective basis which can be referenced and referred in research.

Many techniques exist to reduce the enormous amount of textual input to process thus simplifying analytical work. One interesting and important element is text summarisation. A simple form of summarisation is when we select the sentence(s) with the largest commonality index; that is, a number which represents the similarity beween the text and other elements. One of the basic measures used is the Jaccard formula [2], which allow for the composition of the Jaccardi matrix. The (i,j) element of the Jaccardi matrix is given as follows

$$J_{ij} = \left| \frac{s_i \cap s_j}{s_i \cup s_j} \right| = J_{ji} .$$

Similarity is calculated by calculating row sums,

$$S_i = \sum_j J_{ij} ,$$

and a natural ranking according to the significance of a sentence can be starting from the lowest values (e.g. highest information content or novelty).

After having done some analysis and editing tasks and having trimmed the text to our needs the next task is to analyse the text. One important step is to extract sentiments and decide about the message of the text (e.g. optimistic, pessimistic, neutral).

One method for this process is the Bayesian classification, where we use a training set to "teach" the computer to classify documents based on the occurrence of typical terms (so called prior probabilities) and use the definition of the conditional probability to calculate posterior probabilities to classify new documents in the given classes of sentiments.

Another method frequently applied is the support vector model, which spearates the datasets using a distance maximisation method (e.g. distance between data groups is maximised by fitting (a) separating hyperplane(s)) between).

A simple way can be the word count method where we simple count the number of words with positive and negative sentiment and get a net balance of the text.

2. Applying metrics text analysis assessment

When trying to establish the quality of an algorhitm in text minig, it is important to apply certain metrics. Originally metrics mean a measurement of distance in mathematics, in the current context they provide a means to test for the goodness of the text mining algorithm. Here we present only a few examples from the literature [3, 4].

One important element is the confusion matrix, which describes the goodness of classification using a matrix form. Simply put, assuming a k categories, we have a quadratic K x K matrix, where the rows represent actual categories, columns represent assigned categories, and any cell (i,j) represents a text which is category i and was assigned to category j. Obviously only elements in the diagonal of the matrix represent well classified elements, all other elements which are non-zero represent classification error (thus the notation confusion matrix).

The test is based on a χ^2 critical value, the null hypothesis that in the case of random guessing (a completely useless algorithm) the rows and columns would be independent. Denote with O(i,j) the actual elements of the confusion matrix and E(i,j) the expected element under the assumption of no classification (uniformly distributed random values, e.g. the number of observations in the ith row and jth column divided by the total number of observations).

$$\chi^2_{(K-1)^2} = \sum_i \sum_j \frac{(O(i,j)-E(i,j))^2}{E(i,j)} \qquad (1)$$

Depending on this test statistics we can decide about accepting the algorithm.

Based on the elements of the confusion matrix accuracy can also be tested with the following metrics using the previous notations:

$$A = \frac{\sum_i O(i,i)}{\sum_j M(j)} = \frac{\sum_i O(i,i)}{\sum_i M(i)} \qquad (2)$$

This is simply the sum of the diagonal elements divided by the sum of all elements of the matrix.

Incorrect classification can be sometimes more harmful than no classification at all. Incorrect classification can be simply counted as the percentage of elements which are not correctly assigned (this can be weighted). A logical assumption is that the categories are arranged in a manner where neighbouring categories have proxmitiy in their sentimental content, too. Under such arrangement it is expected that a classification which puts a given category to a category with distinctively different meaning causes much more harm than a misclassification to a category in the "vicinity". In our proposition below we try to give a way to resolve this issue by introducing a vicinity factor in misclassification.

3. Proposed new metrics in text analysis

One important element in text analysis is classification of text. Besides that, in our proposed method it is possible to identify the main market tendencies according to the followings. Assume that the information from the market is organised into n documents (sources) and that at most k distinctive terms are.

Suggestion for systemic error testing

If a classification algorithm is completely precise, we would only receive elements in the main diagonal, that is, the rank of the matrix would be full (equaling the number of rows). If on the other hand we have a systemic error in the algorithm, this would mean a tendency of false classification. In this case a category could be replaced by one or more other categories and the classification would not suffer any loss. For this we suggest a rank probe, that is to calculate the rank of the confusion matrix. If the rank is lower than the order of the matrix (k) that means that one category can be reproduced as a linear combination of other (one or more) categories. In that case the algorithm is generating systemic, inherent errors. If the rank of the confusion matrix is full, then the algorithm contains only random errors.

Communality matrix and determination of principal vectors in news

Concerning miscategorisation as a grave error it is logical to identify a measure to deal with this problem. Assume that categories are assigned in a logical order (e.g. decreasing sentiment, etc.) and that the the algorithm is not degenerative, that is the K confusion matrix is full rank. In that case it is possible to apply linear transformation and gain the Jordan canonical form [5]. In that case there exist at least one real eigenvalue of the matrix, but more importantly the basis of the Jordan-form matrix is composed of the eigenvectors of the original matrix (transformation, or in our case classifying algorithm).

A measure for the degree of miscategorisation can be a simple euclidean distance of the standardised eigenvectors. If the distance is less than a given threshold, then the categorisation can be accepted. If the distance is very large than the algorithm can be considered risky from the aspect of miscategorisation.

4. Empirical results of news analytics

Some elements of the theoretical results were applied to a specific case along the following lines. The Hungarian Oil Companies (MOL) and the Croatian Industrianafte (INA) formed a strategical alliance in 2003 and MOL became the owner of almost 50% of the INA shares. In our short analysis we analysed approximately 850 articles from Hungarian websites (primarily, portfolio.hu). These articles were grouped into three categories based on keyword assessment: bearish (pessimistic), bullish (optimistic) and neutral, and were scored accordingly. In many cases the articles were of political nature and thus had additional layers of information. In cases where multiple messages (perhaps of mixed positive and negative nature) were found the overall aggregate value was considered for that day.

This was matched with the daily movement of MOL share prices on the Budapest Stock Exchange (BUX).

These results were combined in simple difference values as follows. If the information gained from news analytics (three discrete values were possible) were matching the daily movement of prices then we assigned a +0.5 value to the forecast.

If the information derived from the analysed news were different from the share price movement we generated a +1 or -1 value depending on the direction of share price change compared to the forecast.

The information is summarised in the following chart, Figure 1.

It is well visible that the news analytics performed only partially well in forecasting price movements. As this was the contemporaneous (daily change) it is worth to check for the lag phase behaviour of the forecast. This is shown in Figure 2.

From this chart it can also be observed that a given day prediction from news analysis typically resulted in the next day share price movement following the sentiment of the news text.

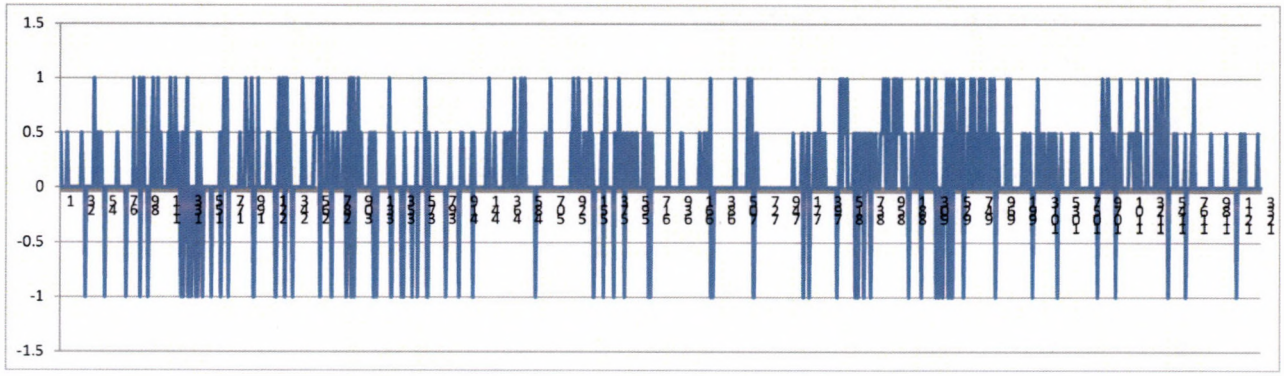

Figure 1. Differences between information of analysed news and share price movements, no lag
(1=share price increase w. negative forecast, 0.5 identical movement, correct forecast,
-1=share price decrease with positive forecast)

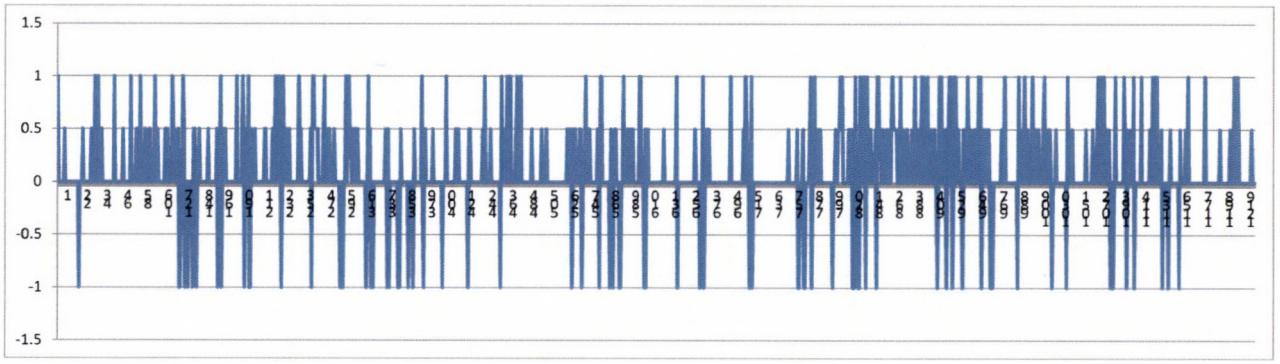

Figure 2. Differences between information of analysed news and share price movements, 1 day lag
(1=share price increase w. negative forecast, 0.5 identical movement, correct forecast,
-1=share price decrease with positive forecast)

5. Conclusion

Although the above results are of limited scope they show that news analytics require increased attention both from the theoretical view and from the view of technical analysis. There is evidence that the market is not fully informed, at least that that full information principle only holds in a weaker form as news analysis is able to provide additional predictive abilities.

References

[1.] Loughran T., McDonald W.: 2014. Measuring readability in financial disclosures. Journal of Finance, Vol. 69, pp. 1643–1671. http://dx.doi.org/10.1111/jofi.12162

[2.] Jaccard P.: 1901. Étude comparative de la distribuition florale dans une portion des Alpes et des Jura. Bull. Soc. Vaudoise Sci. Nat. 37. pp. 547-579.

[3.] Das S. R.: 2014. Text and Context: Language Analytics in Finance, Foundations and Trends R in Finance, Vol. 8, No. 3, pp. 145–260. http://dx.doi.org/10.1561/0500000045

[4.] Das S. R., Chen M.: 2007. Yahoo for amazon! sentiment extraction from small talk on the web, Management Science, Vol. 53, pp. 1375–1388. http://dx.doi.org/10.1287/mnsc.1070.0704

[5.] Molnár S., Szidarovszky F.: 2002. Introduction to Matrix Theory with Applications to Business and Economics, World Scientific, London.

CONTENTS OF NO 28/2015